AD_____

GRANT NUMBER DAMD17-94-J-4410

TITLE: Int-3 Oncogene in Normal and Neoplastic Breast Development

PRINCIPAL INVESTIGATOR: Doctor Jan K. Kitajewski

CONTRACTING ORGANIZATION: Columbia University
New York, New York 10032

REPORT DATE: September 1998

TYPE OF REPORT: Final

PREPARED FOR: Commander
U.S. Army Medical Research and Materiel Command
Fort Detrick, Frederick, Maryland 21702-5012

REPORT DOCUMENTATION PAGE

Form Approved
OMB No. 0704-0188

1. AGENCY USE ONLY *(Leave blank)*	2. REPORT DATE	3. REPORT TYPE AND DATES COVERED
	September 1998	Final (1 Sep 94 - 31 Aug 98)

4. TITLE AND SUBTITLE
Int-3 Oncogene in Normal and Neoplastic Breast Development

5. FUNDING NUMBERS
DAMD17-94-J-4410

6. AUTHOR(S)
Doctor Jan K. Kitajewski

7. PERFORMING ORGANIZATION NAME(S) AND ADDRESS(ES)
Columbia University
New York, New York 10032

8. PERFORMING ORGANIZATION REPORT NUMBER

9. SPONSORING/MONITORING AGENCY NAME(S) AND ADDRESS(ES)
Commander
U.S. Army Medical Research and Materiel Command
Fort Detrick, Frederick, Maryland 21702-5012

10. SPONSORING/MONITORING AGENCY REPORT NUMBER

11. SUPPLEMENTARY NOTES

12a. DISTRIBUTION / AVAILABILITY STATEMENT
Approved for public release; distribution unlimited

12b. DISTRIBUTION CODE

13. ABSTRACT *(Maximum 200*

To study the *int-3* gene in mammary cancer, we isolated the *int-3* proto-oncogene and named it *Notch4*, reserving the *int-3* nomenclature for the oncogenic form. Notch4 is a bona-fide Notch protein. Comparison of the *int-3* gene to *Notch4* suggests that loss of the extracellular domain of Notch4 leads to constitutive activation of this receptor. Elongation and branching of epithelial ducts is required for mammary gland development. Branching morphogenesis of mammary TAC-2 cells was used to examine Notch function in mammary gland development. Notch4(int-3) oncoprotein inhibited branching morphogenesis induced by HGF and TGF-β2. Co-expression of Wnt-1 and Notch4(int-3) demonstrates that Wnt-1 overrides the Notch-mediated inhibition of ductal morphogenesis. Wnt and Notch signaling may play opposite roles in mammary gland development. In situ hybridization revealed that *Notch4* transcripts are primarily restricted to endothelial cells in embryonic and adult life, suggesting a specific role for *Notch4* during development of vertebrate endothelium. In vitro assays using cultured endothelial cells suggest Notch4 activation can promote angiogenesis. We identified sel-10, a member of the CDC4 family of proteins that promotes ubiquitination, as an int-3 binding protein.

14. SUBJECT TERMS	15. NUMBER OF PAGES
Breast Cancer, Mammary Oncogene, Notch, Receptor, Angiogenesis	76
	16. PRICE CODE

17. SECURITY CLASSIFICATION OF REPORT	18. SECURITY CLASSIFICATION OF THIS PAGE	19. SECURITY CLASSIFICATION OF ABSTRACT	20. LIMITATION OF ABSTRACT
Unclassified	Unclassified	Unclassified	Unlimited

FOREWORD

Opinions, interpretations, conclusions and recommendations are those of the author and are not necessarily endorsed by the U.S. Army.

N/A Where copyrighted material is quoted, permission has been obtained to use such material.

N/A Where material from documents designated for limited distribution is quoted, permission has been obtained to use the material.

✓ Citations of commercial organizations and trade names in this report do not constitute an official Department of Army endorsement or approval of the products or services of these organizations.

✓ In conducting research using animals, the investigator(s) adhered to the "Guide for the Care and Use of Laboratory Animals," prepared by the Committee on Care and Use of Laboratory Animals of the Institute of Laboratory Resources, National Research Council (NIH Publication No. 86-23, Revised 1985).

N/A For the protection of human subjects, the investigator(s) adhered to policies of applicable Federal Law 45 CFR 46.

✓ In conducting research utilizing recombinant DNA technology, the investigator(s) adhered to current guidelines promulgated by the National Institutes of Health.

✓ In the conduct of research utilizing recombinant DNA, the investigator(s) adhered to the NIH Guidelines for Research Involving Recombinant DNA Molecules.

✓ In the conduct of research involving hazardous organisms, the investigator(s) adhered to the CDC-NIH Guide for Biosafety in Microbiological and Biomedical Laboratories.

[signature] 12/12/98

PI - Signature Date

Int-3 Oncogene in Normal and Neoplastic Breast Development
Final Report-1998

TABLE OF CONTENTS

INTRODUCTION

I. NATURE OF THE PROBLEM

In the past several years, it has been shown that oncogenes contribute to the pathobiology of breast cancer. Mutational activation of the *Notch4* proto-oncogene has been shown to contribute to experimental mammary gland tumorigenesis in mouse. Several human Notch family genes have also been implicated in human cancers. There is strong evidence that the Notch4/int-3 proteins regulate the cell fate decisions required for the morphogenesis and functional differentiation of the mouse mammary gland. Despite this evidence, work on the role of the *Notch4/int-3* gene in breast cancer is still in its infancy. Extensive studies on other Notch family members (lin-12/Notch) in organisms more tractable to genetic analysis such as Drosophila and C. elegans, demonstrates the evolutionary conservation of these proteins and their fundamental importance in cell fate decisions.

The proposed research will investigate the role of Notch4/int-3 proteins in the normal development of mammary gland and other tissues and study the biochemical properties that are important for int-3 transforming activity. This information will broaden our understanding about the events which control normal mammary gland development and how alterations in those events can lead to neoplastic growth of the mammary gland.

II. BACKGROUND

Mouse mammary tumor virus induces breast cancer in mouse by insertional mutagenesis. In tumors, viral integration can result in activation of the *Notch4* proto-oncogene by promoter insertion and results in expression of a truncated gene product (int-3) (1). The nucleotide sequence of the truncated gene product revealed homology with the Notch/lin-12 gene family (2). The full length cDNA of the *int-3* gene has been successfully cloned, and indeed it bears all the hallmarks of a Notch/lin-12 family gene. We proposed to name the full length *int-3* gene *Notch4*, and reserve the term *int-3* for the truncated oncogenic form which is induced by retroviral insertion. Several lines of evidence confirm a role for int-3 in mammary tumorigenesis. Transfection of a recombinant *int-3* genomic DNA fragment, encoding the truncated oncoprotein, into the HC11 mouse mammary epithelial cell line induces anchorage-independent growth in soft agar (2). Expression of this same genomic fragment *in vivo* as a transgene in a transgenic mouse strain is associated with arrest of normal mammary gland development and impaired differentiation (3), intraductal hyperplasia of mammary epithelium, and a high incidence of focal mammary tumors (adenocarcinomas) (4). It has also been reported that the normal *int-3* gene is endogenously expressed in the mouse mammary gland (5).

cDNA sequence of the 6.5kb full length *Notch4* gene indicates that it is a bona fide Notch family member. The Notch/lin-12 protein family currently consist of eleven members, Notch (Drosophila) (6), lin-12 and glp-1 (C. Elegans) (7-9), Xotch (Xenopus) (10), Notch 1, 2, 3 and 4 (Mouse) (11-15)11-15), Notch 1 and 2 (Rat) (16, 17), NOTCH 1 and 2 (Human) (18, 19). These genes encode for transmembrane receptor proteins. The extracellular domain of Notch/lin-12 family members contains variable numbers of EGF (epidermal growth factor) like repeats and other cysteine rich repeats named lin-12/Notch repeats. The intracellular domain of all Notch/lin-12 family members contains several copies of a repeat sequence, named cdc10 or ankyrin repeat. The cdc10 repeats have recently been implicated as a protein-protein interaction domain. The intracellular domain of this family of proteins also contains a PEST sequence, a nuclear localization signal, and an opa repeat. PEST sequences are found in proteins which are rapidly degraded or may also represent potential phosphorylation sites. An opa repeat is a protein domain that is rich in glutamine and is commonly found in transactivating domains of transcription factors or transcription factor binding proteins (20). The Notch and lin-12 proteins are required for cell-cell interactions that play a pivotal role in cell-fate decisions. For instance, the mechanisms that control how a group of equivalent progenitor cells give rise to a group of cells each with their particular fate. The fundamental importance of these genes during development has been demonstrated by genetic analysis of lin-12, Notch and Xotch mutants

(21-24). In the mouse, null mutants of Notch 1 and 2 are lethal during embryonic development, although the exact cause for this premature death is not known (25).

Genetic and molecular analysis have identified several proteins that participate in Notch signaling. Drosophila *Delta* (26) and *Serrate* (27) and C. elegans *Lag-2* (28) and *Apx-1* encode a family of structurally related ligands for the Drosophila Notch and C.elegans lin-12 and glp-1 receptors respectively. These ligands are transmembrane proteins, containing EGF-like domains and a cysteine rich DSL (Delta-Serrate-Lag-2) domain within the extracellular part of the protein. Recently, mouse homologues of these ligands have been cloned, *Jagged-1* (29) and *Dll-1* (30). These ligands have been demonstrated to regulate Notch receptor activity through cell-cell interactions. The products of three Drosophila genes, deltex, disheveled and suppresser of hairless (Su(H)) have been shown to interact with the intracellular domain of Notch and may thus participate in the intracellular signaling pathway of Notch (31, 32). Furthermore, genetic analysis has revealed similar phenotypes in certain Deltex and Notch mutants.

Deletion of the extracellular part of Notch, Xotch and lin-12 proteins results in a dominant gain of function mutation (21, 22, 33). The truncated gene product encoding for the intracellular part of the receptor exhibits constitutively activated protein function. The phenotype observed in this class of mutants suggests that the truncated gene products delay cell determination and thereby increase the proportion of uncommitted stem cells, leading to a prolonged lifetime of the cell or to a greater number of descendants (21, 22, 33). By analogy to the function of other Notch/lin-12 family members in lower organisms, one can speculate that delay in differentiation and accumulation of pluripotent proliferative stem cells would result in a growth advantage, thereby increasing the probability for secondary oncogenic mutations. This model would propose that Notch proteins contribute to oncogenesis by stimulating stem cell growth and blocking differentiation.

Studies on the Notch protein in Drosophila demonstrated that the intracellular domain of the Notch protein is translocated to the nucleus when a truncated Notch protein (corresponding to the intracellular domain of the protein) is expressed as a transgene in Drosophila embryos (21). Based on the hypermorphic effect of the deletion mutants, and on the presence of a nuclear translocation signal in the intracellular domain of the protein, a hypothetical model would be that ligand binding to the receptor would result in cleavage of the intracellular domain of the receptor and subsequent translocation to the nucleus, where it could interact with its substrate (34). Recent studies have borne out the model of ligand induced nuclear translocation of Notch proteins (35, 36).

Notch/lin-12 gene family members have been implicated in human tumorigenesis. Alteration of NOTCH-1 (also named TAN-1) has been associated with a T lymphoblastic neoplasm (18). The mutation of the NOTCH-1 gene in T lymphoblastic lymphomas is caused by a translocation that results in expression of a truncated gene product. TAN-1 mutations are analogous to the *int-3* activating mutations as a result of MMTV insertion, as well as to the dominant gain of function mutations of Notch, lin-12 and Xotch. Furthermore, human NOTCH-1 and NOTCH-2 (also named hN) were found to be overexpressed in human cervical carcinomas (19).

III. PURPOSE

The overall goal of the work proposed here is to understand in molecular details the function of the Notch4/int-3 proteins in mammary epithelial cells and during mouse mammary gland development, with the long term goal of understanding the role of the *int-3* gene in mammary tumorigenesis.

IV. METHODS OF APPROACH

The overall goal of the work proposed here is to understand in molecular details of the function of the Notch4/int-3 proteins in mammary epithelial cells and during mouse mammary gland development.

We proposed three specific aims to investigate the mechanisms of the functions of Notch4/int-3 proteins in a relatively simple and biological context:

1. Compare the normal int-3 protein to activated int-3 oncoproteins

We intend to first determine the primary sequence of the normal int-3 protein and evaluate whether the normal *int-3* gene encodes a Notch-like transmembrane receptor. We will then compare the biochemical and physiological properties of the normal int-3 protein with that of truncated int-3 oncoproteins. Our aim is to determine what structural alterations lead to oncogenic activation of int-3 and to evaluate if activated int-3 proteins act at the cell surface or the nucleus.

2. Identifying proteins that interact with the intracellular domain of int-3.

To elucidate the molecular mechanisms of the oncogenic effect of activated int-3, we will identify proteins or protein complexes that interact with int-3. Three approaches will be used: (1) affinity purification of associated proteins, (2) library screening with radio-labeled int-3 proteins, and (3) a yeast two-hybrid genetic screen for int-3 associated proteins.

3. Analysis of int-3 expression pattern in the murine mammary gland.

The fact that overexpression of activated int-3 in mouse mammary gland has profound effects on the development of the gland suggests a role of normal *int-3* gene products in mammary gland development. We will determine whether *int-3* gene is normally expressed in the mammary gland. Molecular and immunohistochemical techniques will be used to evaluate where and when in the normal mammary gland the *int-3* gene is expressed.

To fulfill these specific aims, we have proposed five technical objectives for a period of four years.

Task 1: Characterize the full length *int-3* cDNA. (Months 1-12)
Task 2: Study the production, processing and subcellular localization of normal int-3 proteins and int-3 oncoprotein in mammary epithelial cells. (Months 3-18)
Task 3: Evaluate the transforming potential of int-3 proteins. (Month 9-18)
Task 4: Identify proteins that interact with the intracellular domain of int-3. (Month 12-48)
Task 5: Analysis of the int-3 expression pattern in the murine mammary gland. (Months 12-48)

IV* MODIFIED METHODS OF APPROACH

The first two **aims** and first four **tasks** of our original "Methods of Approach" have largely been achieved as outlined in the original proposal.

Aim 3/Task 5 has been altered to pursue findings related to the normal expression of the full-length Notch4 gene. Our original goal was to determine if Notch4/int-3 was normally expressed in mammary epithelium and, if so, when and where in the gland is it expressed. This study was intended to shed light on the role of Notch genes in mammary gland development and oncogenesis.

We altered this **aim** upon discovering that the Notch4 gene was exclusively expressed in endothelium. Activation of expression of the truncated Notch4 gene, int-3, in mammary epithelium occurs when driven by the Mouse Mammary Tumor Virus (MMTV) LTR. As Notch4 is not normally expressed in mammary epithelium, one can propose that an alternate Notch gene plays a role in mammary gland and Notch4 activation by MMTV disrupts this role leading to oncogenesis. Based on the discovery of endothelial expression of Notch4 we modified **Aim 3/task 5** to focus on an analysis of it's potential role in vascular development and/or angiogenesis. The modified **Aim 3**, described here, is designated **Aim 3***.

Aim3* **Analysis of Notch4 expression pattern in the murine vasculature and the potential role of Notch4 in angiogenesis.**

We will determine if Notch 4 is expressed in adult and embryonic endothelium. In situ hybridizations and immuno-histochemical analysis will document the expression pattern of Notch4 in vasculature. In vitro assays using cultured endothelial cells will be used to define a potential role for Notch signaling in angiogenesis.

Task 6: Analysis of the Notch4 expression pattern in murine vasculature.

Task 7: Evaluate the angiogenic or anti-angiogenic potential of Notch signal transduction.

Please Note: The accomplishments of **Aim3*** are largely described in **Chapters III and VII.** Specifically, **Task 6** is described in **Chapter III** and **Task 7** is described in **Chapter VII.**

BODY

The progress of each specific aim will be described in the following Chapters.

Capital roman numerals will designate the Specific Aims/Chapters (**I-VII**).

Chapters that describe a comprehensive body of work, **Chapters IV-VII,** will be presented in manuscript fashion with the following sections:
Introduction, Results, Discussion, Materials & Methods, Figure Legends, Figures.

Figure numbering will be specific to each chapter and designated- Chapter #/Figure #

CHAPTER I.
Specific aim 1.

Compare normal int-3 proteins to activated int-3 proteins.

Task 1. Characterize the full length *int-3* cDNA. (Months 1-12)

This task has been completely fulfilled within the proposed period of time.

The *int-3* oncogene was classified in the lin-12/Notch protein family solely on the basis of its homology to the intracellular part of the lin-12/Notch family members. Previously, there was no direct evidence that demonstrates that the full length *int-3* encodes for a transmembrane protein. By cloning the full length *int-3* cDNA we have demonstrated that the *int-3* gene encodes a transmembrane protein, homologous to the lin-12/Notch family of transmembrane proteins. We have proposed to name the full length gene *Notch4*, and reserve the *int-3* nomenclature when referring to the truncated and oncogenic form of the gene.

A. Cloning truncated *int-3*. We have cloned the truncated *int-3* gene that encodes for the intracellular part of the protein and corresponds to the int-3 mammary oncogene (Fig. 1)

B. Cloning of the full length int-3 We have used the PCR based method of RACE (Rapid Amplification of cDNA Ends) (37, 38) to clone sequences that are located 5' from the truncated *int-3* (the truncated *int-3* transcript is localized at the 3' end of the gene). To clone the *int-3* full length cDNA, we have screened a mouse lung cDNA library. This choice of cDNA library was based on our findings of the mRNA expression analysis of *int-3*. Initially, the probes that were used in this screening analysis were derived from the cloned truncated *int-3*, as well as from the clones obtained by RACE. Positive clones were purified and sequenced and used as probes in successive rounds of screening in order to obtain the full length cDNA of the *int-3* gene. The length of the full length int-3 mRNA is approximately 6.5kb based on our Northern blot analysis.

C. Sequencing *int-3* cDNAs A total of 37 overlapping cDNA clones were analyzed and sequenced to obtain a 6677 bp cDNA sequence. This sequence encodes one long open reading frame of 1964 amino acids, starting with an initiator methionine at nucleotide 347 and terminating with a stop codon at nucleotide 6239. The 6677 bp cDNA corresponds in size to that of *Notch4* transcripts detected by Northern blot analysis; thus, we believe the cloned cDNA represents the full length *Notch4* gene (Fig. 1).

Several differences (insertions, deletions, and single nucleotide changes) were found between the nucleotide sequence of *Notch4* reported here and the previously published *int-3* nucleotide sequence (2). These differences alter the reading frame in several locations within the intracellular domain and may be a result of differences in sequence analysis or possibly mutations found in the tumor derived *int-3* transcript (2) that are not found in the *Notch4* gene. The nucleotide sequence of mouse *Notch4* has been deposited with Genbank under the Accession number U43691.

Analysis of the deduced amino acid sequence of *Notch4* reveals the presence of conserved domains shared by all Notch proteins (see Fig. 1). Notch4 contains EGF-like repeats, Notch/lin-12 repeats, a transmembrane domain, cdc10/ankyrin repeats and a putative PEST domain. The overall homology between Notch4 and other Notch proteins was determined using GCG (Bestfit, gap weight 3.0, length weight 0.1). The Notch4 protein is approximately 60% similar and 43% identical to other vertebrate Notch proteins, and 58% similar and 40% identical to *Drosophila* Notch. Lower homologies were found when compared to the *C. elegans* lin-12 and glp-1 proteins (49% similar and 29% identical).

Two hydrophobic regions in the Notch4 protein sequence were identified by hydropathy analysis (Kyte Doolittle algorithm, data not shown). An N-terminal region contains 19 hydrophobic residues that could function as a signal peptide sequence (Fig. 1) and a putative signal peptidase cleavage site was identified at residue 20. A second hydrophobic region from amino acid residues 1441 to 1465 is of sufficient length (25 amino acids) to behave as a membrane spanning domain and is immediately followed by five consecutive arginine residues that are consistent with a stop transfer signal (Fig. 1).

The extracellular domain of Notch4 contains 29 EGF-like repeats (Figs 1), in contrast to the 36 EGF-like repeats found in murine Notch 1 and rat Notch 2, and to the 34 EGF-like repeats found in murine Notch 3. EGF-like repeats are defined by a cysteine-rich consensus sequence and generally occur in analogous locations in two different Notch proteins.

Notch4 also contains three Notch/lin-12 repeats which are approximately 53% identical to the Notch/lin-12 repeats found in other murine Notch proteins. Between the Notch/lin-12 repeats and the transmembrane domain of Notch4 are 2 cysteines at positions 1388 and 1397 that are conserved among all Notch proteins and may promote receptor dimerization upon ligand binding (39).

The intracellular domain of Notch4 contains the 6 ankyrin/cdc10 repeats found in other Notch proteins. The ankyrin repeat domain of Notch4 is 48%, 52%, and 55% identical to the ankyrin repeat domains of Notch1, Notch2, and Notch3 respectively. In all Notch proteins the number of amino acids between the transmembrane domain and the ankyrin/cdc10 repeats is 110 residues, as it is in Notch4 (Fig. 1). Like other Notch proteins, Notch4 contains a C-terminal PEST domain, albeit of shorter length. In addition, Notch4 lacks a recognizable opa repeat (Fig. 1), such as that found in *Drosophila* Notch. The carboxy-terminal end of Notch proteins, beyond the ankyrin/cdc10 repeats, is the least conserved region among Notch proteins. Within this C-terminal region, Notch4 displays little homology to other Notch proteins and no significant homology to other known proteins. This C-terminal is also much shorter in Notch4 than in other Notch proteins, containing 177 residues, compared to 457 in Notch1, 437 in Notch2, and 329 in Notch3.

Task 2. Study the production, processing and subcellular localization of normal int-3 proteins and int-3 oncoprotein in mammary epithelial cells. (Months 3-18)

This task has been fully completed.

The *int-3* gene was discovered in mouse mammary tumors, induced by MMTV infection. Insertional of *Notch4* gene by MMTV results in the expression of a truncated protein product (int-3) that is able to transform mammary epithelium cells both *in vivo* and *in vitro.*

A. Epitope-tagging of int-3 proteins Before antibodies against the Notch4/int-3 proteins (aim 3) were available, we added an epitope to the Notch4 protein and its deletion mutants including int-3 (40). The epitope we have chosen is derived from the influenza HemAgglutinin (HA) protein and is recognized by a monoclonal antibody 12CA5 (41). cDNAs were cloned into phagemid vectors that contain the sequence encoding the HA epitope situated downstream. Single strands were generated from the phagemids and used in a site-directed mutagenesis protocol with an oligonucleotide designed to loop-out the sequence between the last codon of our proteins and the first codon of the HA tag, to create an in-frame fusion. The HA epitope was fused to the carboxy termini of all the Notch4/int-3 proteins. This method allowed us to detect ectopically expressed Notch4/int-3 fusion proteins in transfection experiments, using anti HA antibodies in immunoblot analysis (Appendix B).

B. Generation of int-3 expressing cell lines *int-3* and int-*3/HA* fusion constructs were sub-cloned into eukaryotic vectors such as pLNCX vector (42) and pQNCX vector (our unpublished data). These vectors utilize the cytomegalovirus immediate early promoter/enhancer to drive expression of the *int-3* gene and the retroviral LTR to drive expression of the *neo* gene, which confers resistance to the drug G418. We have also generated several control retroviral vectors, such as vectors expressing the LacZ gene, vectors expressing an unrelated HA tagged protein, and vectors expressing int-3 without the HA tag. In order to evaluate the transforming potential of int-3, a mammary epithelial cell line programmed to express int-3 was generated by infection with retroviral expression vectors. In this

study we used the TAC-2 mammary epithelial cell line (43). This line was used in an extensive study of the function of int-3 in transformation and branching morphogenesis that is described in detail in **Chapter IV.**

C. Biochemical analysis of int-3(Notch4) proteins produced in cell lines. The deduced amino acid sequence of the full length Notch4 protein predicts that Notch4 is a putative transmembrane protein. We will investigate this hypothesis by studying the intracellular localization of the Notch4 protein. These studies may confirm the predicted transmembrane nature of the Notch4 protein. The biochemical properties of Notch4 will be investigated once mammary epithelial cell lines have been generated that are programmed to express Notch4. A full length Notch4 transcript was assembled and the Notch4 protein was detected in protein lysates of transiently transfected 293T cells (data not shown). The molecular weight of epitope tagged Notch4 is approximately 215 KD. Immunofluorescence experiments on 293T cells transiently transfected with epitope tagged Notch4, cells demonstrated plasma membrane staining (data not shown).

D. Subcellular localization of int-3 proteins The intracellular localization of truncated int-3 was investigated in transiently transfected cells (293T and HeLa cells). We have investigated the intracellular localization by indirect immunofluorescence (44) using the anti-HA antibodies, and have found nuclear localization of truncated int-3. Several deletion mutants have been generated in order to determine which part of the truncated int-3 protein is responsible for its nuclear translocation. These initial studies pointed out two domains that may contain a nuclear translocation signal, one N-terminal and one C-terminal of the ankyrin repeats. Interestingly, deletion of the ankyrin repeats alone did not affect the nuclear localization. Preliminary data suggest that a protein consisting solely of the int-3 ankyrin repeats resides in the cytoplasm (data not shown). These studies will also allow us to investigate whether transformation coalesces with cytoplasmic or nuclear localization of the int-3 protein.

Task 3. Evaluate the transforming potential of int-3 proteins. (Month 9-18).

This task has been completed as an analysis of the morphogenetic effects of int-3 on mammary epithelial cells. This phenotype is thought to be related to the transforming function of int-3 in the mammary gland, as discussed in **Chapter IV**.

Described in detail in Chapter IV.

"Notch and Wnt Regulation of Mammary Gland Morphogenesis".

A. Generate cell lines expressing int-3 proteins We have generated TAC-2 cell lines that stably express int-3 proteins **Chapter IV**.

B. Evaluate the transformed properties of int-3 expressing cell lines

Briefly, we have proposed to study mammary transformation by int-3, we have, instead established a biological assay for int-3 based on its ability to block ductal morphogenesis of cultured mammary epithelial cells. The biological activity of int-3 was studied in the TAC-2 mouse mammary epithelial cell line. TAC-2 cells were isolated based on their ability to undergo branching morphogenesis when grown in a collagen gel matrix (43). This differentiation of the TAC-2 cells into tree-like structures can be specifically induced by treatment with hepatocyte growth factor (HGF). TAC-2 cells that express int-3 protein fail to undergo branching morphogenesis, when grown in the presence of HGF. Control cell lines, TAC-2 cells expressing Lac-Z, and TAC-2 cells expressing the mammary oncogene Wnt-1, were still able to differentiate into tree-like structures when induced with HGF, suggesting that the int-3 induced block of differentiation is specific. To investigate which domain of the int-3 protein is responsible for the block of branching morphogenesis of the TAC-2

cells, we expressed the int-3 deletion mutants described above and examined their effects on TAC-2 cells. We also investigated the growth characteristics of the different TAC-2 cell lines and found no differences in growth rate (day 2) or post-confluence growth rate (day 6) between int-3 expressing TAC-2 cells and control TAC-2 cells or TAC-2 cells expressing Wnt-1, in the presence or absence of HGF. The growth of TAC-2 cells was measured by a commercially available biochemical assay. These experiments suggest that the int-3 oncoprotein prevents differentiation of mammary epithelial cells without affecting the growth characteristics of these cells. The above described data are reminiscent of the mammary gland phenotype of the *int-3* transgenic mice. These animals that overexpress the *int-3* oncogene in the mammary gland fail to develop a normal mammary gland (no branching morphogenesis) and the mammary epithelial cells present display an undifferentiated phenotype. In addition, our experiments also demonstrated that the int-3 and Wnt-1 oncoproteins have opposing activities in the branching morphogenesis pathway in TAC-2 mammary epithelial cells, and that the Wnt-1 oncoprotein can act as a morphogen (as opposed to mitogen) in the TAC-2 assay.

FIGURE LEGENDS

Figure 1.
Deduced amino acid sequence of Notch4 (Genbank Accession number U43691). The boxed regions indicate the major structural elements of the Notch family of proteins, indicated as follows: 29 epidermal growth factor(EGF)-like repeats; 3 Notch/lin12 repeats; Transmembrane domain; 6 cdc10/ankyrin repeats. Putative glycosylation sites are underlined. A putative PEST domain is doubly underlined. The two cysteines thought to promote dimerization are marked with asterisks. The initiating methionine of the int-3 oncoprotein is in bold and marked by an arrow.

Chapter I.
Figure 1

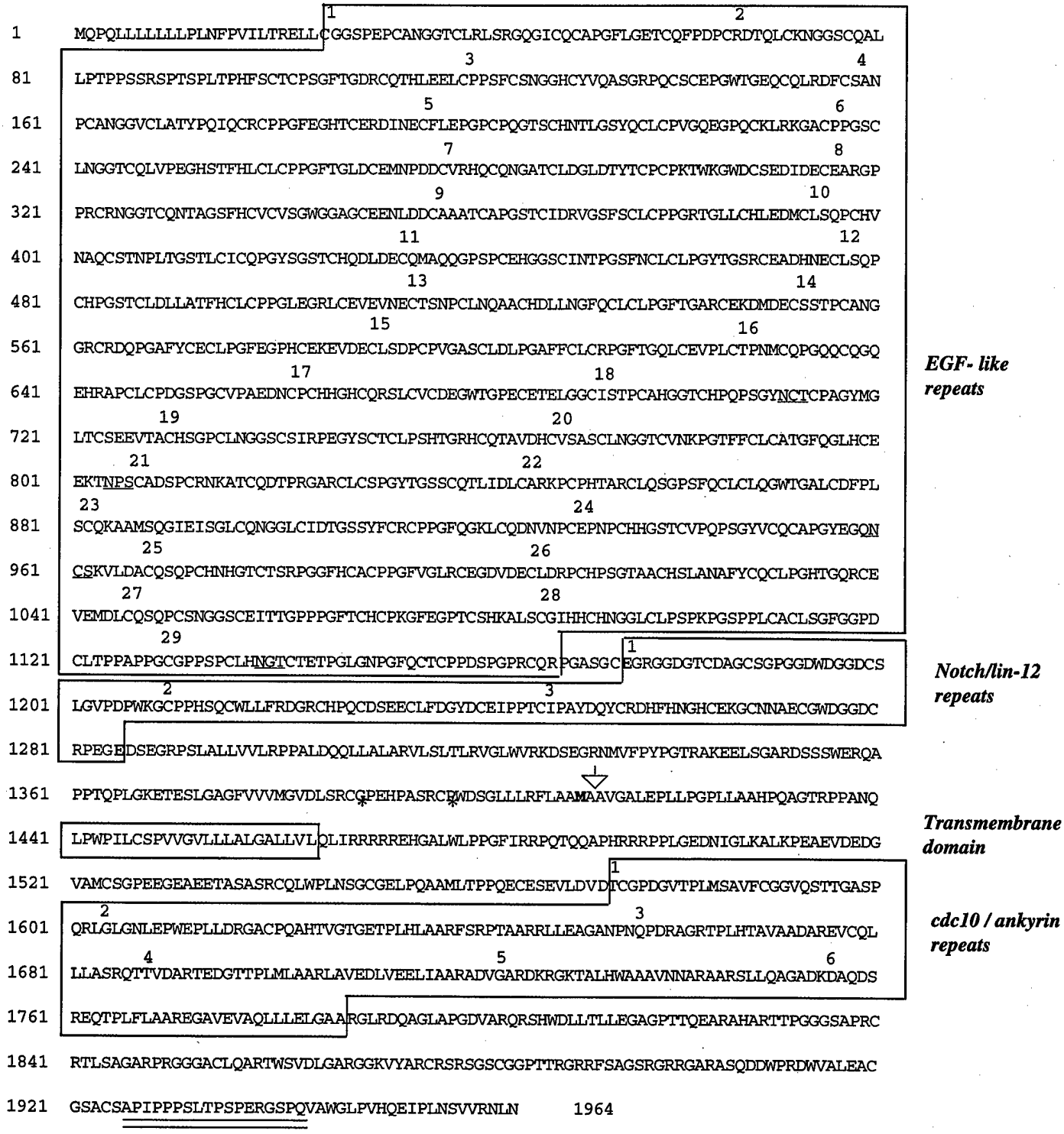

CHAPTER II.
Specific Aim 2
Identify proteins that interact with the intracellular domain of int-3

Task 4. Identify proteins that interact with the intracellular domain of int-3. (Month 12-48).

This task has been completed as the identification and analysis of the Notch/int-3 binding protein Sel-10, described in **Chapters V and VI.**

Analysis of the int-3 binding protein, SEL-10, is described in detail in Chapter V:
"SEL-10, a member of the CDC4 family, binds and regulates Notch/lin-12 proteins"

A. Identify candidate proteins that may interact with the intracellular domain of int-3 (corresponds to task 4a, 4b, 4c) A genetic screen for genes that are involved in Notch/lin-12 signaling has been done in C. elegans by Dr. Iva Greenwald at Columbia University. In collaboration with Dr. Greenwald's lab, we select C. elegans genes identified in their genetic screen according to their genetic and predicted biochemical features, as candidate genes that may encode int-3 binding proteins. The protein products of these candidate genes will be further tested in two-hybrid system and by biochemical and biological approaches. One candidate gene, C. elegans *sel-10*, a CDC4 family member has been shown in our assays to form a complex with C. elegans LIN-12 and mouse int-3 proteins. A human homologue of *sel-10* has been identified through genebank search.

B. Identify int-3 binding proteins using yeast two-hybrid genetic screen (corresponds to task 4d) To study the downstream signaling pathway of Notch4 receptor, we planned to carry out yeast two hybrid screen to search for proteins that interact with the intracellular domain of Notch4. We first generated two bait constructs for two hybrid screen. They contain either the entire intracellular domain or the ankyrin repeats region fused to LexA or GAL4 DNA binding domain. Unfortunately, when we tested the two constructs for their ability to activate LacZ reporter gene expression in yeast on their own, the ankyrin repeat construct gave very robust positive signal while the other construct produced a medium level positive signal. We tried to tackle this problem with bait constructs containing a series of deletion mutants of the intracellular domain of int-3, hoping to get rid of the transcriptional activity of the bait yet keep the intracellular domain as much as possible so that we might still identify Notch4 binding proteins through two hybrid screen. However, all the deletion mutant constructs we have tested are more or less active in β-galactosidase assay (data not shown). We tried different approaches to solve this technical difficulty, including testing our bait constructs in different yeast strains, testing the bait constructs for HIS3 reporter gene activation and adding 3-AT in yeast culture medium to suppress the leakiness of the HIS3 gene. However, under all the conditions we have tested, our bait constructs always display intrinsic transcriptional activity. These constructs, if used for two-hybrid screen, will inevitably cause high background. Therefore, they seem to be inappropriate for two-hybrid screen. But we still co-expressed the bait construct containing the entire intracellular domain with several of our candidate genes in yeast. Although the bait itself gives background expression of LacZ reporter gene, when it is co-expressed with some of our candidate genes, the signal is much stronger than the background. The same results were observed constantly in several independent experiments, suggesting that some of the C. elegans candidate proteins interact with the intracellular domain of Notch4. One of these genes, C. elegans sel-10 is further tested by biochemical approaches.

C. Characterize int-3 binding proteins (corresponds to task 4d) **See Chapter V. for details.** The interactions between C. elegans SEL-10 and LIN-12 or int-3 is confirmed by co-immunoprecipitation assay. Epitope-tagged (HA or myc) SEL-10 was co-transfected into 293T cells with either LIN-12intraHA or int-3. We then use antibodies to immunoprecipitate LIN-12intraHA or int-3 and probe for SEL-10 proteins. Our results indicate that the intracellular domains of LIN-12 or Notch4 exist in the same protein complex as SEL-10. These results are confirmed by immuoprecipitating SEL-10 first and then probing for the existence of LIN-12intraHA or int-3.

CHAPTER III.
Specific aim 3

Analyze int-3 expression pattern in murine mammary gland.

Specific aim 3*
Analyze Notch4 expression pattern in murine vasculature

Task 5: Analysis of the int-3 expression pattern in the murine mammary gland. (Months 12-48)
Task 6: Analysis of the Notch4 expression pattern in murine vasculature.

This task has been partially completed and altered, as outlined in the modified aims section. As an alternative to studying the int-3 expression pattern in the murine mammary gland we analyzed the expression pattern in murine vascular, the normal site of expression of *Notch4/int-3*.

We proposed to analyze the expression pattern of the Notch4 protein as well as the *Notch4* mRNA. Such analysis will give us further insights in the function of the Notch4 protein. We planned to study the expression pattern of *Notch4* in different mouse tissues to determine if the Notch4 protein is expressed in a tissue specific manner, and we will investigate whether *Notch4* is expressed in the mammary gland and whether this expression is developmentally regulated.

A. Generate int-3 specific antibodies To study the biological and biochemical behavior of the Notch4 and int-3 proteins, we have successfully generated rabbit antiserum against a GST fusion protein of Notch4. An intracellular fragment of Notch4 protein, which is C-terminal to the ankyrin repeats, was fused to GST protein. This fragment is the least homologous domain among different murine Notch proteins and therefore, it was chosen as immunogen to avoid cross-reactivity with other proteins. The specificity of the antiserum as well as its ability to recognize Notch4/int-3 proteins in Western blot and immunoprecipitation assays has been determined, **see Chapter VII**.

B. Immunohistochemical analysis of int-3 proteins in mammary tissue We are in the process of using the polyclonal antibodies against Notch4 in immunohistochemistry experiments. Preliminary data have confirmed the endothelial cell specific expression of Notch4 in adult mouse kidney glomeruli **(Chapter VII).**

C. Northern blot analysis of int-3 expressed in mammary tissue We have not analyzed mammary gland expression but have determined the expression pattern of Notch4/int-3 in adult and embryonic tissues. *Notch4* mRNA expression was studied by Northern blot analysis and in situ hybridization using probes derived from the 3' UTR. *Notch4* gene encodes for a 6.5 kb transcript that is highly expressed in lung, heart and kidney in adult tissues, Figure 1. Several shorter *int-3* transcripts were observed in adult testis, and were later shown to be the products of aberrant transcriptional events in post-meiotic spermatids, Figure 2. The *Notch4* transcript is expressed at all stages of mouse development (day 6.5 to 15.5) (data not shown).

D. In situ hybridization analysis of int-3 RNA in mammary tissue In situ hybridization (using the same probe as in the Northern blot analysis) was performed to determine the cellular origin of *Notch4* expression during mouse development, and revealed endothelial specific expression in mouse embryos, Figure 3. In situ hybridization on adult lung tissue was performed and revealed endothelial cell specific expression of *Notch4* , Figure 4.

FIGURE LEGENDS

Figure 1.
Expression analysis of Notch4 in adult mouse tissues. Panel A: Northern blot using riboprobe transcribed from the 3' UTR of *Notch4* (probe D in Fig. 5.), Panel B: the same blot was reprobed with a GAPDH probe. The transcript sizes of 6.7kb, 1.5kb, and 1.1 kb are indicated and were estimated in reference to 28S and 18S rRNA migration.

Figure 2.
Expression analysis of Notch4 testis transcripts. Panel A: Notch4 testis transcripts are expressed in post-meiotic germ cells. Northern blot analysis from staged and germ cell deficient testes with probe C and a GAPDH probe. Note that GAPDH transcripts appear as two isoforms in the adult testis. RNA was isolated from testes of day 7 p.n., day 17 p.n., adult, W^v/W, and $W/+$ mice as indicated. Panel B: Northern blot analysis of several adult tissues with probe A, derived from the 5' UTR of Notch4, and a GAPDH probe. Panel C: Schematic representation of truncated Notch4 transcripts as compared to the full length coding potential. Relative position of probes used in Northern blot analysis is shown. Conserved elements of Notch family proteins are indicated. MMTV integration site reported in (2) is indicated by an arrow. Novel 5' sequences of testes cDNAs are indicated.

Figure 3.
Notch4 is expressed in embryonic endothelial cells. Panel A and B: phase and darkfield photomicrograph of a horizontal section of a 9 days p.c. embryo hybridized with a cRNA probe corresponding to Notch4. Strong labeling is detectable over the anterior cardinal vein (white arrow). Diffuse labeling is also present throughout the developing nervous system and at higher level over the tip of the neural folds (red arrow). Panel C-F: Phase and darkfields images of a horizontal section of a 13.5 days p.c. embryo hybridized for Notch4 showing the venous and arterial system anterior to the lung, including dorsal aorta arch, aortic and pulmonary tract. Panel E and F are higher magnification of the area framed in panel C. Embryonic vessels are labeled and, as shown in panel E and F, labeling is restricted to the endothelial cells lining the vessels. Arrow denotes the gut which does not have detectable signal in the epithelium.

Figure 4.
Notch4 is expressed in adult lung endothelial cells. Panel A and B: phase and darkfield photomicrographs of an adult mouse lung hybridized with a cRNA probe corresponding to Notch4. Punctate staining is observed over the alveolar walls in a pattern indicative of capillaries. No labeling is observed over the pseudostratified squamous epithelium (black and white arrows) nor over the smooth muscle cells (red arrows).

Chapter III.
Figure 1

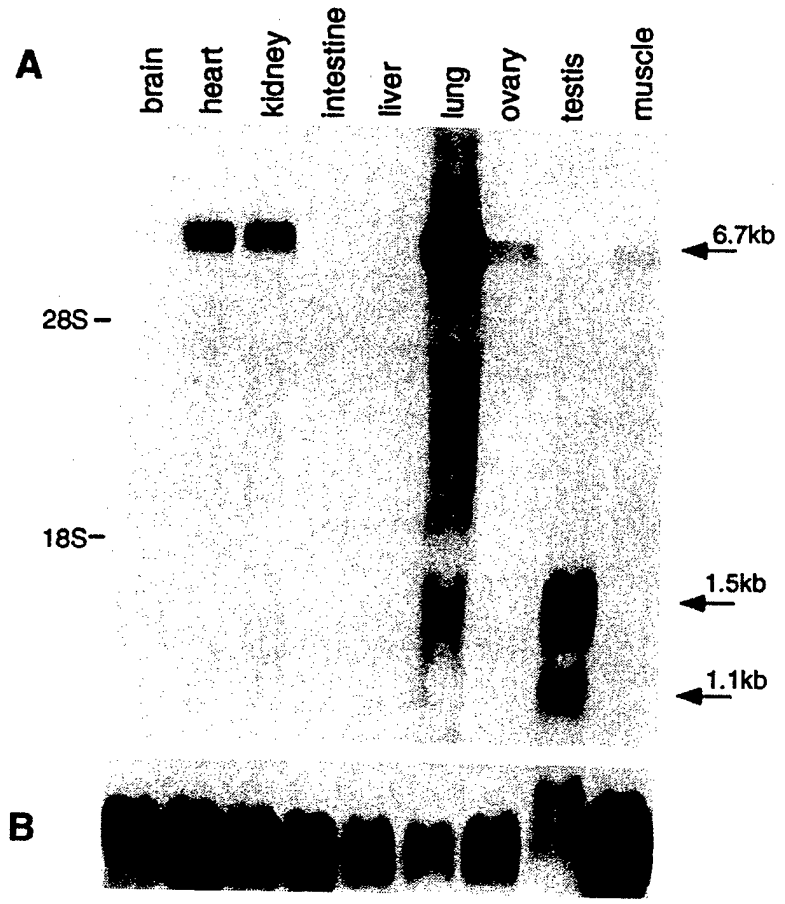

Chapter III.
Figure 2

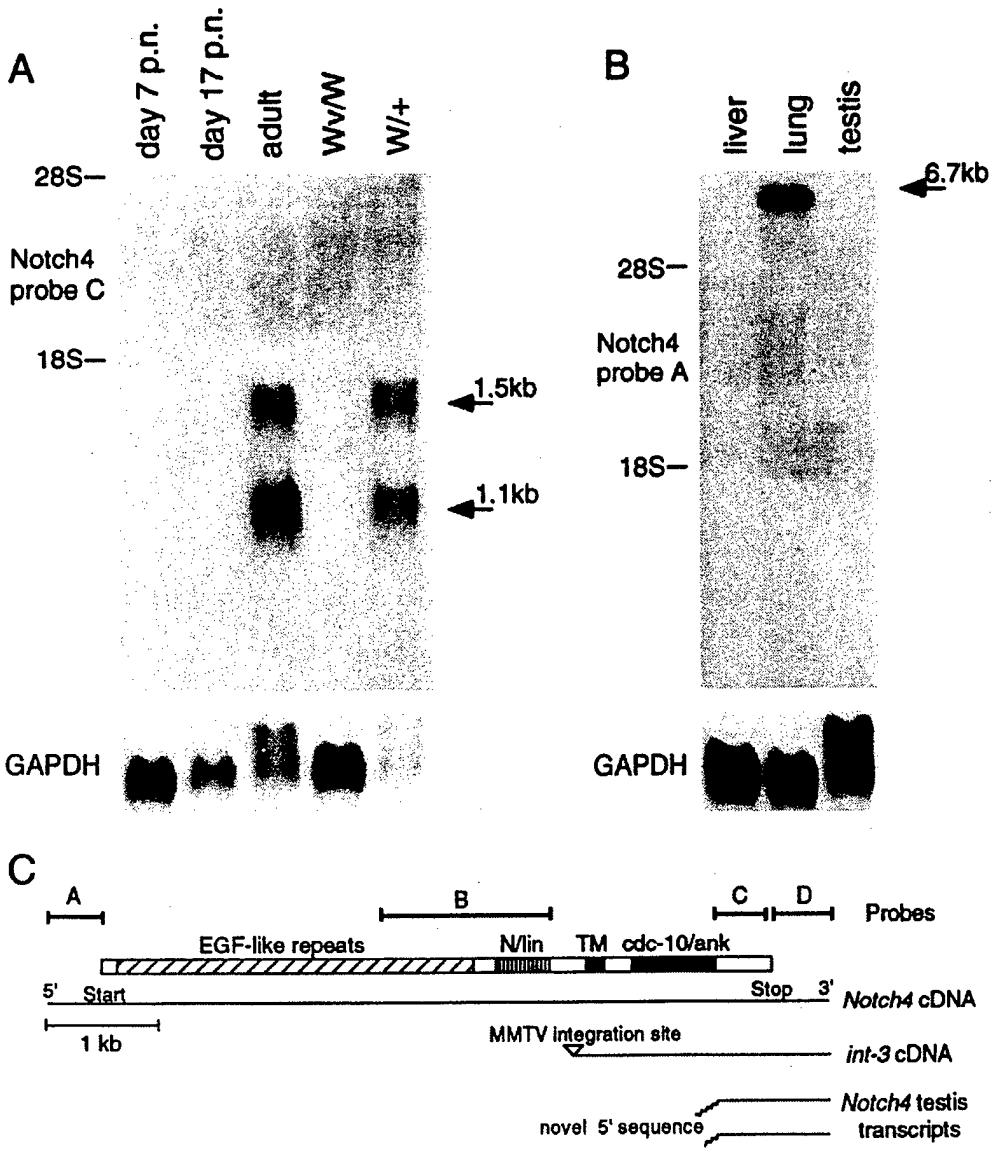

Chapter III.
Figure 3

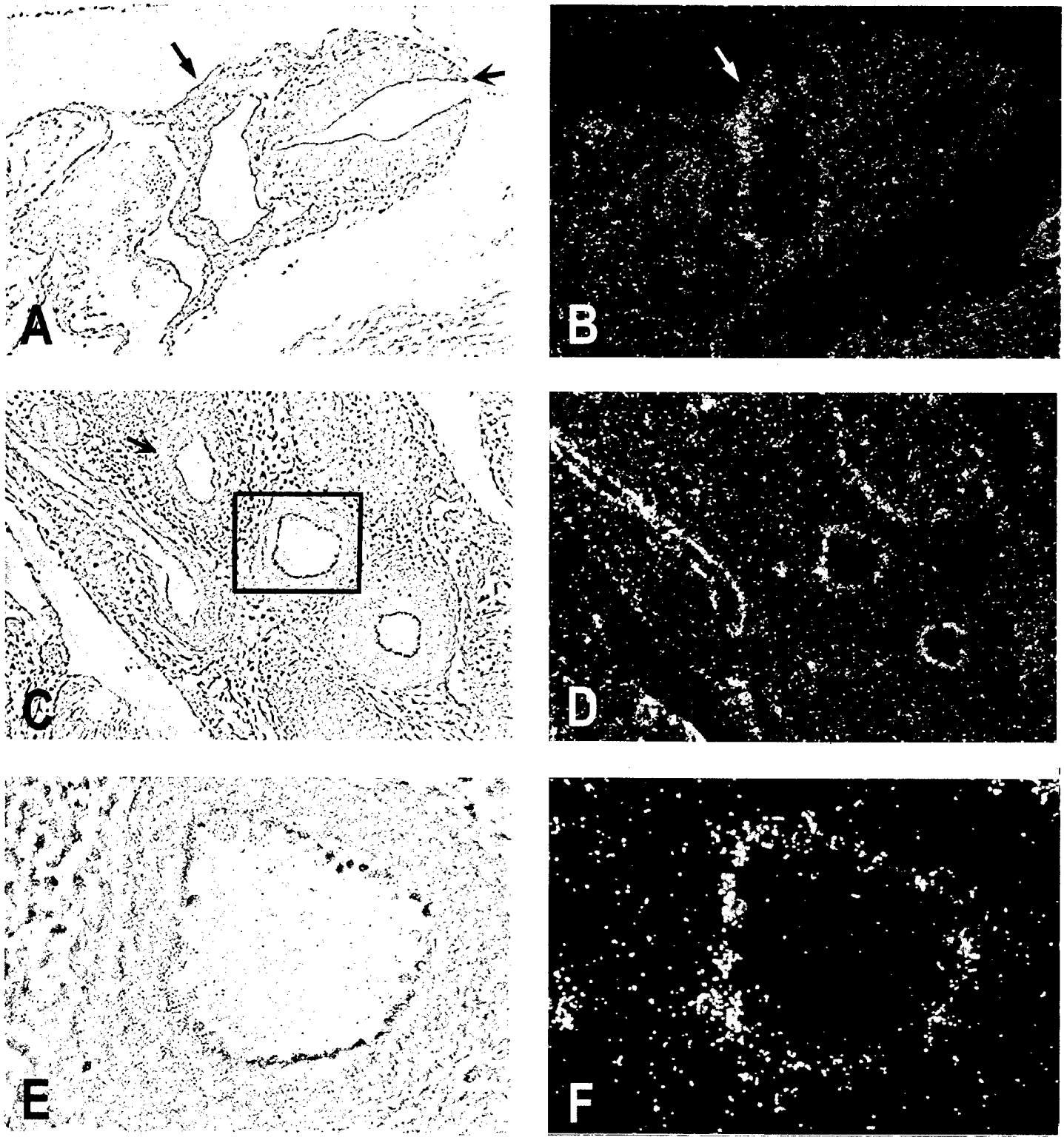

Chapter III.
Figure 4

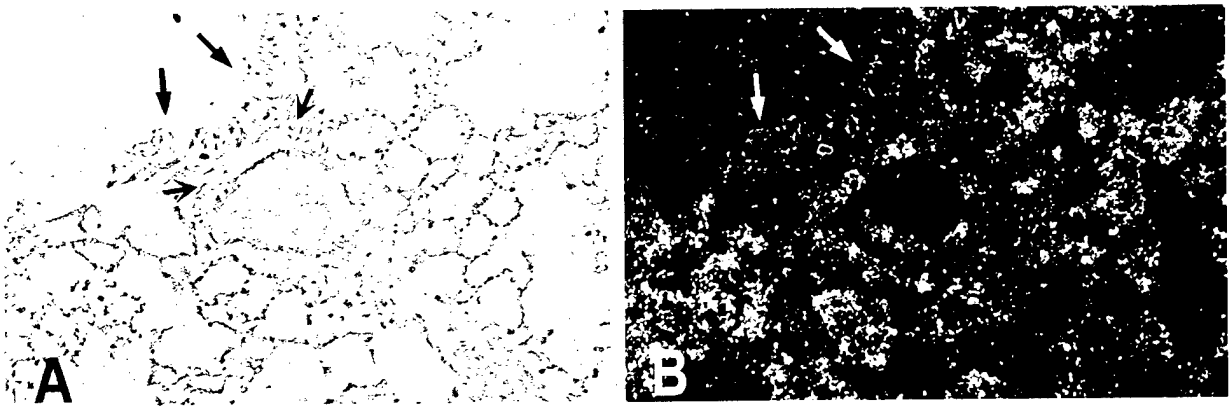

CHAPTER IV.
Notch and Wnt Regulation of Mammary Gland Morphogenesis

INTRODUCTION

The development of the murine mammary gland involves an intricate sequence of proliferative, morphogenetic and differentiative events, which gradually results in the formation of an arborized tree-like structure of epithelial ducts. Postnatal development of the mammary gland is influenced by gonadal hormones, with distinct developmental stages occurring during puberty, estrous, pregnancy and lactation. At birth, the mammary epithelial ducts have few side-branches. During puberty, the epithelial ducts rapidly elongate and branch, and give rise to a highly organized epithelial structure with terminal end buds and lateral buds. The terminal end buds are the major sites of proliferation, whereas the lateral buds differentiate into alveoli during each estrous cycle. During pregnancy, the alveoli rapidly increase in size and number resulting in the development of fully differentiated lobules, which will produce milk at lactation. The mammary gland remodels after lactation ceases, and this process is characterized by the involution of the secretory lobules and regression to the ductal tree observed at puberty.

Mesenchymal-epithelial and epithelial-epithelial interactions are essential in the regulation of growth and development of the murine mammary gland. Peptide growth factors, such as Epidermal growth factor (EGF) (45), Fibroblast growth factors (FGF) (46), Hepatocyte growth factor (HGF), Insulin-like growth factor II (IGF-II) (47), Neuregulin (NRG) (48), and Transforming growth factor–β (TGF–β) (49, 50), have been implicated as regulators of mammary gland development based on their expression patterns and, in some cases, on their abilities to affect the development of the mammary gland. HGF (or scatter factor) is expressed in the mammary mesenchyme during ductal branching, whereas its tyrosine kinase receptor c-met is expressed in the mammary epithelial ducts at all stages (51). HGF can promote branching morphogenesis of the mammary ductal tree (43, 48, 51, 52) in several experimental settings. TGF–β1 is expressed in the epithelial compartment of the mammary gland at all stages, except during lactation (49, 53). In vivo, TGF–β1 has been shown to inhibit ductal out-growth from the mammary end buds (50, 54). In vitro however, TGF–β1 has been shown to induce opposite effects depending on its concentration. TGF–β1 at high concentrations (0.5-5 ng/ml) inhibit ductal elongation and branching of TAC-2 mammary epithelial cells, whereas at low concentrations (5-100 pg/ml) it is able to stimulate these biological processes (55).

The Wnt family of secreted growth factors are also implicated as regulators of the developing mouse mammary gland (56). *Wnt* genes are expressed during ductal development of the gland (*Wnt*-2, *Wnt*-5a, *Wnt*-7 and *Wnt*-10b) and during lobular development at pregnancy (*Wnt*-4, *Wnt*-5b and *Wnt*-6), and the expression of most *Wnt* transcripts is down regulated during lactation (57, 58). This pattern of expression during periods of morphogenesis has led to a proposed role for *Wnt* genes in morphogenetic events during mammary gland development. *Wnt* gene expression has been documented in both the stromal and epithelial compartments of the mammary gland, raising the possibility of involvement in both stromal-epithelial and epithelial-epithelial interactions (58, 59). The *Wnt*-1 gene is not normally expressed within the mouse mammary gland, however its expression can contribute to tumorigenesis when activated by insertion of mouse mammary tumor virus (MMTV) proviral DNA in MMTV-induced mammary tumors (60). Mammary gland tumors develop in transgenic mice where ectopic *Wnt*-1 gene expression is controlled by the MMTV promoter; these mice display hyperplasia of the mammary epithelium and an increased incidence of tumors (61).

The *Notch4* gene was also identified as a frequent target for insertional activation by MMTV proviral DNA in MMTV-induced mammary gland tumors (2, 5). The *Notch4* gene encodes for a large transmembrane receptor protein (62, 63). The int-3 oncoprotein is activated by MMTV insertion and corresponds to a truncated form of Notch4 which has most of its extracellular domain deleted (62); this mutated version of Notch4 will be referred to as Notch4(int-3). In contrast to *Wnt*-1, expression of the *Notch4(int-3)* oncogene as a transgene in the mouse mammary gland results in impaired development of the mammary gland which no longer generates a tree-like structure of epithelial ducts. Instead, a hyperproliferative mass of undifferentiated epithelial cells is observed near the nipple, from which undifferentiated mammary carcinomas rapidly develop (4).

The aim of this study was to define the roles of both Wnt and Notch signaling in mammary gland ductal morphogenesis. Using a previously described model in which TAC-2 mammary epithelial cells grown in collagen gels form branching cords or tubules in response to HGF or TGF–β1 (43, 55), we demonstrate that activation of the Wnt and Notch signaling pathways has opposite effects on branching morphogenesis. Wnt-1 acts to induce branching morphogenesis whereas Notch4(int-3) inhibits branching morphogenesis by either HGF or TGF–β. Wnt-1 has the capacity to overcome the Notch4(int-3) mediated inhibition of branching morphogenesis.

The development of the murine mammary gland involves an intricate sequence of proliferative, morphogenetic and differentiative events, which gradually results in the formation of an arborized tree-like structure of epithelial ducts. Postnatal development of the mammary gland is influenced by gonadal hormones, with distinct developmental stages occurring during puberty, estrous, pregnancy and lactation. At birth, the mammary epithelial ducts have few side-branches. During puberty, the epithelial ducts rapidly elongate and branch, and give rise to a highly organized epithelial structure with terminal end buds and lateral buds. The terminal end buds are the major sites of proliferation, whereas the lateral buds differentiate into alveoli during each estrous cycle. During pregnancy, the alveoli rapidly increase in size and number resulting in the development of fully differentiated lobules, which will produce milk at lactation. The mammary gland remodels after lactation ceases, and this process is characterized by the involution of the secretory lobules and regression to the ductal tree observed at puberty, reviewed in (64-66).

Mesenchymal-epithelial and epithelial-epithelial interactions are essential in the regulation of growth and development of the murine mammary gland. Peptide growth factors, such as Epidermal growth factor (EGF) (45), Fibroblast growth factors (FGF) (46), Hepatocyte growth factor (HGF), Insulin-like growth factor II (IGF-II) (47), Neuregulin (NRG) (48), and Transforming growth factor–β (TGF–β) (49, 50), have been implicated as regulators of mammary gland development based on their expression patterns and, in some cases, on their abilities to affect the development of the mammary gland. HGF (or scatter factor) is expressed in the mammary mesenchyme during ductal branching, whereas its tyrosine kinase receptor c-met is expressed in the mammary epithelial ducts at all stages (51). HGF can promote branching morphogenesis of the mammary ductal tree (43, 48, 51, 52) in several experimental settings. TGF–β1 is expressed in the epithelial compartment of the mammary gland at all stages, except during lactation (49, 53). In vivo, TGF–β1 has been shown to inhibit ductal out-growth from the mammary end buds (50, 54). In vitro however, TGF–β1 has been shown to induce opposite effects depending on its concentration. TGF–β1 at high concentrations (0.5-5 ng/ml) inhibit ductal elongation and branching of TAC-2 mammary epithelial cells, whereas at low concentrations (5-100 pg/ml) it is able to stimulate these biological processes (55).

The Wnt family of secreted growth factors are also implicated as regulators of the developing mouse mammary gland (56). *Wnt* genes are expressed during ductal development of the gland (*Wnt*-2, *Wnt*-5a, *Wnt*-7 and *Wnt*-10b) and during lobular development at pregnancy (*Wnt*-4, *Wnt*-5b and *Wnt*-6), and the expression of most *Wnt* transcripts is down regulated during lactation (57, 58). This pattern of expression during periods of morphogenesis has led to a proposed role for *Wnt* genes in morphogenetic events during mammary gland development. *Wnt* gene expression has been documented in both the stromal and epithelial compartments of the mammary gland, raising the possibility of involvement in both stromal-epithelial and epithelial-epithelial interactions (58, 59). The *Wnt*-1 gene is not normally expressed within the mouse mammary gland, however its expression can contribute to tumorigenesis when activated by insertion of mouse mammary tumor virus (MMTV) proviral DNA in MMTV-induced mammary tumors (60). Mammary gland tumors develop in transgenic mice where ectopic *Wnt*-1 gene expression is controlled by the MMTV promoter; these mice display hyperplasia of the mammary epithelium and an increased incidence of tumors (61).

The *Notch4* gene was also identified as a frequent target for insertional activation by MMTV proviral DNA in MMTV-induced mammary gland tumors (2, 5). The *Notch4* gene encodes for a large transmembrane receptor protein (62, 63). The int-3 oncoprotein is activated by MMTV insertion and corresponds to a truncated form of Notch4 which has most of its extracellular domain deleted (62); this mutated version of Notch4 will be referred to as Notch4(int-3). In contrast to *Wnt*-1, expression of the *Notch4(int-3)* oncogene as a transgene in the mouse mammary gland results in impaired development of the mammary gland which no longer generates a tree-like structure of epithelial ducts. Instead, a hyperproliferative mass of undifferentiated epithelial cells is observed near the nipple, from which undifferentiated mammary carcinomas rapidly develop (4).

The aim of this study was to define the roles of both Wnt and Notch signaling in mammary gland ductal morphogenesis. Using a previously described model in which TAC-2 mammary epithelial cells grown in collagen gels form branching cords or tubules in response to HGF or TGF–β1 (43, 55), we demonstrate that activation of the Wnt and Notch signaling pathways has opposite effects on branching morphogenesis. Wnt-1 acts to induce branching morphogenesis whereas Notch4(int-3) inhibits branching morphogenesis by either HGF or TGF–β. Wnt-1 has the capacity to overcome the Notch4(int-3) mediated inhibition of branching morphogenesis.

RESULTS

When suspended in collagen gels, TAC-2 mammary epithelial cells form small slowly growing colonies with a morphology ranging from irregular shaped cell aggregates to poorly branched structures. Under these same conditions, TAC-2 cells grown in the presence of either HGF or TGF–β1 develop an extensive network of branching cords that consist of elongated epithelial cords or tubules with multiple branch points (43, 55). This TAC-2 cell phenotype is thus reminiscent of the branching morphogenesis of epithelial ducts in the mammary gland and provides an experimental model to study the roles of growth factors and receptors in the development of the mammary gland. To investigate the role of Wnt and Notch signaling in mammary epithelial cell growth and morphogenesis we ectopically expressed either the Wnt-1 or activated Notch4(int-3) oncoproteins and analyzed their effects on branching morphogenesis of TAC-2 cells. The results described below represent those found with several independently derived cell lines, including independent lines that were programmed to express proteins using a different promoter, as noted in the text.

Wnt-1 stimulates TAC-2 cell branching morphogenesis.

The biological activity of Wnt proteins was evaluated by generating TAC-2 cells ectopically expressing a *Wnt*-1 cDNA. TAC-2 cell lines programmed to express *Wnt*-1 (TAC-2 Wnt-1) were generated using the retroviral vector pLNCX to drive *Wnt*-1 expression from the CMV promoter . As a control, TAC-2 cells were generated that were programmed to express LacZ (TAC-2 LacZ). To evaluate the expression levels of Wnt-1 proteins in the cell lines generated, the *Wnt*-1 cDNA was fused at the carboxy terminus to the haemagglutinin-epitope (HA) tag, allowing us to detect Wnt-1 proteins in immunoblot analysis using the anti-HA monoclonal antibody (Fig. 1). Cell extracts from TAC-2 cell lines contained Wnt-1 proteins (Fig. 1) that migrated as a series of proteins with molecular weights between 41 and 45 kD, due to differential glycosylation. The ectopic expression of Wnt-1 proteins in TAC-2 Wnt-1 cells can be significantly increased by treating cells with sodium butyrate (2mM), which enhances transcription of the CMV promoter (Fig. 1). In order to evaluate the effects of different protein levels on branching morphogenesis of TAC-2 cells, experiments were done either in the presence or absence of sodium butyrate. We found that addition of sodium butyrate to the TAC-2 branching morphogenesis assay did not alter or enhance the TAC-2 cell phenotypes described below.

TAC-2 cells programmed to express LacZ give rise to small colonies with poorly branched cords when grown in collagen gels for four days (Fig. 2A). Addition of either HGF (20 ng/ml) or TGF–β2 (50 pg/ml) to the culture induces pronounced changes in colony morphology, resulting in the formation of long branching cords or tubules (Fig. 2B and 2C). We utilized TGF–β2 in our assays, which we found has an identical activity as TGF–β1 in the induction of branching morphogenesis of TAC-2 cells (55). When TAC-2 cells are programmed to express Wnt-1 proteins, cell colonies form cords with moderate branching even in the absence of exogenous growth factors (compare Fig. 2A and 2D). When TAC-2 Wnt-1 cells are grown in the presence of either HGF or TGF–β2 (Fig. 2E and 2F), a highly extensive branching network is observed. This network of epithelial tubules is significantly more extensive when compared to control TAC-2 LacZ cells grown under identical conditions. An identical phenotype was observed in TAC-2 cell lines programmed to express either a non-epitope tagged *Wnt*-1 cDNA or a HA epitope tagged *Wnt*-1 cDNA transcribed from a SV40 based retroviral vector (data not shown). Thus, Wnt-1 activity was confirmed in at least three independently produced TAC-2 cell lines.

The morphological analysis of TAC-2 cell cultures suggested that Wnt-1 cooperates with either HGF or TGF–β2 in the induction of branching morphogenesis. To characterize combined effects of Wnt-1 and HGF, quantitative evaluation of cord length and the number of branch points was conducted (Fig. 3A and 3B). Both analyses showed that the branched network formed by TAC-2

Wnt-1 cells grown under control conditions was comparable to that found for HGF-treated TAC-2 LacZ cultures. When TAC-2 Wnt-1 cells are grown in the presence of HGF, both cord length and number of branch points is significantly greater than the combined values for TAC-2 Wnt-1 cells without HGF and TAC-2 LacZ cells grown with HGF (Fig. 3A and 3B). Thus, Wnt-1 and HGF act in a cooperative fashion to induce branching morphogenesis of TAC-2 cells.

To determine whether the effects of Wnt-1 on TAC-2 cell branching morphogenesis are due to effects on the growth characteristics of TAC-2 cells we compared the growth of the TAC-2 cell lines generated. TAC-2 cells were plated at different densities on collagen coated dishes, either in the presence or absence of HGF, and viable cell numbers were determined either two or six days after plating. No significant differences in cell number were found between control TAC-2, TAC-2 LacZ, or TAC-2 Wnt-1 cell lines grown in either the presence or absence of HGF (data not shown). When grown under these conditions, TAC-2 Wnt-1 cells and control TAC-2 cells both displayed contact inhibition at confluence and had similar morphological characteristics. Hence, the effects of Wnt-1 on TAC-2 branching morphogenesis are not correlated with mitogenic activity of Wnt-1 and are dependent on growth in three dimensional collagen gels. Identical results were obtained with TAC-2 cell lines that were programmed to express Wnt-1 using a SV40 based retroviral vector.

To further characterize morphogenetic activities of Wnt-1 proteins, we analyzed TAC-2 cells induced to form cyst structures in collagen gel cultures. When TAC-2 LacZ cells are grown in collagen gels in the presence of hydrocortisone and cholera toxin, they form spheroidal cysts enclosing a widely patent lumen, as previously observed with non-transfected TAC-2 cells (43)(Fig. 4A, C, E). In contrast, under the same experimental conditions, TAC-2 Wnt-1 cells form branching structures (Fig. 4B, D, F). This clearly indicates that Wnt-1 expression modifies the spatial arrangement of TAC-2 cells and therefore has a morphogenetic effect.

Notch4(int-3) inhibits TAC-2 cell branching morphogenesis.

Notch4 activity in branching morphogenesis was evaluated by expressing an activated form of the Notch4 receptor, Notch4(int-3), in TAC-2 cells. TAC-2 cell lines programmed to express the Notch4(int-3) proteins were generated using the retroviral vector pLNCX and will be referred to as TAC-2 int-3. Notch4(int-3) was HA-epitope tagged at the carboxy terminus to allow detection of ectopically expressed proteins. Immunoblot analysis using anti-HA antibodies detected Notch4(int-3) proteins that migrate with an approximately molecular weight of 60 kD, corresponding well to their predicted molecular weight (Fig. 1).

When TAC-2 int-3 cells are grown in collagen gels and incubated in the presence of either HGF or TGF–β2 (Fig 2H and 2I), cell colonies no longer form elongated cords like control cultures (Fig 2B and 2C). Instead, HGF- or TGF–β2-treated TAC-2 int-3 cell colonies form small aggregates or structures with rudimentary branches which are similar in appearance to those formed by either TAC-2 LacZ or TAC-2 int-3 colonies grown in the absence of HGF or TGF–β2 (Fig 2A and 2G). An identical phenotype was observed in at least three independently produced cell lines, including TAC-2 cells programmed to express a non-epitope tagged *Notch4(int-3)* cDNA or a HA epitope tagged *Notch4(int-3)* cDNA transcribed from a SV40 based retroviral vector (data not shown). Interestingly, we found that a smaller percentage of TAC-2 int-3 cells give rise to colonies in collagen gels with respect to TAC-2 LacZ cells (230±32 colonies/cm2 in TAC-2 int-3 cells versus 795±114 colonies/cm2 in TAC-2 LacZ cells), which suggests that Notch4(int-3) expression reduces plating (colony formation) efficiency in collagen gels. Accordingly, to avoid overestimating the inhibition of HGF-induced cord elongation in TAC-2 int-3 cells, the quantitative analysis of cord length and branching was carried out on a per colony basis, rather than on a per field basis (see Materials and Methods). This analysis demonstrated that, despite the fact that colonies formed by TAC-2 int-3 cells are slightly more elongated and branched than those formed by TAC-2 LacZ cells, their morphogenetic response to HGF is markedly decreased (Fig. 3C and 3D).

We analyzed the growth characteristics of the TAC-2 int-3 cell line, as described for TAC-2 Wnt-1 cells. TAC-2 int-3 cells plated on collagen coated dishes, either in the presence or absence of HGF, displayed no significant differences in cell number, morphology, or growth post-confluence when compared with TAC-2 controls (data not shown). Identical results were obtained with TAC-2 cell lines programmed to express Notch4(int-3) using a SV40 based retroviral vector. Hence, the effects of Notch4(int-3) on TAC-2 branching morphogenesis are not correlated to changes in the growth properties in the cells.

The carboxy terminus of the Notch4(int-3) is not required for activity.

The Notch4(int-3) oncoprotein, has most of the extracellular domain of Notch4 deleted and consists of the transmembrane and intracellular domains. To investigate which region(s) of Notch4(int-3) proteins are required and sufficient for activity, a series of Notch4(int-3) deletion mutants were generated (schematized in Fig. 5A). Four Notch4(int-3) deletion mutants were made and designated ΔNT (deletion of the amino terminal domain), ΔCDC (deletion of cdc10 repeat domain), ΔCT (deletion of the carboxy terminal domain) and ΔNTΔCT (N-terminal and C-terminal deletion) (Fig. 5A). All four mutant int-3 cDNAs were HA-epitope tagged at their carboxy termini and TAC-2 cell lines programmed to express each deletion mutant were generated using the retroviral vector pLNCX. Immunoblot analysis using anti-HA monoclonal antibodies demonstrated expression of Notch4(int-3) deletion proteins of appropriate molecular weight in each respective cell line (Fig. 5B). The ΔNTΔCT Notch4(int-3) deletion protein with predicted molecular weight of 25 kD co-migrates with a non specific anti-HA antibody background band (Fig. 5B), however, was detected in a separate analysis of both untreated TAC-2 ΔNTΔCT cells or cells treated with sodium butyrate (Fig. 5C). TAC-2 cell lines expressing the four different Notch4(int-3) deletion mutants were grown in collagen gels as described above, and the ability of each Notch4(int-3) deletion mutant to inhibit HGF induced branching morphogenesis of TAC-2 cells was analyzed. As shown in Fig. 6, TAC-2 cells expressing either ΔNT (Fig. 6A and 6B), ΔCDC (Fig. 6C and 6D) or ΔNTΔCT (Fig. 6G and 6H) are responsive to HGF induced branching morphogenesis. In contrast, when grown in the presence of HGF, ΔCT expressing TAC-2 cells (Fig. 6E and 6F) display an identical phenotype as the TAC-2 int-3 cells. Hence, the carboxy terminus of the Notch4(int-3) is not required for Notch-mediated inhibition of TAC-2 branching morphogenesis. Thus, in this assay the activity of the Notch4(int-3) oncoprotein can be conferred by the amino terminus and cdc10 repeats.

Branching morphogenesis in cells co-expressing Wnt-1 and Notch4(int-3) oncoproteins.

The activation of the Wnt-1 and Notch signaling pathways resulted in opposite effects on HGF- or TGF–β2-induced branching morphogenesis of TAC-2 cells. To explore the interactions between these two signaling pathways, we investigated the effect of simultaneous expression of both Wnt-1 and Notch4(int-3) proteins on TAC-2 branching morphogenesis. The above described TAC-2 LacZ and TAC-2 int-3 cell lines, which were generated with the pLNCX expression vector, were now also programmed to express Wnt-1 using the retroviral vector pLHTCX. This vector drives gene expression from the CMV promoter and contains the hygromycin resistance gene. In this fashion, four additional TAC-2 cell lines were generated that were named TAC-2 LacZ/ctr, TAC-2 LacZ/Wnt-1, TAC-2 int-3/ctr and TAC-2 int-3/Wnt-1 (where ctr denotes control empty pLHTCX vector). To determine appropriate protein expression in each of these four cell lines, immunoblot analysis showed Notch4(int-3) and Wnt-1 proteins were expressed as expected and at levels similar to those previously found to confer activity (data not shown). Each of the four cell lines were grown in collagen gels to determine their ability to undergo HGF- or TGF–β2-induced branching morphogenesis (Fig. 7). This assay was repeated three times with similar results. Doubly infected control cells TAC-2 LacZ/ctr (Fig. 7A, B, C) remained responsive to both HGF and TGF–β demonstrating that two rounds of drug selection did not affect the phenotype of the TAC-2 cell lines. As observed previously for TAC-2 Wnt-1 cells, TAC-2 LacZ cells that are now programmed to express Wnt-1 (Fig. 7D, E, F) form small colonies that undergo modest branching even in the absence of HGF or TGF–β2; these cells form extensive elongated branches when grown in the presence of HGF or TGF–β2. The activity found for Notch4(int-3), that is the inhibition of HGF- and TGF–β-induced branching morphogenesis, was also found in the TAC-2 int-3/ctr cell line (Fig. 7G, H, I). Wnt-1 and Notch4(int-3) co-expressing cells, TAC-2 int-3/Wnt-1, are able to form colonies displaying branching and elongation and have an appearance similar to that of TAC-2/LacZ/Wnt-1 cells (Fig. 7J). An examination of several fields reveal that TAC-2 int-3/Wnt-1 cells displayed increased responses when treated with either HGF or TGF–β, thus these cells now regain responsiveness to these factors (Fig. 7K, L). Our results indicate that Notch activation attenuates responsiveness of TAC-2 cells to both HGF and TGF–β and that Wnt-1 can override the Notch activity in TAC-2 cells.

DISCUSSION

In this study, we have detailed a regulatory hierarchy involved in the branching morphogenesis of TAC-2 mammary epithelial cells. This regulation includes four distinct signaling pathways; the Wnt, Notch, HGF, and TGF–β signaling cascades. Using an in vitro model that reflects the branching morphogenesis exhibited during mammary gland development we have assessed the potential interactions between several different signaling pathways. This approach has allowed us to establish the relationships between these pathways. One remarkable feature of the regulation of branching morphogenesis we describe is its similarity to the regulatory pathways leading to morphogenetic events during Drosophila development.

Wnt proteins as branching morphogens in the mammary gland.

Formation of branching cords is induced in collagen gel cultures of TAC-2 cells by the addition of either HGF or low concentrations of TGF–β. Wnt-1 proteins induce moderate branching and elongation of TAC-2 cell tubules in the absence of added HGF or TGF–β2. The extent of Wnt-1 induced branching morphogenesis of TAC-2 cells is comparable to the induction by either HGF or TGF–β2. Our evidence suggests that Wnt-1 acts as a morphogen in this capacity. First, Wnt-1 induces a change in a morphogenetic event, the formation of branched epithelial tubules or cords. Second, Wnt-1 does not appear on its own to alter the growth properties of the TAC-2 cells. Finally, Wnt-1 can induce branching in an environment where cysts typically form; that is, in hydrocortisone and cholera toxin treated cultures. Such cultures form spheroidal cysts enclosing a widely patent lumen. In this environment, peptide growth factors that display mitogenic and not morphogenetic properties would increase the size of the cyst but the spheroidal structure would be maintained. In contrast, Wnt-1 alters the morphogenetic behavior in such a way that new branch points are formed and the structures take on a tubular morphology.

Several Wnt proteins are expressed in the mammary gland during periods of morphological changes of the ductal epithelium (*Wnt*-2, *Wnt*-5a, *Wnt*-7 and *Wnt*-10b) (57, 58). Ectopic expression of Wnt-1 *in vivo* suggests a role for Wnt proteins in cell proliferation during mammary gland development; however, morphogenetic changes also occur in response to Wnt-1. It is has been proposed that the Wnt-1 expression mimics the activity of endogenous mammary gland Wnt proteins. A transgenic line driving expression of *Wnt*-1 to the mammary gland displays a hyperplastic phenotype, indicative of increased proliferation (61). In addition, both virgin females and males display a marked increase in the number of terminal branches, and in fact resemble the hormonally stimulated glands normally observed in pregnant animals. Tissue reconstitution experiments in which *Wnt*-1 is ectopically expressed in mammary epithelium also result in a hyperplastic gland where duct epithelium show abundant fine side-branches, suggesting that Wnt-1 may instruct the epithelium to form branches (67). This phenotype is most likely not simply a consequence of proliferation as it is not seen with a variety of other oncogenic proteins which when ectopically expressed in the mammary gland induce hyperplasia without increasing branching (68).

The Wnt signal transduction pathway is mediated in part through b-catenin, a protein associated with cadherins, and which is necessary for the adhesive functions of adherens junctions (69). Wnt-1 signaling results in stabilization of the cytoplasmic pool of b-catenin (70, 71), which then can associate with downstream targets in the cytoplasm to transduce signals that lead to regulation of target gene expression (72, 73). TAC-2 cells programmed to express Wnt-1 in fact display increased levels of cytosolic b-catenin, when compared to TAC-2 LacZ cells (our unpublished data). This stabilization may be regulated by the phosphorylation of b-catenin on serine/threonine residues, possibly by glycogen synthase kinase 3 (GSK-3) (74). Recent evidence has demonstrated the importance of b-catenin/cadherin interactions in regulating cell adhesion, cell migration and epithelial phenotype in embryonic development (75). The activation of b-catenin by Wnt-1 induced signaling may result in changes of the adhesive and migratory characteristics of mammary epithelial cells and consequently affect ductal morphogenesis of TAC-2 cells.

Cooperative interactions between Wnt-1 and HGF or TGF–β.

In response to the combined effects of Wnt-1 and HGF, TAC-2 cells form a network of elongated and branching tubules that is far more extensive than the branching cords observed when TAC-2 cells are grown in the presence of Wnt-1 or HGF singularly. We propose that the combined

effect of HGF addition and Wnt-1 expression is not the result of the sum of their independent activities on branching morphogenesis, but that Wnt signaling synergizes with the HGF/c-met tyrosine kinase pathway. The possibility that Wnt proteins cooperate in vivo with the HGF/c-met pathway in the regulation of mammary morphogenesis is supported by the overlapping temporal patterns of *Wnt* genes and HGF/c-met expression (52, 57, 58).

One potential area where these two signaling pathways could converge might be through their effects on the catenin and cadherin proteins. The cooperation between Wnt-1 and HGF may be explained by their combined activation of b-catenin. b-catenin has been detected in a complex with the EGF receptor and can be phosphorylated in response to EGF and HGF (76, 77). In addition, the Ras pathway is essential for the biological activity induced by HGF/c-met (78) and b-catenin has been demonstrated to be a substrate for tyrosine kinases and to become tyrosine phosphorylated in cells expressing activated Src and Ras (79). Another catenin-like protein, p120, which was identified as a substrate of Src and several receptor tyrosine kinases, interacts with the cadherin–β-catenin complex and may participate in regulating the adhesive function of cadherins (80). EGF is also able to stimulate branching morphogenesis of TAC-2 cells, although not to the same extent as HGF, whereas NGF, bFGF, IGF-II and KGF can not (43). These activities correlate with the reported phosphorylation of b-catenin by the EGF and HGF signal transduction pathways (77). It is yet unclear how tyrosine phosphorylation of b-catenin might regulate its activity. Tyrosine phosphorylated b-catenin is found in a detergent soluble pool (76, 81), which may reflect specific phosphorylation of a free pool of b-catenin. Since both Wnt-1 and HGF signaling can converge on b-catenin, it is therefore possible that the observed cooperation between HGF and Wnt-1 is due to their combined action on b-catenin activity.

Wnt-1, HGF, and TGF–β could induce branching morphogenesis by regulating the adhesive and migratory properties of TAC-2 cells through modulation of extracellular matrix components and their interaction with their receptors. Since HGF has been demonstrated to decrease adhesion of TAC-2 cells to collagen and to enhance the deposition of type IV collagen it is also possible that the observed cooperation between HGF and Wnt-1 is due to their combined effect on cell-substrate adhesion. TGF–β signaling involves receptors with serine/threonine kinase activity which are known to regulate the synthesis and degradation of extracellular matrix molecules and to induce matrix organization. Induction of branching morphogenesis by TGF–β could be mediated by a remodeling of extracellular matrix components and cell-substrate interactions. The Wnt signal transduction pathway may also regulate cell-substrate interactions, and the combined activity of both Wnt-1 and TGF–β may explain their cooperative activities on the branching morphogenesis of TAC-2 cells.

In *Drosophila*, wingless (*wg*) and the TGF–β homologue *Decapentaplegic* (*Dpp*) have been shown in some cases to act in combination to regulate gene transcription during inductive events. In particular, Wg and Dpp have been shown to act in combination during limb development (82, 83) and to induce *Ultrabithorax* expression during endoderm induction (84). Wnt-1 and TGF–β signaling may similarly converge to affect gene transcription during branching morphogenesis in the mouse mammary gland.

Notch inhibits branching morphogenesis of mammary epithelial cells.

We demonstrate that Notch activation inhibits both the HGF and TGF–β induced branching morphogenesis of TAC-2 mammary epithelial cells. The precise mechanism of this inhibition is unclear. Activation of Notch signaling has been demonstrated to inhibit or alter the cell fate commitment or differentiation of a variety of different cell types (85, 86). For instance, *C. elegans* Lin-12 controls cell fate decisions during gonadogenesis, *Drosophila Notch* acts to control cell fate during neuroblast and photoreceptor cell differentiation, an activated *Xenopus Notch* can affect epidermal and neural crest cell development, and an activated mouse *Notch*1 can control cell fate during myogenesis and neurogenesis of cultured mouse cells (85, 86). Transgenic mice that use the MMTV viral promoter to express the Notch4(int-3) oncoprotein, the activated form of Notch4, display severely impaired mammary ductal growth (4). When *Notch4(int-3)* is expressed from the whey acidic protein promoter, whose expression is restricted to the secretory mammary epithelial cells, the differentiation of the secretory lobules of the transgenic animals is profoundly inhibited (87). These experiments demonstrate that *Notch4(int-3)*, like many other activated *Notch* genes, can act as a regulator of cell fate decisions in the mammary gland of mice. Little is known about the spatial and temporal pattern of *Notch* gene expression in the mammary gland, however, *Notch4* is expressed *in*

vivo in the murine mammary gland (3, 5). *Notch* genes may thus regulate the cell fate decisions occurring during mammary gland development that lead to the branched epithelial strutcture of the gland.

We have found that Notch activation can affect the response of TAC-2 mammary epithelial cells to either HGF or TGF–β. Since HGF acts through a tyrosine kinase receptor and TGF–β acts through serine/threonine kinase receptors, the affects of Notch activation may involve more than specific inhibition of a particular signaling cascade. Notch may regulate the competency of TAC-2 cells to respond to several different factors, possibly by shifting TAC-2 cells to a fate that is not predisposed to undergoe branching morphogenesis. This model would be consistent with the proposed activites of Notch proteins in several different organisms. Alternately, these signaling pathways may be controlled by Notch at a point at which they may converge to induce expression of genes important for branching morphogensis. Recently, the intracellular domain of LIN-12, a *C. elegans* Notch, has been demonstrated to associate with EMB-5, which encodes for a cytoplasmic protein containing a SH2 domain (88). This finding raises the possibility that the Notch signaling proteins may interact directly with those elicited by tyrosine kinase receptors, such as the HGF receptor (c-met).

We have demonstrated that the domain, carboxy terminal to the cdc10 repeats, of the Notch4(int-3) oncoprotein is not required for biological activity. However, the amino terminal domain and the cdc10 repeats are required for Notch4(int-3) activity. These findings are consistent with previous observed data for other *Notch* genes. The RAM23 domain which is localized between the transmembrane and cdc10 repeats has been demonstrated to be the binding site of CBF-1, a downstream and essential element in Notch signaling (89). Deletion of the amino terminal domain of Notch4(int-3), which contains the RAM23 domain, may eliminate binding to CBF-1, and hence destroy Notch4(int-3) activity. The region of the LIN-12 protein that includes the RAM-23 domain and cdc10 repeats appears to interact with another downstream and positive regulator, EMB5 (88). Point mutations and deletions within the cdc10 repeats result in loss of function of Notch proteins (90). Our data thus indicates that Notch4 may interact and be regulated through similar mechanisms.

Competing influences of Wnt and Notch signaling in branching morphogenesis.

When TAC-2 cells are programmed to express both Wnt-1 and Notch4(int-3), the cells are able to undergo branching morphogenesis. In Wnt-1 and Notch4(int-3) coexpressing TAC-2 cells, branching morphogenesis can be increased by either HGF or TGF–β; that is, the cells regain responsiveness to these factors. The phenotype observed in Wnt-1 and Notch4(int-3) coexpressing cells was similar to that of TAC-2 cells expressing only Wnt-1. The opposite biological activities of Wnt-1 and Notch4(int-3) observed in the TAC-2 cell assay correlate well with the mammary gland phenotype observed in Wnt-1 and Notch4(int-3) transgenic mice that ectopically express these proteins in the mammary gland (4). Although both oncogenes increase mammary tumor development, Wnt-1 stimulates a hyperplastic phenotype with increased ductal development whereas Notch4(int-3) inhibits ductal development.

Wnt-1 can override the Notch4(int-3)-mediated inhibition of branching morphogenesis providing the first evidence of interaction between these two signaling pathways in vertebrates. The dominance of Wnt-1 over activated Notch we have observed in murine cells parallels the functional relationship proposed for *Drosophila Wnt* (*wingless*) and *Notch* during *Drosophila* development (91). In this study, genetic analysis suggests a pathway convergence between wingless and Notch signaling resulting in opposing effects during patterning of the developing *Drosophila* wing. Activation of the wingless signal leads to regulation of Notch activity, possibly by *Drosophila* dishevelled, a cytoplasmic protein that is also a positive mediator in the Wnt-1 signal transduction pathway. Analysis using a yeast interaction trap system demonstrated that Dishevelled physically associates with the intracellular domain of Notch. The antagonism between Wnt-1 and Notch4(int-3) seen in branching morphogenesis may also be mediated by common regulators of the two signaling pathways such as Dishevelled.

During mammary gland development, the growth and differentiation of the gland is regulated by mesenchymal-epithelial and epithelial-epithelial interactions. Cells often receive different signals simultaneously and must integrate them in order to take on the correct proliferative, morphogenetic or differentiative response. Notch inhibition of ductal morphogenesis may be an early event in ductal morphogenesis. An attractive mechanism for overcoming Notch and allowing ductal morphogenesis to initiate or progress would be to activate the expression of a *Wnt* gene(s). Wnt could then serve the

dual function of suppressing Notch activity and initiating branching morphogenesis. Wnt signaling may then cooperate with other signaling pathways, such as those mediated by HGF and TGF–β, in order to complete branching morphogeneis. Our study thus has revealed complex interactions between the signal transduction pathways of Wnt, Notch, HGF and TGF–β, in regulating the branching morphogenesis of mammary epithelial cells.

MATERIALS AND METHODS

Reagents. Recombinant human HGF (rhHGF) was provided by Genentech, Inc. (San Francisco, CA). Recombinant TGF–β2 was provided by Dr. G. Gunderson (Columbia University, New York, NY). Rat tail collagen solution was obtained from Upstate Biotechnology Inc. (Lake Placid, NY). Anti-HA monoclonal antibody (12CA5) was from Berkeley Antibody Co. (Richmond, CA) and HRP-conjugated sheep anti-mouse immunoglobulin G from Amersham (Arlington Heights, IL).

cDNA clones. The murine *Notch4(int-3)* cDNA corresponds to a truncated *Notch4* cDNA; residues 4551 to 6244 of *Notch4* (Uyttendaele et al. 1996). An oligonucleotide encoding the haemagglutinin (HA) antigenic determinant was appended to the 3' end of the *Notch4(int-3)* and *Wnt*1 cDNA's. Eighteen codons were added that specify the amino acid sequence SMAYPYDVPDYASLGPGP, including the nine residue HA epitope (underlined). HA-tagged *Notch4(int-3)* and *Wnt*1 cDNAs were created by subcloning each cDNA into Bluescript KS (Stratagene) with the coding region of the HA epitope situated downstream of the newly inserted cDNA. These two sequences were made co-linear by "loop-out" mutagenesis using oligonucleotides designed to eliminate the stop codon and non-coding 3' sequence of the *Notch4(int-3)* and *Wnt*1 cDNAs. Oligonucleotides used in this procedure are as follows;
Notch4(int-3): CGG TTG TAA GAA ATC TGA ACT CCA TGG CCT ACC CAT ATG
Wnt-1: CGC GCG TTC TGC ACG AGT GTC TAT CCA TGG CCT ACC C .
The 5' end of each oligo is complementary to the C-terminus of *Notch4(int-3)* or *Wnt*1 cDNA and their 3' ends anneal to HA epitope-encoding sequence (underlined). Mutagenesis was done with the Muta-Gene*in vitro* mutagenesis kit (Bio Rad, Richmond, CA). The presence of each fusion was confirmed by DNA sequencing. *Notch4(int-3)* cDNA deletion mutants were generated from the epitope-tagged *Notch4(int-3)* construct by restriction enzyme cloning, and were named ΔNT, ΔCDC, ΔCT and ΔNTΔCT. The ΔNT deletion mutant corresponds to nucleotides 4921 to 6244 of the *Notch4* sequence. The ΔCDC deletion mutant corresponds to nucleotides 4551 to 4864 and to nucleotides 5706 to 6244 of the *Notch4* sequence. The ΔCT deletion mutant corresponds to nucleotides 4551 to 5718 of the *Notch4* sequence. The ΔNTΔCT deletion mutant corresponds to nucleotides 4921 to 5718 of the *Notch4* sequence.

Cell culture. The TAC-2 cell line was derived from NMuMG cells as described previously (43). TAC-2 cell were grown on collagen-coated dishes in Dulbecco's modified Eagle's medium (DMEM, GIBCO) supplemented with 10% fetal calf serum (FCS, GIBCO). The Bosc 23 retrovirus packaging cell line (Pear et al. 1993) was obtained from Dr. W. Pear (MIT, MA) and grown in DMEM containing 10% FCS. Both culture media were supplemented with penicillin (500 i.u./ml) and streptomycin (100ug/ml). Both cell lines were grown at 37°C in 8% CO_2.

Cell line generation. HA-tagged cDNAs were inserted into the retroviral vector pLNCX (42) wherein neomycin phosphotransferase (neo) expression is controlled by the murine leukemia virus LTR, and cDNA transcription is controlled by the cytomegalovirus (CMV) enhancer/promoter. The retroviral vector pLHTCX was derived from pLNCX, however the neo gene is replaced by a hygromycin-resistence gene. Populations of TAC-2 cells, expressing either HA-tagged *Notch4(int-3)* or *Wnt*1 cDNA, were prepared by retroviral infection. Recombinant retroviruses were generated by transiently transfecting constructs into the BOSC 23 cell line by calcium phosphate co-precipitation, as previously described (92). Retroviral infection of TAC-2 cells was done by culturing cells with viral supernatants collected from transfected BOSC 23 cells two day post-transfection. Infections were done in the presence of 4 μg/ml polybrene for 12 hours after which medium was replaced to DMEM + 10% FCS. One day post-infection the culture medium was replaced to DMEM + 10% FCS containing

500 µg/ml Geneticin (GIBCO BRL Life Technologies, Grand Island, NY) or 200 µg/ml hygromycin B (Sigma Chemical Co.). Colonies appeared 5 days later and were pooled into medium containing 250 µg/ml Geneticin or 200 µg/ml hygromycin B. These resultant populations, each comprised of at least 50 clones, were used in assays described below.

Collagen cell culture assays. TAC-2 cell lines were harvested using trypsin-EDTA, centrifuged, and embedded in three-dimensional collagen gels as previously described (43). Briefly, 8 volumes of rat tail collagen solution (approximately 1.5 mg/ml) were mixed with 1 volume of 10x minimal essential medium (GIBCO) and 1 volume of sodium bicarbonate (11.76 mg/ml) in a sterile tube kept on ice to prevent premature collagen gellation. TAC-2 cells were resuspended in the cold mixture at cell densities of 2 or 4 x 10^4 cells/ml and 0.5 ml aliquots were dispensed into 16-mm wells of 24 multiwell plates (Becton Dickinson Labware). After the collagen mixture had gelled, 1ml of complete medium (DMEM + 10% FCS) with or without HGF or TGF-β2 was added to each well. TAC-2 collagen gel cultures were initially done in the presence and absence of 2mM sodium butyrate, but since no difference in phenotypes was observed, the sodium butyrate was omitted in all experiments. Media were changed every 2 days, and after 3 to 5 days, cell cultures were photographed with a Nikon ELWD 0.3 phase contrast microscope on Kodak T-Max film (100 X magnification).

Quantification of cord lenth and branching. TAC-2 cells were suspended at $5x10^3$ or $1x10^4$ cells/ml incollagen gels (500 µl) cast into 16-mm wells of 4-well plates (Nunc, Kampstrup, Rosklide, Denmark) and incubated in 500 µl complete medium in the presence or the absence of 10ng/ml HGF. After 7 days, the cultures were fixed with 2.5% glutaraldehyde in 0.1M cacodylate buffer, and at least 3 randomly selected fields (measuring 2.2 mm x 3.4 mm) per experimental condition in each of 3 separate experiments were photographed with a Nikon Diaphot TMD inverted photomicroscope. The total length of the cords present in each individual colony was measured with a Qmet 500 image analyzer (Leyca Cambridge Ltd., Cambridge, UK). Cord length was considered as "0" in: a) colonies with a spheroidal shape, and b) slightly elongated structures in which the length to diameter ratio was less than 2. Quantification of branching was performed by counting all branch points in each colony. Values of cord length and branching obtained from the largest colonies are an underestimate, since in these colonies a considerable proportion of cords were out of focus and therefore could not be measured. Values were expressed either as mean cord length and number of branch points per photographic field (55) or as mean cord length and number of branch points per individual colony (43). The mean values for each experimental condition were compared to controls using the Student's unpaired T-test.

Immunoblot analysis. HA-tagged Notch4(int-3), Notch4(int-3) deletion mutants and Wnt-1 proteins from lysates of TAC-2 cell populations were analyzed by immunoblotting. To maximize protein expression, TAC-2 cells were treated with 2mM sodium butyrate for 16 hours prior to lysis. Cells were washed twice with cold PBS and then removed from dishes in 1.5 ml PBS using a rubber policeman. Cells were pelleted by centrifugation at 2,000x g at 4°C for 5 min. and lysed in 90 µl TENT buffer (20 mM Tris, pH 8.0, 2 mM EDTA, 150 mM NaCl, 1% Triton-X100) containing 1 mM phenylmethylsulfonyl fluoride, 10 mg/ml aprotinin, 2 mg/ml leupeptin, 1 mg/ml pepstatin, at 4°C for 30 min. Lysates were clarified by centrifugation at 10,000xg at 4°C for 10 min., and protein contents were determined using the BioRad Protein determination kit. Lysates containing 40 µg protein were electrophoresed in 10% SDS-polyacrylamide gels. Proteins were transferred from gels onto nitrocellulose by electroblotting, and then blocked overnight at 4°C in TBST (10 mM Tris, pH 8.0, 150 mM NaCl, 0.2% Tween-20) containing 1% bovine serum albumin (fraction V). Blots were then incubated in anti-HA monoclonal antibody (12CA5) diluted 1:100 in TBST at room temperature. After four hours, the blot was washed three times for 5 min. each in TBST. Blots were exposed to a 1:16,000 dilution of HRP-conjugated sheep anti-mouse IgG. Blots were washed as above and then incubated 1-2 min. in enhanced chemiluminescence reagents (Amersham Inc, IL) and exposed to X-ray film (Fujifilm, Fuji Photo Film Co., LTD., Tokyo).

FIGURE LEGENDS FOR CHAPTER IV.

Figure 1.
Immunoblot analysis on TAC-2 cell lysates using anti-HA antibodies. TAC-2 cells programmed to express either LacZ, Wnt-1 or int-3 were grown in the presence or absence of sodium butyrate. Wnt-1 and int-3 proteins of appropriate molecular weight can be detected in the respective TAC-2 cell lines, and the level of protein expression can be increased by sodium butyrate treatment.

Figure 2.
TAC-2 cell ductal morphogenesis assay. TAC-2 cells programmed to express LacZ (A,B,C), Wnt-1HA (D,E,F), or int-3HA (G,H,I) were grown in collagen gels either in the absence of exogenous growth factor (A,D,G), in the presence of HGF (B,E,H), or TGF–β2 (C,F,I). HGF and TGF–β2 induce branching morphogenesis of TAC-2 LacZ cells (compare A to B or C). Wnt-1 expression in TAC-2 cells induces modest branching morphogenesis of TAC-2 cells in the absence of either HGF or TGF–β2 (compare D to A), and robust branching is observed when TAC-2 Wnt-1 cells are grown in the presence of either HGF or TGF–β2 (compare E to B, and to C). TAC-2 cells programmed to express int-3 fail to undergo branching morphogenesis when grown in the presence of either HGF or TGF–β2 (compare G to H or I, H to B, and I to C).

Figure 3.
Wnt-1 and HGF have cooperative effects on branching morphogenesis of TAC-2 cells, while expression of int-3 inhibits HGF-induced branching morphogenesis. TAC-2 LacZ, TAC-2 Wnt-1 and TAC-2 int-3 cells were suspended in collagen gels at $5x10^3$ cells/ml (A and B) or $1x10^4$ cells/ml (C and D) and incubated with either control medium or 10ng/ml HGF for 7 days. In each of 3 separate experiments, at least three randomly selected fields per condition were photographed. The total additive length of all cords in each field (A), the number of cord branch points per field (B), the total additive length of all cords in each individual colony (C), and the number of cord branch points per colony (D) was determined as described in Materials and Methods. Values are mean ± s.e.m.; n=3. Values for HGF are significantly ($P<0.001$) different when compared to controls (except for TAC-2 int-3 cells) and values are significantly different ($P<0.001$) when TAC-2 LacZ and TAC-2 Wnt-1 cell lines are compared. Similar results were obtained by evaluating cord length and branching per individual TAC-2 LacZ andTAC-2 Wnt-1 colony (data not shown).

Figure 4.
Differential behavior of TAC-2 LacZ cells and TAC-2 Wnt-1 cells in hydrocortisone-supplemented cultures. Cells were suspended in collagen gels at $5x10^3$ cells/ml and incubated for 10 days with 1 μg/ml hydrocortisone and 50 ng/ml cholera toxin. Under these conditions, TAC-2 LacZ cells form thick-walled spheroidal cysts enclosing a widely patent lumen (A,C,E), as previously shown for untransfected cells. In marked contrast, TAC-2 Wnt-1 cells form branched structures consisting of either short tubules (B), cords containing small mutifocal lumina (D) or apparently solid cords (F). The three-dimensional structures illustrated in A,C,E and B,D,F are representative of the vast majority of colonies formed by TAC-2 LacZ and TAC-2 Wnt-1 cells, respectively. Magnification = 180x.

Figure 5.
Schematic representation of int-3 deletion mutants (A) and immunoblot analysis on TAC-2 cell lysates using anti-HA antibodies (B, C). TAC-2 cells programmed to express either DNT, DCDC, DCT, and DNTΔCT were grown in the presence or absence of sodium butyrate. The int-3 deletion proteins are epitope tagged and deletion proteins of appropriate molecular weight can be detected in the respective TAC-2 cell lines, and the level of protein expression can be increased by sodium butyrate treatment. Panel C, immunoblot analysis on lysates of TAC-2 LacZ and TAC-2 DNTΔCT cells, as in panel B, demonstrating the presence of the DNTΔCT deletion protein.

Figure 6.
TAC-2 cell ductal morphogenesis assay with int-3 mutants. TAC-2 cells programmed to express ΔNT (A,B), ΔCDC (C,D), ΔCT (E,F), and ΔNTΔCT (G,H) were grown in collagen gels either in the absence of exogenous growth factor (A,C,E,G), or in the presence of HGF (B,D,F,H). HGF induces branching

morphogenesis of TAC-2 ΔNT cells (B), TAC-2 ΔCDC cells (D) and TAC-2 ΔNTΔCT cells (H) TAC-2 ΔCT cells fail to undergo branching morphogenesis when grown in the presence of either HGF (F).

Figure 7.
TAC-2 cell ductal morphogenesis assay. TAC-2 cells programmed to express LacZ/ctr (A,B,C), LacZ/Wnt-1 (D,E,F), int-3/ctr (G,H,I), or int-3/Wnt-1 (J,K,L) were grown in collagen gels either in the absence of exogenous growth factor (A,D,G,J), in the presence of HGF (20 ng/ml)(B,E,H,K), or in the presence of TGF–β2 (50 pg/ml)(C,F,I,L). HGF and TGF–β2 induce branching morphogenesis of TAC-2 LacZ/ctr cells (compare A to B or C). Wnt-1 expression in TAC-2 cells induces modest branching morphogenesis of TAC-2 LacZ/Wnt-1 cells in the absence of either HGF or TGF–β2 (D), and robust branching is observed when TAC-2 LacZ/Wnt-1 cells are grown in the presence of either HGF (E) or TGF–β2 (F). TAC-2 cells programmed to express int-3/ctr fail to undergo branching morphogenesis when grown in the presence of either HGF (H) or TGF–β2 (I). TAC-2 cells programmed to express both int-3 and Wnt-1 undergo branching morphogenesis in the absence of exogenous growth factor (J), and form a robust branching network when grown in the presence of HGF (K) or TGF–β2 (L) in a similar manner when compared to TAC-2 cells programmed to express Wnt-1 solely (D,E,F).

Chapter IV

Figure 1

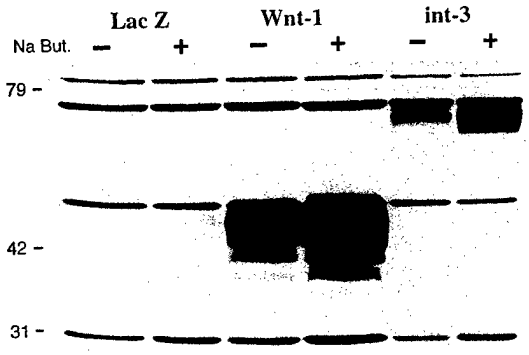

8863f1.lay

Chapter IV

Figure 2

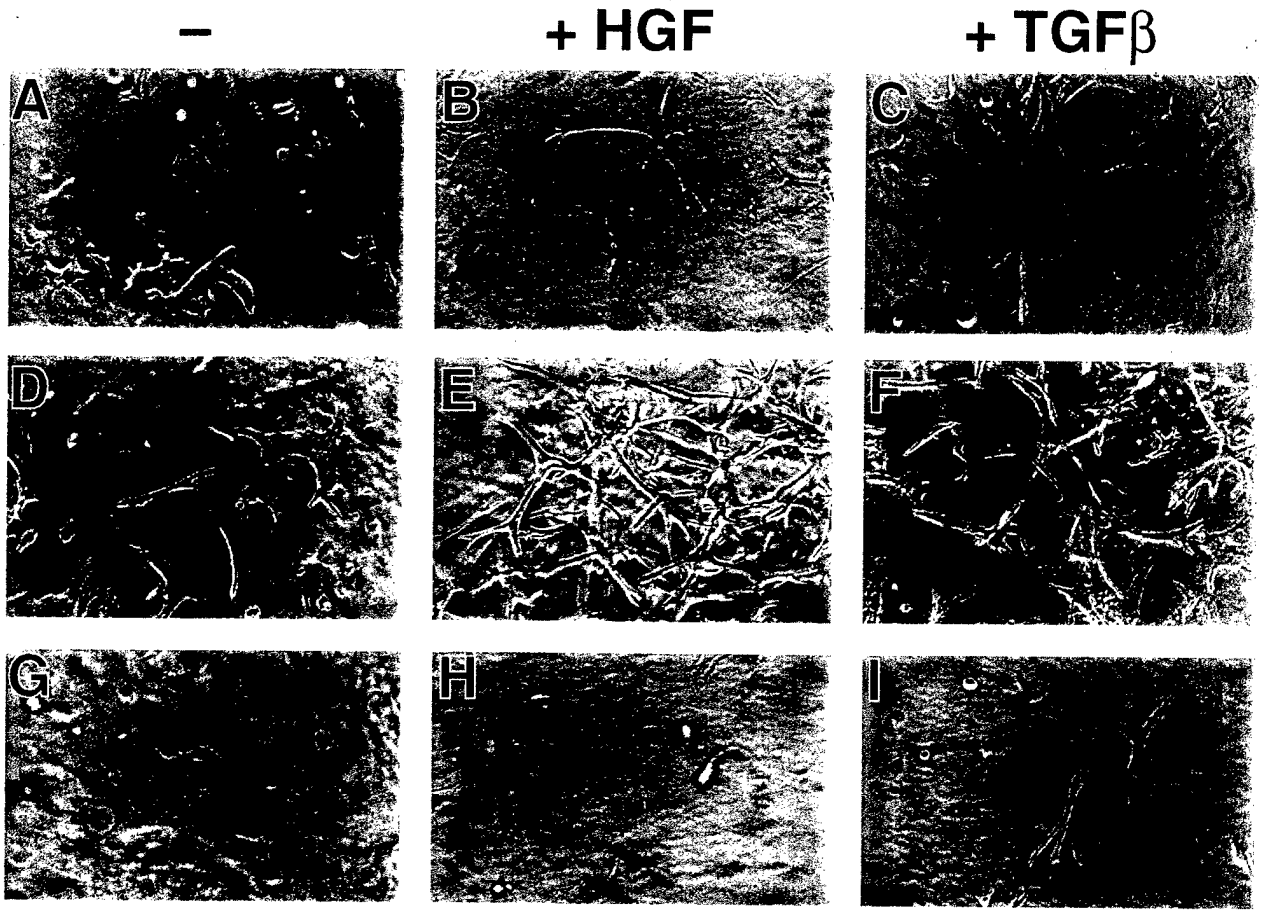

8863f2.lay

Chapter IV

Figure 3

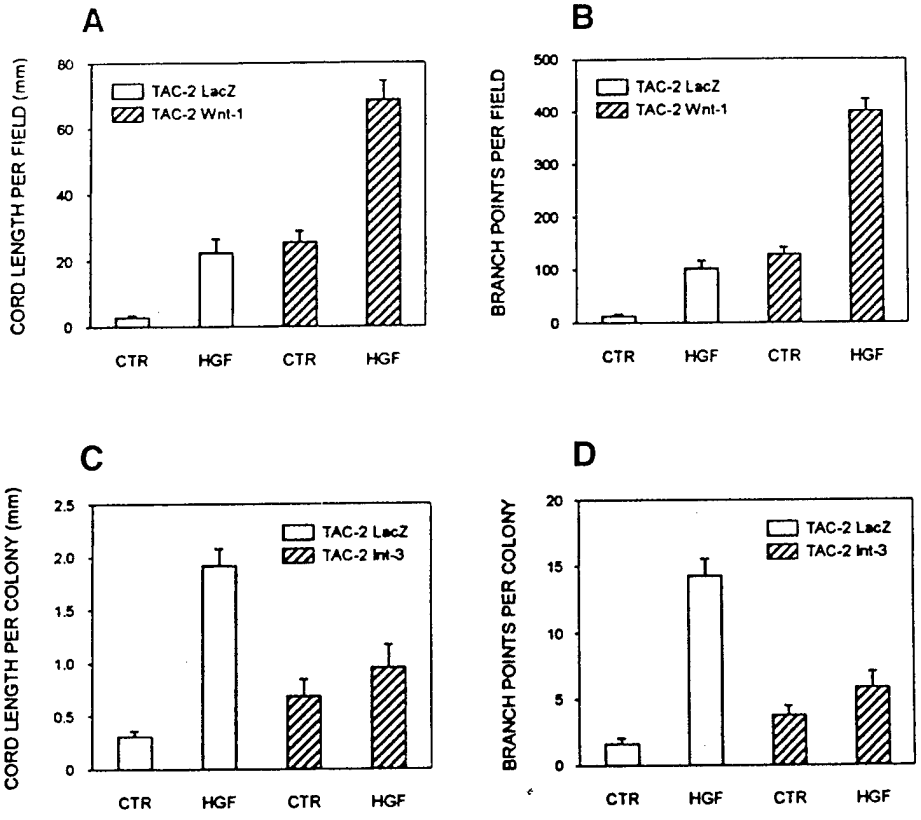

Chapter IV

Figure 4

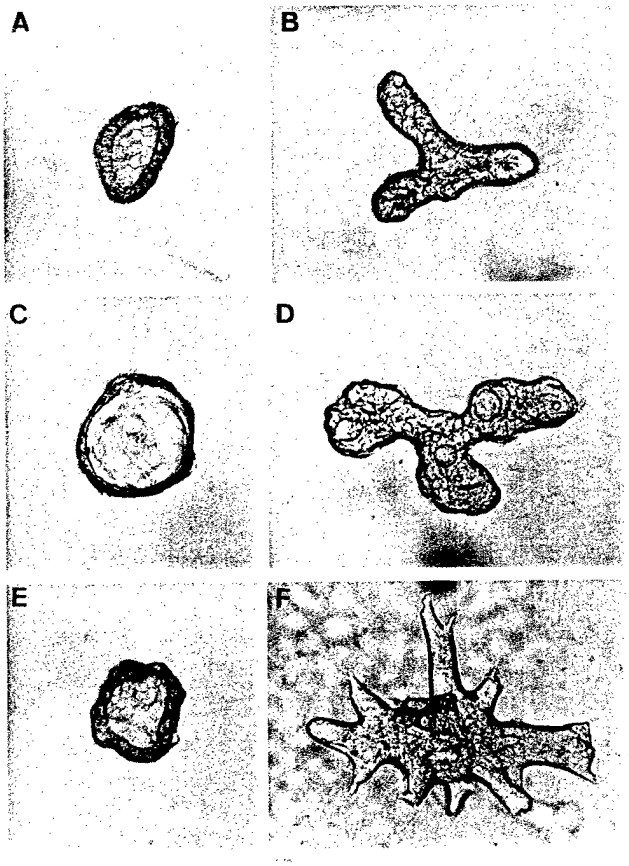

8863f4.lay

Chapter IV

Figure 5

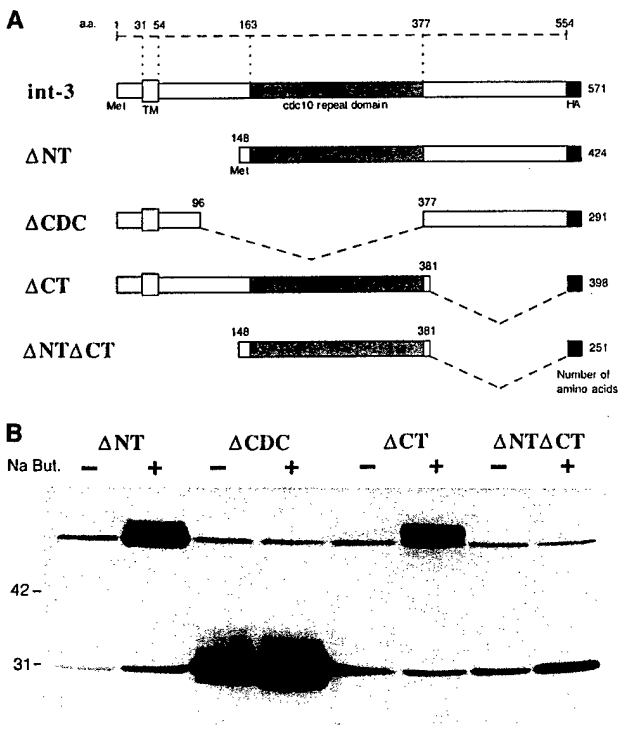

8863f5ab.lay

Chapter IV

Figure 6

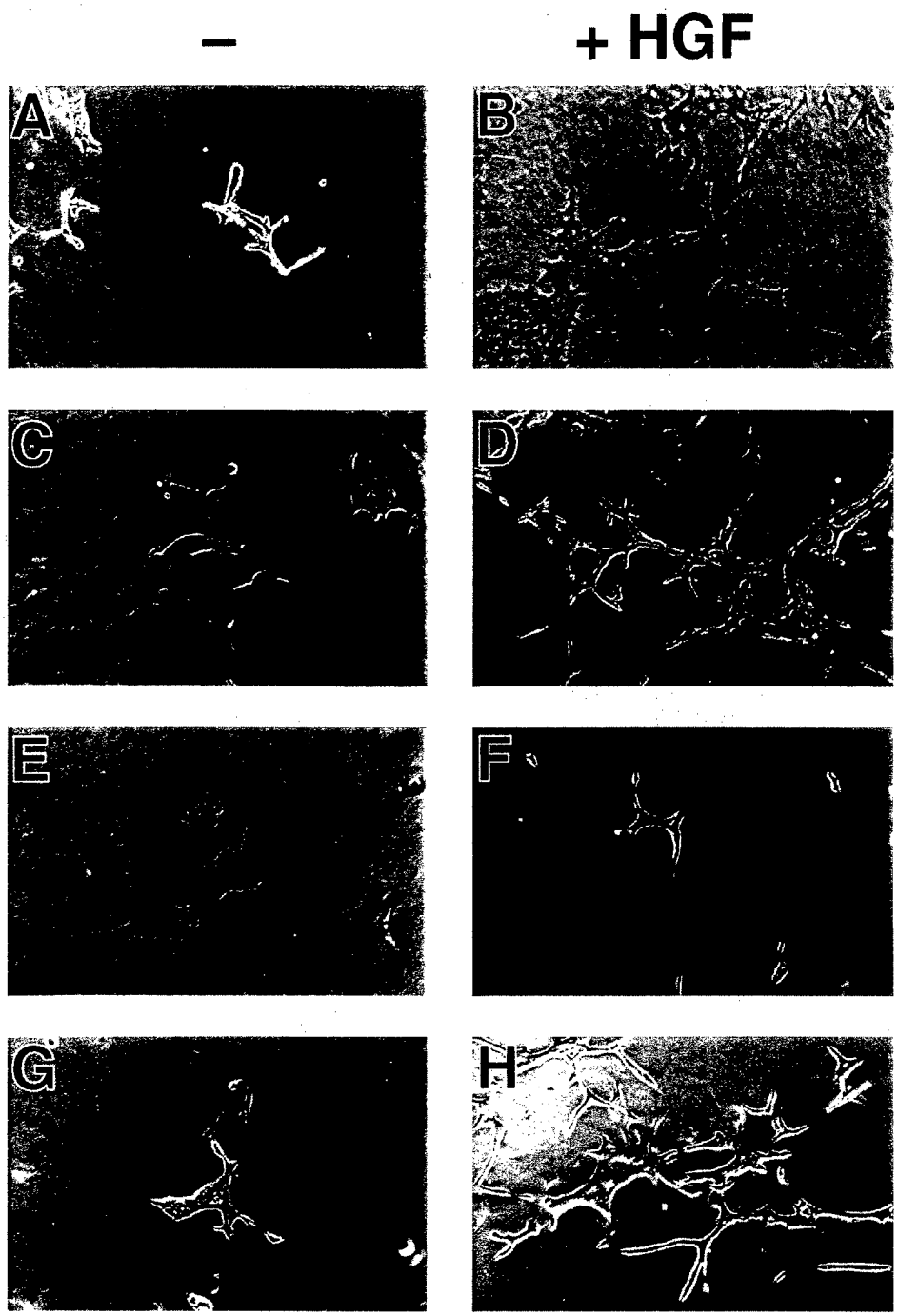

8863f6.lay

Chapter IV

Figure 7

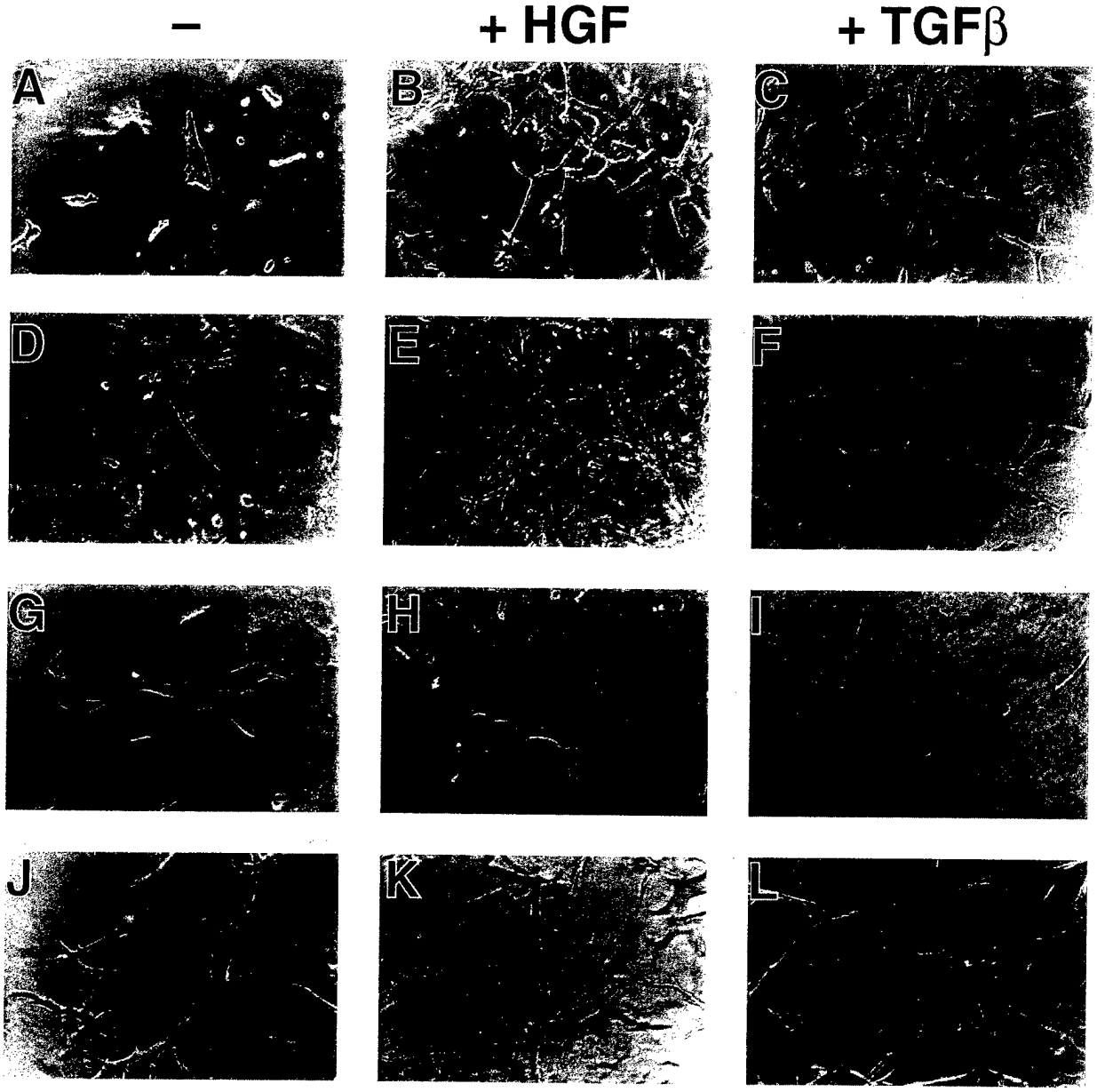

8863f7.lay

CHAPTER V.

SEL-10, a member of the CDC4 family, binds and regulates Notch/lin-12 proteins.

INTRODUCTION

Many cell-cell interactions that specify cell fate are mediated by receptors of the LIN-12/Notch family and ligands of the Delta/Serrate/LAG-2 (DSL) family (reviewed in (86). *C. elegans* affords an opportunity to study a simple case of lateral specification involving an interaction between two cells of the hermaphrodite gonad. These cells, named Z1.ppp and Z4.aaa, are initially equivalent in their developmental potential: each has an equal chance of becoming the anchor cell (AC), a terminally differentiated cell type that is necessary for vulval development, or a ventral uterine precursor cell (VU), which contributes descendants to the ventral uterus. However, in any given hermaphrodite, only one of these cells will become the AC, while the other becomes a VU (93).

Laser ablation studies have shown that this process of lateral specification, the AC/VU decision, depends on interactions between Z1.ppp and Z4.aaa (94, 95). Furthermore, genetic studies have indicated that *lin-12*-mediated signalling controls the AC/VU decision: if *lin-12* activity is inappropriately elevated, Z1.ppp and Z4.aaa become VUs, while if *lin-12* activity is reduced, Z1.ppp and Z4.aaa become ACs (96). Genetic mosaic analysis (95) and reporter gene studies (97) have indicated that both Z1.ppp and Z4.aaa initially express *lin-12* and *lag-2*, but that a stochastic small variation in ligand and/or receptor activity is subsequently amplified by a feedback mechanism that influences *lin-12*and *lag-2* transcription. Thus, Z1.ppp and Z4.aaa assess their relative levels of *lin-12* activity as part of the decision-making process, before either cell commits to the AC or VU fates, and the feedback mechanism ensures that only one of the two cells will become an AC and the other will become a VU.

Many components in the Notch/lin-12 pathway are highly conserved in animals as distantly related as *C. elegans*, Drosophila, and vertebrates. The identification of genes that influence *lin-12* activity during the AC/VU decision may reveal other conserved factors that participate in signal transduction or regulate the activity of *Notch/lin-12* proteins. sel-10 was identified as a negative regulator of lin-12 activity in a screen for suppressors of phenotypes associated with partial loss of *lin-12* activity (98). Sequence analysis revealed that SEL-10 is a member of the CDC4 family of F-box/WD40 repeat containing proteins. CDC4, the most extensively studied member of this family, is a Saccharomyces cerevisiae protein that is involved in the ubiquitin-mediated degradation of cell cycle regulators such as SIC1 (reviewed in (99). CDC4 binds to SIC1, thereby targeting the ubiquitination machinery to this substrate (R. Deshaies, personal communication). CDC4 family proteins exit in many other species. Slimb, a CDC4 homologue in Drosophila has been shown to target armadillo for degradation by the ubiquitination pathway (100). Based on the results of these studies, we tested SEL-10 for its ability to interact with LIN-12 and int-3.

RESULTS

SEL-10 encodes a protein of the CDC4 family

The *sel-10* gene, used in the studies described here, was cloned in the laboratory of Dr. Iva Greenwald. Sequence information has been submitted to Genbank (accession number AF020788). A BLAST search (101) using the predicted SEL-10 protein sequence revealed that it contains two previously identified amino acid sequence motifs (Fig. 1A-C). First, there is a motif (102) that is now called the F-Box, after its occurrence in cyclin F (103). The F-Box motif has been implicated in protein-protein interactions, and is found in a large variety of proteins, many of which contain other recognizable motifs C-terminal to the F-Box (103). Second, there are seven tandem WD40 repeats, also known as ßtransducin repeats, a conserved repeat of approximately 40 amino acids named for the common appearance of Trp-Asp (WD) at the end of the repeat (reviewed in (104). There is a great deal of functional diversity among WD40 repeat-containing proteins.

The presence of an F-box N-terminal to a set of seven WD40 motifs is the hallmark of the CDC4 family of WD40 repeat-containing proteins, indicating that SEL-10 belongs to this family. Furthermore, separate BLAST searches with just the SEL-10 F box or the SEL-10 WD40 repeats identified members of the CDC4 family as the most similar. The F-Box motif present in proteins within the CDC4 subfamily is more conserved than among other F-Box-containing proteins (Figure 3B), and there is more extensive homology around the F-box (102). In addition, the alignment of the WD40 repeats of SEL-10 and CDC4 (Fig. 3C) reveals that a given WD40 repeat is more similar between yeast and worms than are the repeats within a given species.

A recent database search has revealed potential human and rat SEL-10 orthologs (Fig. 1 D). The limited sequence information available to date for the human gene begins in the sixth WD40 repeat and extends to the C terminus, and in this region, there is 60% sequence identity. BLAST searches of the available databases using the SEL-10 sequence C-terminal to the WD40 repeats has not identified any other highly conserved sequences.

C. elegans SEL-10 physically interacts with LIN-12(intra) and murine Notch4(int3)

We probed for potential interactions between SEL-10 and the intracellular domains of LIN-12/Notch proteins, specifically LIN-12(intra), the intact intracellular domain (see (21) and Notch4(int3), the intact intracellular domain with some additional sequences produced by the *int3* mutation (2, 62). We initially used the yeast two-hybrid system (105) and our preliminary results suggested that SEL-10 physically interacted with the *C. elegans* LIN-12 intracellular domain, the *C. elegans* GLP-1 intracellular domain (GLP-1 is another *C. elegans* LIN-12/Notch protein; see (9), and the mouse Notch4(int3) intracellular domain (data not shown).

To examine further whether SEL-10 binds LIN-12/Notch proteins, we carried out co-immunoprecipitation experiments using transfected mammalian cells (Fig. 2). 293T (Bosc23) cells (human embryonic kidney cells) were transiently transfected with hemagglutinin (HA)-tagged LIN-12(intra) and/or myc-tagged SEL-10 (see Materials and Methods). Transfected cells were lysed and LIN-12(intra)HA was precipitated with anti-HA antibodies (Fig. 2A) or, alternatively, SEL-10myc was immunoprecipitated with anti-myc antibodies (Fig. 2B). The immunoprecipitates were subjected to immunoblot analysis to identify bound proteins, and probed with anti-myc or anti-HA antibodies as indicated. Under both conditions, the immunoprecipitates were found to contain both LIN-12HA and SEL-10myc. This result suggests that SEL-10 and LIN-12 are able to interact physically, either directly or in a complex.

We also examined whether the *C. elegans* SEL-10 protein would interact with the murine Notch4(int-3) protein. Cells were transfected with Notch4(int-3) and/or SEL-10HA, and immunoprecipitation was performed with cell lysates using either anti-Notch4 antibodies (Fig 2C) or anti-HA antibodies (Fig. 2D). Immunoblot analysis demonstrated that the immunoprecipitates contained a complex of Notch4(int-3) and SEL-10 proteins; thus, SEL-10 is able to complex with Notch4(int-3) protein.

The observations that *sel-10* negatively regulates *lin-12* activity, that SEL-10 resembles CDC4, and that SEL-10 physically interacts with LIN-12 taken together strongly suggest that SEL-10 functions biochemically like CDC4 to promote LIN-12 turnover. We have attempted to examine the effect of co-expressing *C. elegans* SEL-10 on the steady state levels and ubiquitination of Notch4(int-3) and observed a modest decrease in the steady state level (data not shown); however, at this time the mechanism underlying this decrease is not clear. Furthermore, there appears to be polyubiquitination of Notch4(int-3) even in the absence of transfected SEL-10, perhaps due to the activity of an endogenous mammalian *sel-10*-like gene.

DISCUSSION

We propose that the mechanism by which *sel-10* affects *lin-12* activity may be by controlling Notch/LIN-12 protein levels. Sequence analysis indicates that SEL-10 is related to the Saccharomyces cerevisiae protein CDC4, which promotes the ubiquitin-dependent degradation of cell cycle regulators (reviewed in (99). CDC4 complexes with its substrates (R. Deshaies, personal communication), and we have found that *C. elegans* SEL-10 complexes with the intracellular domain of LIN-12. Proteins related to SEL-10 exist in mammals, and *C. elegans* SEL-10 physically complexes with Notch4(int3),

the intracellular domain of murine Notch4. These observations suggest that negative regulation of LIN-12/Notch by SEL-10 may be an evolutionarily conserved feature.

SEL-10 may target LIN-12/Notch proteins for ubiquitin-mediated degradation

The attachment of ubiquitin to substrates involves a series of protein complexes. Ubiquitin is activated by linkage to an E1 ubiquitin activating enzyme, then transferred to an E2 ubiquitin conjugating enzyme. Some ubiquitination events also require the action of a third complex, termed E3. It is thought that E3 complexes may contribute to substrate specificity (reviewed in (99, 106). The Saccharomyces cerevisiae protein Cdc4p may function in an E3 complex. *CDC4* is one of a group of genes that also includes *CDC34*, *CDC53*, and *SKP1*; together, the proteins encoded by these genes directly regulate the level of the cyclin dependent kinase inhibitor SIC1, which must be destroyed for progression from G1 to S phase. CDC34 is an E2 ubiquitin conjugating enzyme ((107), and the current view is that CDC4, CDC53, and SKP1 function as an E3 complex (see (103, 108). Based on our analysis of *sel-10* and the data for *CDC4*, we propose that SEL-10 functions as part of an E3 complex to target the intracellular domains of LIN-12/Notch proteins for ubiquitin-dependent degradation.

The carboxy terminal region of all LIN-12/Notch proteins contain PEST sequences and one or more lysines immediately C-terminal to the cdc10/SWI6 motifs. The presence of PEST sequences often indicates that ubiquitin-mediated turnover occurs, although the two are not necessarily strictly correlated (109). With respect to the CDC34/CDC4-mediated events, it appears that the PEST sequences couple phosphorylation of the substrate to attachment of ubiquitin to lysine residues (reviewed in (99). However, the PEST sequence found in the carboxy terminal region of all Notch/LIN-12 proteins may not be required for SEL-10-mediated degradation of Notch/LIN-12 proteins, because *sel-10* mutations can still enhance the gain-of-function phenotype of a *glp-1* allele (110) that is truncated prior to the PEST sequence.

An important issue to consider in the context of SEL-10 as a component of an E3 complex is its specificity for Notch/LIN-12 proteins. The available *C. elegans* genetic data suggest that *sel-10* is an allele-nonspecific, gene-specific suppressor of *lin-12*, supporting a role for SEL-10 specifically in regulating the activity of LIN-12, or perhaps a small set of proteins including LIN-12. Allele-nonspecificity is indicated by the observation that mutations in *sel-10* suppress/enhance all *lin-12* alleles tested (98) E.J.A.Hubbard, unpublished observations). Gene-specificity is suggested by the fact that mutations in *sel-10* have not been identified in numerous screens in many laboratories for suppressors of hypomorphic mutations in genes encoding proteins other than Notch/LIN-12 proteins; furthermore, sel-10 mutation has not been observed to suppress various marker mutations used in routine strain constructions or of hypomorphic alleles of several other genes encoding receptor proteins (E.J.A.Hubbard, unpublished observations).

Potential roles for sel-10 *in oncogenesis*

Mammalian tumors induced by expression of Notch4(int3) or other truncated forms of Notch largely consisting of the intact intracellular domain are thought to result from constitutive Notch activity (2, 18, 62). Since SEL-10 downregulates Notch activity, it may act to restrain either normal or oncogenic functions of activated Notch, and hence suppress cell growth. If so, loss-of-function mutations in vertebrate *sel-10* could contribute to oncogenesis mediated by Notch by elevating the level of Notch protein. For instance, human T acute lymphoblastic leukemias, which in the majority of cases do not contain oncogenic Notch alterations (111), and human breast tumors, which thus far have not been reported to contain oncogenic Notch alterations, may carry mutations in other proteins that influence *Notch* activity, such as *sel-10* homologs.

MATERIALS AND METHODS

Plasmids for cell culture experiments

Plasmids used in the transient transfection experiments were constructed in pLNCX (42) or pQNCX (Qingyou Yan and J.K., unpublished observations), vectors that drive gene expression under the control of a CMV promoter.

pQNClacZ contains the bacterial *lacZ* gene.

pQNClin-12(intra)HA encodes a protein with a methionine-containing hemagglutinin epitope fused in frame N-terminal to LIN-12(intra) at amino acid 939.

pLNCint-3 contains cDNA corresponding to the *Notch4* region expressed in the *int3* insertion, beginning at amino acid 1411. The Notch4(int3) protein includes the entire intracellular domain of Notch4 and additional sequences.

pQNCsel-10myc (pJH186) encodes a protein with six myc epitope tags (112) fused in frame to cDNA 1A at amino acid 13 of SEL-10.

pQNCsel-10HA (pJH184) encodes a protein with a methionine-containing hemagglutinin epitope from pACT2 ((113) fused in frame (along with a short stretch of polylinker) to cDNA 1A at amino acid 13.

Transfection , Immunoprecipitations, and Western Blot Analysis

293T (Bosc23) cells ((92) were maintained in DMEM with 10% fetal bovine serum (FBS). A confluent plate of cells was split 1:3 the day prior to transfection. For one 60mm plate of cells, 4μg of each plasmid DNA was transfected using the calcium phosphate precipitation method. The total amount of DNA was kept constant by supplementation with vector DNA or lacZ-containing plasmids.

Two days after transfection, cells were harvested and lysed in TENT buffer (50mM Tris·Cl (pH8.0), 2mM EDTA, 150mM NaCl, 1% Triton-X 100) containing protease inhibitors (2μg/ml aprotinin, 2μg/ml leupeptin, 2μg/ml pepstatin, 0.5mM PMSF). Lysates were clarified by centrifugation at 10,000g for 10 minutes and protein content was determined using the BioRad Protein determination kit and samples were normalized for protein content. Extracts were precleared with sepharose CL-4B beads, incubated with antibodies (3μl of anti-Notch4 antiserum, 50μl of 12CA5 anti-HA supernatant, or 200 μl of 9E10 anti-myc supernatant) for six hours at 4°C, then incubated with 40μl of 50% slurry of protein A-sepharose for 1 hour at 4°C. The protein A-sepharose beads were washed with TENT buffer three times by vortexing for 10 minutes, beads were boiled in 30μl 1X protein loading buffer, and then electrophoresed on a 10% SDS-polyacrylamide gel and transferred onto nitrocellulose membrane. The blot was blocked overnight at 4°C with TBST (10mM Tris, pH 8.0, 150mM NaCl, 0.2% Tween 20) containing 1% bovine serum albumin (TBST-BSA). The blot was then incubated with 1° antibody diluted (1:2,000 anti-Notch4; 1:50 for 12CA5; 1:10 for 9E10) in TBST-BSA for 1 hour, washed three times for 5 minutes each with TBST, and incubated with 2° antibody in TBST-BSA for 1 hour. After three washes, the signal was visualized by chemiluminescence (Amersham, ECL).

The anti-Notch4 antiserum (G.W. and J.K., unpublished observations) is directed against the C-terminal region of Notch4 (residues 1788-1964) (62). 12CA5 anti-HA antibody was obtained from Berkeley Antibody Co., Richmond, CA. 9E10 anti-myc antibody was prepared from culture supernatants of the 9E10 hybridoma (114).

FIGURE LEGENDS

Figure 1.
SEL-10 is a member of the CDC4 family of F-box/WD40-repeat proteins. The CDC4 sequence (accession number X05625) is from Genbank. There are other potential CDC4 family members in the database; limited sequence data for a potential SEL-10 ortholog is given in part D. Reverse contrast letters indicate amino acid identity.

A) Schematic depiction of SEL-10 and CDC4, drawn to scale. The percentage of identical amino acids in each region is indicated. Members of the CDC4 family all have this general organization, with some variability in the length and sequence of their amino and carboxy termini.

B) Alignment of SEL-10 and CDC4 F-Boxes.

C) Alignment of WD40 repeats from SEL-10 and CDC4.

D) Alignment of SEL-10 and a potential human ortholog. Partial sequence of a human cDNA encoding a sequence highly similar to the C terminus of SEL-10 was obtained from Genbank (accession number H22962) and was extended into the WD40 repeats by direct sequencing of clone ym50h08.s1 (G.W. and J.K., unpublished observations). The predicted amino acid sequence encoded by the available human cDNA sequence is shown. The database also contains partial sequence information for a rat cDNA (Genbank accession number H34371) that is predicted to encode a peptide that is 100% identical to the last 35 amino acids of the available human sequence (data not shown).

Figure 2.
Coimmunoprecipitation of *C. elegans* SEL-10 with either *C. elegans* LIN-12(intra) or murine Notch4(int3) from transfected 293T cells.

(A) Samples were immunoprecipitated with anti-HA antibody and the Western blot was probed with anti-myc to visualize SEL-10myc (top panel) or anti-HA to visualize LIN-12(intra)HA (bottom panel). Arrow indicates the expected mobility of SEL-10myc.

(B) Samples were immunoprecipitated with anti-myc antibody and the Western blot was probed with anti-HA (top panel) or anti-myc (bottom panel). Arrow indicates the expected mobility of LIN-12(intra)HA.

(C) Samples were immunoprecipitated with anti-Notch4 antibody and the Western blot was probed with anti-HA to visualize SEL-10HA (top panel) or anti-Notch4 to visualize Notch4(int3) (bottom panel). Arrow indicates the expected mobility of SEL-10HA.

(D) Samples were immunoprecipitated with anti-HA antibody and the Western blot was probed with anti-Notch4 (top panel) or anti-HA (bottom panel). Arrow indicates the expected mobility of Notch4(int3).

For details see Materials and Methods. Lane 1, pQNClacZ. Lane 2, pQNClin-12(intra)HA + pQNClacZ. Lane 3, pQNClacZ + pQNCsel-10myc. Lane 4, pQNClin-12(intra)HA + pQNCsel-10myc. Lane 5, mock transfected cells. Lane 6, pLNCint3 + pQNCX. Lane 7, pLNCX + pQNCsel-10HA. Lane 8, pLNCint3 + pQNCsel-10HA.

Chapter V

Figure 1

A. Schematic representation of SEL-10 and CDC4

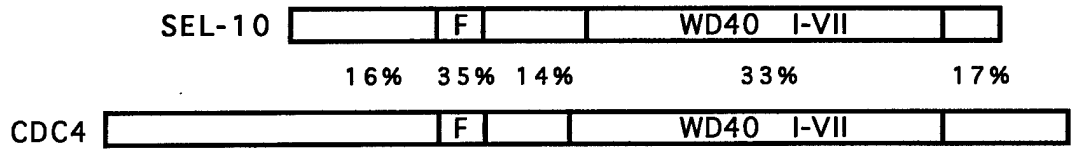

B. Alignment of F-Box

```
SEL-10   127   LPVELGMKILHNLTGYDLLKVAQVSKNW.KLISEIDKIWKSLG
CDC4     278   LPFEISLKIFNYLQFEDIINSLGVSQNWNKIIRKSTSLWKKLL
```

C. Alignment of WD40 repeats

```
I     SEL-10  253   GHEDHVITCMQIHDDVLVTGSDDNTLKVWC
      CDC4    419   GHMTSVITCLQFEDNYVITGADDKMIRVYD

II    SEL-10  294   GHTGGVWTSQISQCGRYIVSGSTDRTVKVWS
      CDC4    460   GHDGGVWALKYAHGG.ILVSGSTDRTVRVWD

III   SEL-10  336   GHTSTVRCMAMAG....SILVTGSRDTTLRVWD
      CDC4    502   GHNSTVRCLDIVEYKNIKYIVTSGRDNTLHVWK

IV    SEL-10  376   GHHAAVRCVQFDGTTVVSGGYDFTVKIWN
      CDC4    569   GHMASVRTVSGHGNIVVSGSYDNTLIVWD

V     SEL-10  416   GHNNRVYSLLFESERSIVCSGSLDTSIRVWD
      CDC4    609   GHTDRIYSTIYDHERKRCISASMDTTIRIWD

VI    SEL-10  461   GHTSLTSGMQLRGNILVSCNADSHVRVWD
      CDC4    671   GHTALVGLLRLSDKFLVSAAADGSIRGWD

VII   SEL-10  501   GHR..SAITSLQWFGRNMVATSSDDGTVKLWD
      CDC4    710   HHTNLSAITT.FYVSDNILVSGSENQFN.IYN
```

D. Alignment of partial sequence of potential human SEL-10 ortholog

```
                    WD VI                          WD VII
Ce SEL-10 480   NADSHVRVWDIHEGTCVHML...SGHRSAITSLQWFGRNMVATSSDDGTV
Hs SEL-10       NADSTVKIWDIKTGQCLQTLQVPNKHQSAVTCLQ.FNKNFVITSSDDGTV

Ce SEL-10 527   KLWDIERGALIRDLVTLDSGGNGGCIWRLCSTSTMLACAVGSRNNTEETK
Hs SEL-10       KLWDLKTGEFIRNLVTLESGGSGGVVWRIRASNTKLVCAVGSRNGTEETK

Ce SEL-10 577   VILLDFD
Hs SEL-10       LLVLDFD
```

Chapter V

Figure 2

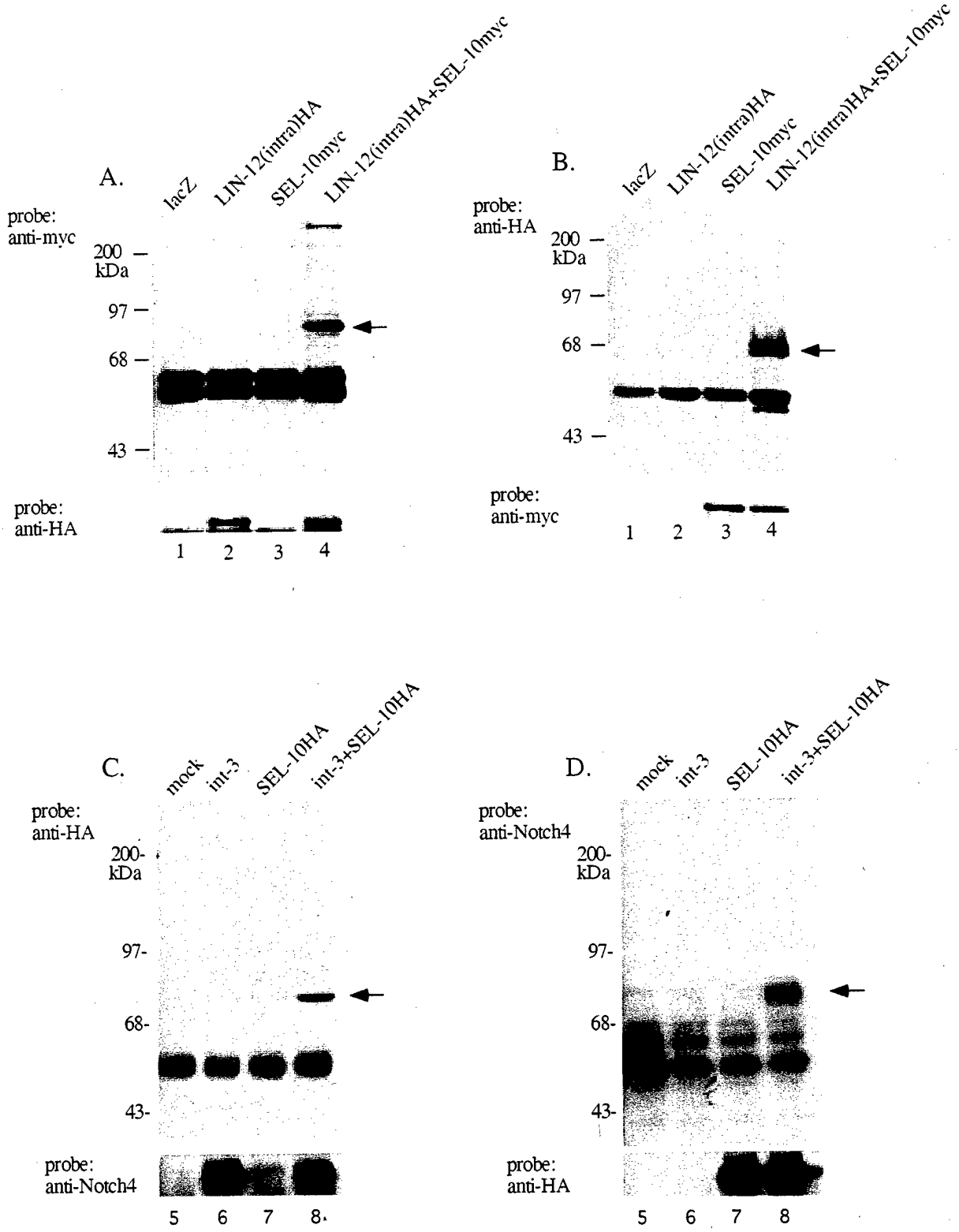

CHAPTER VI.
Functional and Physical interaction between SEL-10 and SEL-12 presenilin.

INTRODUCTION

Alzheimer's disease (AD) is a major cause of dementia among elderly people. The brains of affected individuals have a characteristic pathology, including hallmark amyloid plaques and neurofibrillary tangles. The main constituent of amyloid plaques is Aβ42(43), an amyloid beta peptide processing product. The "amyloid hypothesis" posits that deposition of this peptide causes AD; however, the mechanism by which this peptide exerts its toxic effect is unclear (115, 116). Familial forms of Alzheimer's disease have enabled the identification of genes that may illuminate the underlying molecular basis of the disease. In addition to the gene encoding the β-amyloid precursor protein (β-APP) itself, familial AD mutations have defined two additional genes, which encode the proteins presenilin 1 (PS1) and presenilin 2 (PS2). Mutations in the presenilins account for a significant portion (up to 60%) of early-onset familial AD cases. Presenilins appear to have eight transmembrane domains, and most studies have localized presenilins to endoplasmic reticulum/Golgi subcellular compartments (117). There is a growing body of evidence that presenilins are involved in the trafficking or processing of a selective group of proteins that includes APP and LIN-12/Notch proteins, but the mechanism of presenilin function remains unknown.

Individuals carrying mutations in PS1 or PS2 have elevated levels of Aβ42(43) (118), and elimination of PS1 activity reduces the proteolysis of β-APP. It has therefore been suggested that one approach to anti-amyloidogenic therapy for Alzheimer's disease is reducing presenilin activity. *C. elegans* is a simple model organism to identify genes that may serve as the basis for such therapies. In *C. elegans*, there are two functional presenilin genes, *sel-12* and *hop-1*. The *sel-12* gene was found in a genetic screen for mutations that suppress the phenotypic effects of a constitutively active transmembrane receptor of the LIN-12/Notch family (119). The SEL-12 protein appears to be a bona fide presenilin, since human PS1 or PS2 can substitute for SEL-12 in *C. elegans* (120). Another *C. elegans* gene, *hop-1*, encodes a somewhat more divergent protein that also appears to be a bona fide presenilin, since HOP-1 can substitute for SEL-12 (121). Furthermore, genetic studies suggest that *sel-12* and *hop-1* are functionally redundant in facilitating the activity of LIN-12/Notch proteins in several cell fate decisions (121).

Genetic screens for suppressers of mutations in the *C. elegans sel-12* presenilin constitute one approach to identifying factors that may regulate presenilin level or activity. *sel-12* mutations cause a highly penetrant egg-laying defective (Egl) phenotype (119). Suppressers can be easily identified by looking for the presence of eggs among the progeny of mutagenized *sel-12* mutant hermaphrodites or by constructing double mutants carrying mutations in candidate genes and mutations in *sel-12*. In principle, loss-of-function mutations that suppress the Egl defect of *sel-12* mutants might augment or stabilize mutant SEL-12 proteins or HOP-1(+), or reduce or bypass the need for presenilin activity. *sel-10*, a gene previous identified as a negative regulator of lin-12/Notch activity, has also been shown to regulate SEL-12 presenilin level or activity. Truncation mutations of *sel-10* suppress the Egl phenotype caused by loss-of-function mutation of *sel-12*. Based on the homology between SEL-10 and Cdc4p family of F-box/WD40 repeat containing proteins (98, 122), it is proposed that SEL-10 regulate SEL-12 activity by targeting it for degradation by the ubiquitination pathway.

Our study here explores the physical association between SEL-10 and SEL-12.

RESULTS AND DISCUSSION

A schematic drawing showing relevant features of the SEL-10 and SEL-12 proteins is shown in Fig. 1. The positions of epitope tag insertions are also indicated.

Expression of epitope-tagged SEL-10 and SEL-12 in mammalian cells.

We tagged SEL-10 with either a six-myc epitope or an HA epitope at the amino terminus (Fig. 1) as described in Materials and Methods. 293T cells were transfected with expression plasmids encoding these epitope-tagged proteins. Protein detection was conducted by immunoprecipitation from transfected cell lysates followed by Western blotting of the immunoprecipitates. When this procedure was performed with anti-myc antibodies to detect SEL-10myc, we detected a prominent species of 80 kD, the expected molecular mass of SEL-10myc (Fig. 2A, lanes 2 and 4). When it was performed with anti-HA antibodies to detect SEL-10HA, we detected a major species of 68kD, the expected molecular mass of SEL-10HA (Fig. 3A, lanes 2 and 4).

We tagged SEL-12 with an HA epitope at the carboxy terminus or a six-myc epitope in the intracellular loop (Fig. 1; Materials and Methods). When immunoprecipitation and blotting was performed, we detected the SEL-12HA or SEL-12myc proteins as multiple species, including several of higher molecular weight than predicted (Fig. 2C, lanes 3 and 4; Fig. 3C, lanes 3 and 4). (Differences in the patterns may be attributed to the location of the epitope tags and sensitivity of the detecting antibodies.) The multiplicity and pattern of epitope-tagged SEL-12 species strongly resembles the multiplicity and pattern of similarly epitope-tagged human presenilin forms (123). Biochemical analysis of human presenilins has revealed that higher molecular weight species also contain ubiquitin and/or increase upon treatment with proteasomal inhibitors (123-125). It is not clear why high molecular weight, polyubiquitinated forms of presenilins are evident in the absence of inhibitors of the proteasome, and it will be interesting to determine if there are other factors that regulate the rate or extent of polyubiquitinated-presenilin turnover.

Physical interactions between SEL-10 and SEL-12.

If SEL-10 does indeed target presenilins for degradation, then SEL-10 would be expected to associate physically with presenilins. We assessed potential physical interactions between SEL-10 and SEL-12 by co-immunoprecipitation using transiently transfected mammalian cells. When lysates of transfected cells containing SEL-10myc and SEL-12HA (C terminal-tag) were precipitated with either anti-myc antibodies (Fig. 2A, D) or anti-HA antibodies (Fig. 2B, C), the immunoprecipitates were found to contain both SEL-10myc and SEL-12HA. These results demonstrate that SEL-10 and SEL-12 presenilin are able to form a complex, suggesting that presenilins may be targeted by SEL-10.

However, when lysates of transfected cells containing SEL-10HA and SEL-12myc (loop tag) were analyzed for co-immunoprecipitation, we were unable to detect a physical interaction (Fig. 3B, D). This lack of association raises two interesting points. First, the lack of co-immunoprecipitation of loop-tagged SEL-12myc with SEL-10HA supports the interpretation that the interaction we observed between SEL-12HA and SEL-10myc is specific, and is not simply the result of nonspecific aggregation of SEL-12 and SEL-10 due to the experimental conditions. Second, the cytosolic loop of SEL-12 has a region with features of a PEST sequence (109) and potential phosphorylation sites. The WD40 region of Cdc4p has been shown to bind to phosphorylated target proteins to promote their degradation (126). The failure of co-immunoprecipitation when the epitope tag is placed in the loop may indicate that this region is mediating the interaction between SEL-10 and SEL-12, and the proximity to the PEST sequence is additionally provocative.

We note that co-immunoprecipitation experiments similar to those described here as well as yeast two-hybrid experiments have identified other proteins that interact physically with the presenilin intracellular loop region. Two studies have provided evidence that the presenilin loop region interacts with β-catenin, a family of proteins that are components of cell junctions and of the Wnt signal transduction pathway, and δ-catenin, a novel β-catenin-related protein (127, 128). Another study has provided evidence that the presenilin loop region interacts with the microtubule associated protein tau and with glycogen synthase kinase-3β, which can phosphorylate tau as well as intermediates in the Wnt signal transduction pathway (129). However, no evidence for the functional relevance of these interactions has been reported yet.

Concluding remarks. Proteins highly related to SEL-10 exist in mammals (122, 126); our unpublished observations; M.E. Gurney, personal communication). The physical and functional interactions between SEL-10 and SEL-12 in *C. elegans* raise the intriguing possibility that SEL-10 is part of a conserved mechanism that regulates presenilin level or activity in mammals. Functional analysis of SEL-10-related proteins in mammalian cell culture and genetic systems will be necessary to assess this possibility.

MATERIALS AND METHODS

Plasmids for cell culture experiments.
Plasmids used in the transient transfection experiments were constructed in pQNCX (Qingyou Yan and J.K., unpublished observations), vectors that drive gene expression under the control of a CMV promoter.

pQNClacZ contains the bacterial lacZ gene.

pQNCsel-10myc encodes a protein with six myc epitope tags (112) fused in frame to the N-terminus of SEL-10 at amino acid 13.

pQNCsel-10HA encodes a protein with a hemagglutinin epitope tag fused in frame to the N-terminus of SEL-10 at amino acid 13

pQNCsel-12myc encodes a protein with six myc epitope tags fused in frame to the SEL-12 loop region between amino acids 336 and 337.

pQNCsel-12HA encodes a protein with a hemagglutinin epitope fused in frame to the C-terminus of SEL-12 at amino acid 441.

Transfections, immunoprecipitations, and Western blot analysis.
293T (Bosc23) cells (92) were maintained in DMEM with 10% fetal bovine serum (FBS). A confluent plate of cells was split 1:3 the day prior to transfection. For one 60 mm plate of cells, 4 μg of each plasmid DNA was transfected using the calcium phosphate precipitation method. The total amount of DNA was kept constant by supplementation with lacZ-containing plasmids.

Two days after transfection, cells were harvested and lysed in TENT buffer (50 mM Tris·Cl (pH8.0), 2 mM EDTA, 150 mM NaCl, 1% Triton-X 100) containing protease inhibitors (2 μg/ml aprotinin, 2 μg/ml leupeptin, 2 μg/ml pepstatin, 0.5 mM PMSF). Lysates were clarified by centrifugation at 10,000g for 10 minutes and protein content was determined using the BioRad Protein Assay Kit and samples were normalized for protein content. Extracts were precleared with sepharose CL-4B beads, incubated with antibodies (50 μl of 12CA5 anti-HA supernatant, or 200 μl of 9E10 anti-myc supernatant) for six hours at 4°C, then incubated with 40 μl of 50% slurry of protein A-sepharose for 1 hour at 4°C. The protein A-sepharose beads were washed with TENT buffer three times by vortexing for 5 minutes, beads were boiled in 30 μl 1X protein loading buffer, and then electrophoresed on a 10% SDS-polyacrylamide gel and transferred onto nitrocellulose membrane.

A Western blot was first blocked overnight at 4°C with TBST (10mM Tris, pH 8.0, 150mM NaCl, 0.2% Tween 20) containing 1% bovine serum albumin (TBST-BSA). The blot was then incubated with 1° antibody diluted (1:50 for 12CA5; 1:10 for 9E10) in TBST-BSA for 1 hour, washed three times for 5 minutes each with TBST, and incubated with 2° antibody in TBST-BSA for 1 hour. After three washes, the signal was visualized by chemiluminescence (Amersham, ECL).

12CA5 anti-HA antibody was obtained from Berkeley Antibody Co., Richmond, CA. 9E10 anti-myc antibody was prepared from culture supernatants of the 9E10 hybridoma.

FIGURE LEGENDS

Figure 1.
Schematic view of the SEL-10 and SEL-12 proteins. For SEL-10, the F-box and WD40 repeats, as well as the position of *ar41* (W323STOP), are indicated. For SEL-12, thick vertical lines represent the eight transmembrane domains, and the *sel-12(ar131)* (C60S) and *sel-12(ar171)* (W225STOP) mutations are indicated. Information about the SEL-10 sequence is from (122) and information about the SEL-12 sequence is from (119) with a correction as in ((120).

Figure 2.
Coimmunoprecipitation of SEL-10myc with SEL-12HA.

(A) Samples were immunoprecipitated with anti-myc antibody and the Western blot was probed with anti-myc to visualize SEL-10myc.

(B) Samples were immunoprecipitated with anti-HA antibody and the Western blot was probed with anti-myc to visualize SEL-10myc associated with SEL-12HA. The immunoglobulin heavy chain is more prominent because it is a longer exposure than in other panels.

(C) Samples were immunoprecipitated with anti-HA antibody and the Western blot was probed with anti-HA to visualize SEL-12HA.

(D) Samples were immunoprecipitated with anti-myc and the Western blot was probed with anti-HA to visualize SEL-12HA associated with SEL-10myc.

Lane 1, lacZ expression plasmid. Lane 2, sel-10myc expression plasmid. Lane 3, sel-12HA expression plasmid. Lane 4, sel-10myc+sel-12HA expression plasmids. All transfections were normalized for DNA content with lacZ expression plasmid.

Figure 3.
SEL-12 epitope-tagged in the loop region does not associate with SEL-10.

(A) Samples were immunoprecipitated with anti-HA antibody and the Western blot was probed with anti-HA to visualize SEL-10HA. In A, B and D, the immunoglobulin heavy and light chains are visible at approximately 50 kD and 28 kD, respectively.

(B) Samples were immunoprecipitated with anti-myc antibody and the Western blot was probed with anti-HA to determine if SEL-10HA is present.

(C) Samples were immunoprecipitated with anti-myc antibody and the Western blot was probed with anti-myc to visualize SEL-12myc. Arrows denote the multiple apparent SEL-12myc species, which are reminiscent of the multiple human presenilin species that have been reported (123).

(D) Samples were immunoprecipitated with anti-HA and the Western blot was probed with anti-myc to determine if SEL-12myc is present.

Lane 1, lacZ expression plasmid. Lane 2, sel-10HA expression plasmid. Lane 3, sel-12myc expression plasmid. Lane 4, sel-10HA+sel-12myc expression plasmids. All transfections were normalized for DNA content with lacZ expression plasmid.

Chapter VI

Figure 1

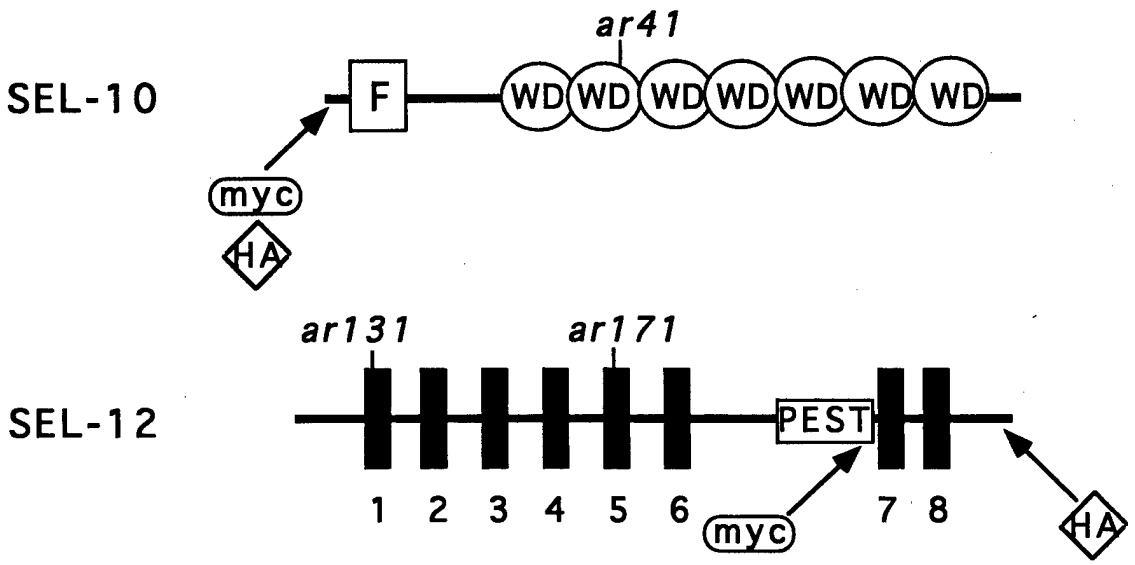

Chapter VI

Figure 2

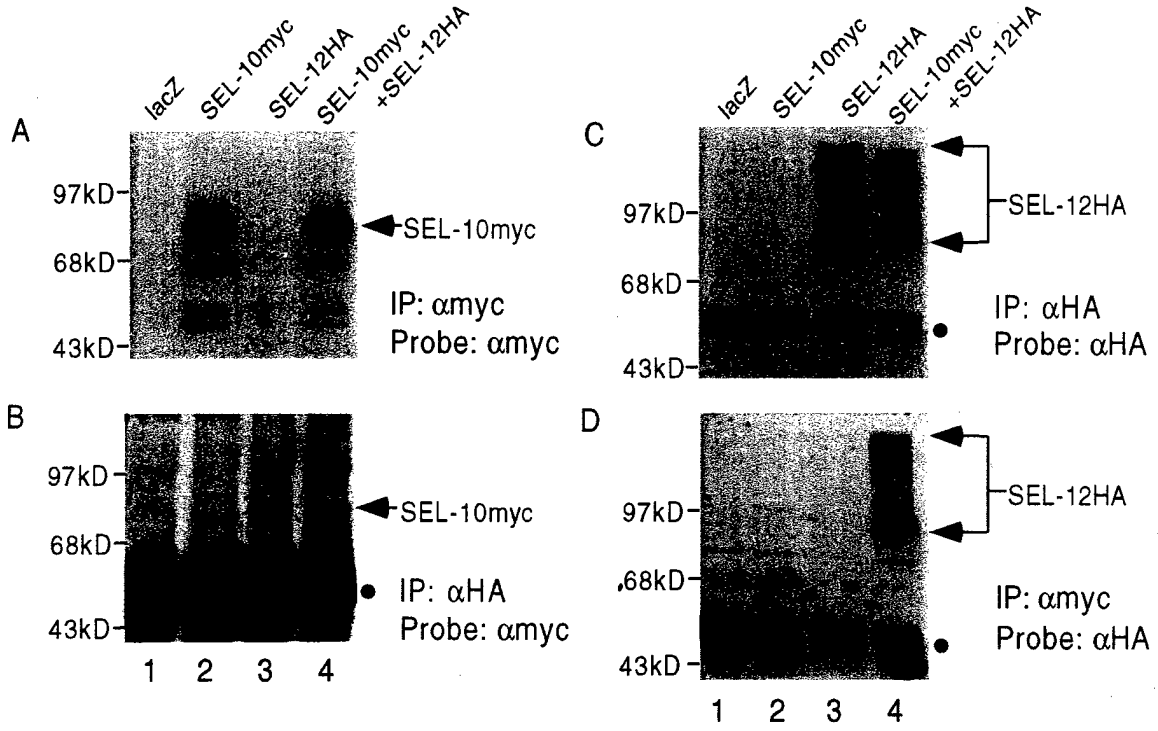

Chapter VI

Figure 3

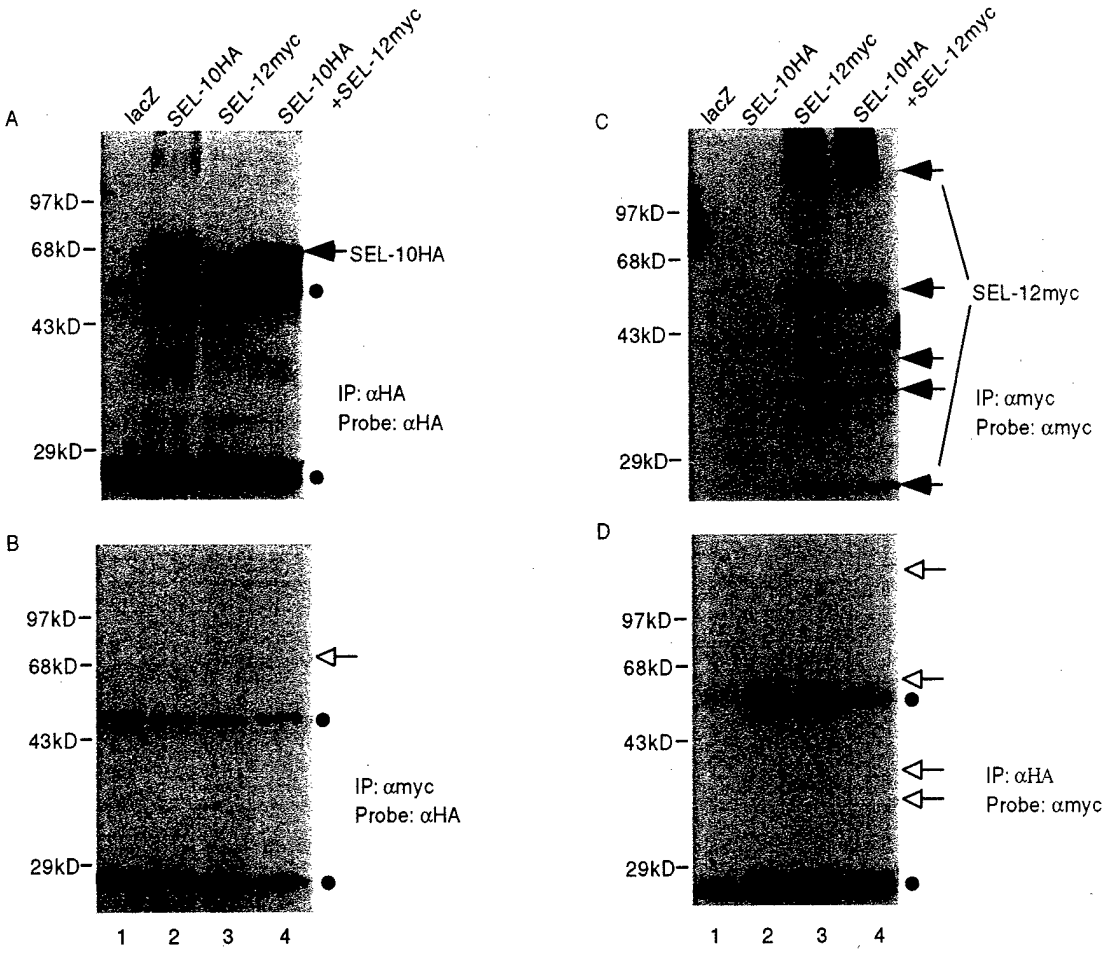

CHAPTER VII.

Notch4 and Jagged-1 induce microvessel differentiation of rat brain endothelial cells

Note: This section describes work propose for Specific aim 3*

"Analysis of the potential role of Notch4 in angiogenesis."

Task 7: Evaluate the angiogenic or anti-angiogenic potential of Notch signal transduction.

INTRODUCTION

Notch4 is a member of the Notch/lin-12 family of transmembrane receptors that are involved in cell fate determination (86, 90). Like other Notch proteins, Notch4 extracellular domain is characterized by both Epidermal Growth Factor (EGF)-like repeats and lin-12/Notch repeats (LNR), and the intracellular domain contains ankyrin/cdc10 repeats (62). Analysis of invertebrate Notch/lin-12 mutants support a function for Notch/lin-12 receptors in intercellular signaling events that control cell fate. Mutants that delete the extracellular domain of *C. elegans lin-12* or *Drosophila Notch* result in dominant gain-of-function phenotypes. The int-3 form of Notch4, Notch4/int-3, was identified based on its oncogenic effects in the mouse mammary gland and encodes only the transmembrane and intracellular domain of Notch4 (1, 62, 63). Notch4/int-3 behaves as a constitutively activated receptor (4, 87, 130). Similar activating mutations in the *Notch1* gene have been identified in T lymphoblastic leukemia and can lead to neoplastic transformation in vitro (18, 131).

Drosophila Delta (132) and *Serrate* (27) and *C. elegans Lag-2* (133) and *Apx-1* (134) encode a family Notch/lin-12 ligands that are transmembrane proteins whose extracellular domains contain EGF-like repeats and a DSL domain (Delta-Serrate-Lag-2). Based on homology to the *Drosophila* ligands, Notch ligands have also been identified in vertebrates. *Jagged*-1, a rat homologue of *Drosophila Serrate*, contains the hallmarks of a Notch ligand (29). Other putative mouse Notch ligands Delta-like 1 (30) and Delta-like 3 (135) have been identified and are closely related to *Drosophila* Delta. More recently, a human *Jagged-2* gene has been identified (136). Although several Notch ligands and Notch receptors have been identified in mammals, it is not clear if ligands display distinct specificity's towards different receptors.

Several genes encoding Notch ligands or receptors are expressed in the endothelium. *Notch4* is expressed primarily in endothelial cells of the vasculature of mouse embryos and adult tissues (62, 137). Notch1 and Jagged-1 are also expressed in the endothelium, as well as a variety of other tissues (14, 138-140). Recently, *Jagged-1* was identified as gene induced during angiogenesis *in vitro* (141). A role of Notch in vascular development is suggested by analysis of mice with targeted disruption of genes encoding Notch ligands or Notch regulatory components. Mice deficient in either Delta like-1 (Dll1) (142, 143) or Jagged-1 develop severe hemorrhages (T. Gridley and G. Weinmaster, unpublished data). Mice with a targeted disruption of the *Presenilin1* gene(143, 144), which facilitates Notch activity, display a loss of expression of *Notch1*, *Dll1* and exhibit hemorrhages in the brain and spinal cord. Evidence for involvement of Notch genes in vascular disorders has come from an analysis of a human hereditary adult onset condition causing stroke and dementia. CADASIL (cerebral autosomal dominant arteriopathy with subcortical infarcts and leukoencephelopathy) is a human disorder manifested by stroke and dementia and characterized by non-amyloid and non-artherogenic angiopathy of cerebral arterioles (145). The CADASIL locus maps to the human *Notch3* gene and mutations in *Notch3* have been defined in CADASIL patients (146). Thus, alterations in Notch signaling may disrupt development and integrity of the vasculature.

As Notch functions in cell fate regulation in *Drosophila* and *C. elegans*, Notch receptors and their ligands expressed in endothelium may similarly control cell fate decisions during vascular development. We used the Rat brain endothelial cell line, RBE4, to study the role of Notch in endothelial cell differentiation. Ectopic expression of an activated Notch4/int-3 or of Jagged-1 in RBE4 cells induced cellular structures with morphological and biochemical properties of endothelial microvessels. Thus, activation of the Notch signaling pathway can promote endothelial differentiation.

RESULTS

Notch4 expression in kidney endothelial cells.

We previously described endothelial cell specific expression of Notch4 mRNA in mouse embryos and adult mouse lung, as analyzed by *in situ* hybridization (62). To define the pattern of Notch4 protein expression, we generated an anti-Notch4 rabbit antiserum directed against a GST fusion protein containing the carboxy-terminus of Notch4 (122). The presence of endogenous Notch4 protein was analyzed in mouse kidney sections, as the kidney contains characteristic glomeruli with endothelial cell clusters in the renal cortex. We first analyzed Platelet Endothelial Cell Adhesion Molecule-1 (PECAM), an extracellular protein specifically expressed in endothelial and platelet cells. Antibodies against PECAM were used as a positive control in these experiments as they stained glomeruli (Fig. 1B). As shown in Fig. 1D, anti-Notch4 antibody specifically detects glomeruli in the kidney cortex in a similar pattern as the anti-PECAM antibody (Fig. 1B). Thus, data presented here demonstrates endothelial expression of Notch4 protein in the kidney.

The anti-Notch4 antibody was used to detect ectopically expressed Notch4 and Notch4/int-3 proteins by immunoblot analysis (Fig. 2C). Transiently transfected 293 cells expressed either HA epitope-tagged or non-epitope-tagged versions of Notch4 and Notch4/int-3. Immunoblot analysis of extracts from these cells displayed the full length Notch4 and Notch4/int-3 proteins which migrate with an approximate molecular weight of 220 and 70 kD respectively (Fig. 2B and C).

RBE4 microvessel outgrowth is induced by activated Notch4 and Jagged-1.

Previous work has shown that the RBE4 cell line grown on collagen coated plates display a cobblestone morphology (147). When cultured in the presence of basic Fibroblast Growth Factor (bFGF), RBE4 cells change to a spindly morphology. When grown post-confluence, bFGF induces RBE4 cells to develop multi-cellular aggregates that arise from the monolayer. These three-dimensional aggregates consist of sprouts that extend above the monolayer and organize into curvilinear and bifurcating structures, resembling microvessels. bFGF-induced RBE4 microvessels contain high activity of alkaline phosphatase (ALP) and gamma glutamyl transpeptidase (γGTP), which are specific enzymatic markers for differentiated endothelium and brain capillaries respectively (147).

RBE4 cell lines were programmed to express the HA-tagged Notch4/int-3, Jagged-1 and LacZ proteins using the retroviral vector pLHTCX. RBE4 cell lines programmed to express Notch4 were generated by direct transfection of the HA-tagged *Notch4* cDNA. All three recombinant proteins were detected by immunoblot analysis of the respective RBE4 cell lines and migrated with their predicted molecular weight (220kD for Notch4, 70kD for Notch4/int-3, 150 kD for Jagged-1, see Fig. 2D).

The consequences of activating the Notch signaling pathway by ectopic expression of ligand (Jagged-1) or an activated receptor (Notch4/int-3) was analyzed in RBE4 cells. Control RBE4 cells expressing LacZ (RBE-LacZ) growth arrest at confluence and do not develop three dimensional structures (Fig. 3A). When confluent RBE-LacZ cells were grown with bFGF (5 ng/ml), they form modest sprouts and microvessels (data not shown). RBE-LacZ were indistinguishable from wild type RBE4 cells grown under identical conditions. RBE4 cells programmed to express either Jagged-1 (RBE-Jagged-1) or Notch4/int-3 (RBE-Notch4/int-3) develop sprouts and three dimensional capillary-like structures (Fig. 3C and D). These structures were not dependent on the presence of bFGF. These microvessel structures either float in the cell culture medium (although originating from a mount formed on the tissue culture plate) or are attached to the tissue culture plate. The extent of microvessel induction by Notch4/int-3 is far greater when compared to Jagged-1, as demonstrated in Fig. 3E and F. RBE4 cells programmed to express Notch4 (RBE-Notch4) do not form any microvessel structures (Fig. 3B). RBE-Notch4/int-3 or RBE-Jagged-1 cells displayed a more spindle shape morphology and do not form the cobblestone monolayer, as observed in RBE-LacZ or RBE-Notch4 (compare Fig. 3C and D with A or B). This morphological change is similar to when wild type RBE4 cells are treated with bFGF (147).

Microvessel structures induced by Jagged-1 and Notch4/int-3 in RBE4 cells were analyzed histochemically for the activities of two blood-brain barrier-associated enzymes, γGTP and ALP. These enzymes are specifically expressed in the brain vasculature, and their expression is induced by bFGF treatment of RBE4 cells (147). ALP activity was detected in microvessel structures induced by either Notch4/int-3 (Fig. 4B) or by Jagged-1 (data not shown). γGTP activity was also detected in both

RBE-Jagged-1 (Fig. 4C) and RBE-Notch4/int-3 (data not shown). The detection of both ALP and γGTP activities was specific for microvessel structures and not found in surrounding monolayer cells. RBE4 cell lines that did not exhibit microvessels, RBE-LacZ and RBE-Notch4, did not display ALP or γGTP activities (data not shown).

Activation of the Notch signal transduction pathway in RBE4 cells.

Jagged-1 and Notch4/int-3 expression resulted in similar phenotypes in RBE4 cells, thus we hypothesized that RBE4 cells must express endogenous Notch receptors that can be activated by Jagged-1. Northern Blot analysis demonstrated endogenous expression of *Notch1*, *Notch3* and *Notch4* transcripts (Fig. 5A). We also found that RBE4 cells express endogenous *Jagged-1* transcripts (Fig. 5A). We could not make a statement about the relative levels of expression of *Notch* and *Jagged* transcripts as each lane in Fig. 5A utilized a different riboprobe.

Activation of Notch signaling has been reported to induce endogenous genes encoding Notch receptors and ligands (136). This induction can serve as a measure of signal activation and may lead to positive feedback control of *Notch* genes by their ligands (97). To measure Notch signaling output in RBE4 cells, we assessed the level of endogenous *Notch* receptor and *Notch* ligand gene transcripts by northern blot analysis (Fig. 5B). RBE-Notch4/int-3 have increased levels of endogenous *Notch4* (6.7 kb) and *Jagged-1* transcripts (5.9 kb) (Fig. 5B, lane 2). The *Notch4*-specific riboprobe corresponds to the carboxy-terminal domain of *Notch4*, and can detect both ectopic *Notch4/int-3* transcripts (1.8 kb) and endogenous *Notch4* transcripts (6.7 kb). Notch4/int-3 expression in RBE cells specifically led to increased levels of endogenous *Notch4* transcripts (Fig. 5B, lane 2) and not endogenous *Notch1* (Fig. 5B, lane 2) or *Notch3* transcripts (data not shown). RBE-Jagged-1 cells also have increased levels of endogenous *Notch4* transcripts (Fig. 5B, lane 4). Again this activation is restricted to the endogenous *Notch4* gene since the levels of *Notch1* (Fig. 5B lane 4) and *Notch3* (data not shown) transcripts remain unchanged. We were not able to ascertain if Jagged-1 expressing RBE4 cells up-regulated endogenous *Jagged-1*, since both the ectopic and endogenous *Jagged-1* transcripts migrate with a similar molecular size (5.9 kb). RBE-Notch4 cells do not have increased levels of *Notch1* (Fig. 5B, lane 3), *Notch3* (data not shown) or *Jagged-1* transcripts (Fig. 5B, lane 3). The level of *Notch4* transcripts in these cells could not be evaluated since we can not distinguish by size between endogenous and ectopic *Notch4* transcripts.

RBE4 cell lines were generated with retroviral vectors designed to express genes via an internal CMV promoter; however, gene expression may also be driven by the retroviral LTR leading to expression of two different sized transcripts. CMV-driven transcripts correspond to 1.8 kb for *Notch4/int-3*, 6.7 kb for *Notch4* and 5.9 kb for *Jagged-1* (Fig. 5B). Larger transcripts encompassing the complete retroviral genome originate from the LTR resulting in transcripts that are 3.5 kb larger than the CMV-driven transcripts. The LTR-driven transcripts are denoted in Fig. 5B (LTR) and correspond to 5.3 kb for *Notch4/int-3*, 10.2 kb for *Notch4* and 9.4 kb for *Jagged-1* (Fig. 5B). To clearly distinguish between the activated endogenous *Notch4* transcripts (6.7 kb) and the LTR-driven *Notch4/int-3* transcript (5.3 kb) a short exposure of a different northern blot from RBE-Notch4/int-3 cells is shown in Fig. 5B (lane 5 and 6). Fig. 5B lanes 2 and 6 both demonstrate that Notch4/int-3 activates expression of the endogenous *Notch4* gene (6.7 kb).

DISCUSSION

To investigate the role of Notch4 and Jagged-1 in endothelial cell differentiation we used an angiogenic *in vitro* model system, the RBE4 cell line. Previous studies have demonstrated that bFGF, a well characterized angiogenic factor, induces microvessel formation and the expression of markers specific for either differentiated endothelium (ALP) or the blood-brain barrier (gGTP) (147). Ectopic expression of either Notch4/int-3 or Jagged-1 in RBE4 cells also results in the induction of microvessel structures that express both ALP and gGTP. Full length Notch4 expression did not elicit any observable phenotype. These studies suggest that Notch4/int-3 and Jagged-1 induce a biological activity in RBE4 cells that is similar to that induced by a known angiogenic agent bFGF. Thus, in rat brain endothelial cells, Notch activation results in an angiogenic response characterized by microvessel formation. Thus, Notch activation may regulate the angiogenic process in endothelium where Notch4 is found to be expressed, such as the vasculature of the adult kidney and lung.

Our data support the concept that Notch4/int-3 is a constitutive activated Notch allele as it induces a phenotype that is identical to when endogenous Notch receptors are activated by Jagged-1. We also note that ectopic expression of full length Notch4 in RBE4 cells does not result in Notch signal activation, thus receptor overexpression does not lead to constitutive receptor activation. It may also suggest that RBE4 cells do not express a Notch4 ligand. Alternately RBE4 cells may not express Notch4 ligands at levels sufficient to activate the ectopically expressed Notch4 receptor. The induction of microvessel structures by Notch4/int-3 appears to be more robust when compared to the induction by Jagged-1 suggesting that a constitutive activated form of the Notch4 receptor is more potent in its activity than a Notch ligand (Jagged-1).

Since Jagged-1 is able to induce a biological activity that is similar to Notch4/int-3, we hypothesize that RBE4 cells must express endogenous Notch receptors which can be activated by Jagged-1. Northern blot analysis demonstrated that the Notch1, Notch3 and Notch4 genes are expressed in RBE4 cells. Notch1 and Notch4 are known to be expressed in endothelium *in vivo* (14, 62, 137-140) and Notch3 may function in the vasculature (146). RBE4 cells also express Jagged-1 when analyzed by Northern blot. Thus, although RBE4 cells express endogenous transcripts that encode for both Notch proteins and one of their ligands, they do not spontaneously form microvessel structures. This observation may suggest that the levels of Notch proteins or ligands in RBE4 cells are insufficient to activate the Notch pathway.

We demonstrated that the Notch signal transduction pathway is activated in RBE4 cells expressing either Notch4/int-3 or Jagged-1. Activation of Notch signaling results in up-regulation of the endogenous Notch4 and Jagged-1 transcripts. Thus, the observed microvessel induction of RBE4 cells correlated with Notch signal activation. Both Jagged-1 and Notch4/int-3 expression resulted in a similar up-regulation of the endogenous Notch4 gene but neither altered the levels of Notch1 and Notch3 transcripts. Activation of a particular Notch signaling pathway, in this case Notch4, led to transcriptional activation events that are specific for distinct endogenous *Notch* genes. The observation that Jagged-1 results in an identical transcriptional activation pattern as activated Notch4/int-3 may suggest that Jagged-1 is a Notch4 ligand.

Previous work has demonstrated that activation of the Notch signal transduction pathway in mammalian cells inhibits differentiative or morphogenetic events. For instance, activated Notch1 and Notch2 are able to inhibit myogenic differentiation(29, 148), and myeloid differentiation (149), and activated Notch4 (Notch4/int-3) is able to inhibit branching morphogenesis of mammary epithelial cells (130). In contrast, we found that activated Notch4/int-3 promoted the differentiation of RBE4 cells. Cell fate determination may involve either inhibition or promotion of differentiative steps. Our data is thus a clear demonstration that Notch signal activation can regulate cell fate decisions that involve the promotion of differentiation in mammalian cells.

Cell fate and cell differentiation decisions likely play important roles during vascular development. Although some factors have been identified that regulate vascular growth, little is known about how these or other factors may regulate cell fate decisions (150). Our data suggest that Notch proteins and their ligands can promote differentiation and may be important in regulating cell fate decisions in the developing vasculature.

MATERIALS AND METHODS

Immunohistochemistry. Frozen mouse kidney sections were fixed in 100% acetone and rinsed in 0.1% Triton X-100 in PBS (PBST). Tissue sections were incubated in blocking solution (5% goat serum, 3% BSA in PBS) for 1 hour. Sections were covered with 1^0 antibody in dilution solution (1% goat serum, 3% BSA in PBS) for 12 hours at 4^0 C. The anti-mouse CD 31 (anti-PECAM) antibody (PharMingen) was used at a concentration of 3 mg/ml, the anti-mouse Notch4 immune-serum and pre-immune serum were diluted 500X. Tissue sections were rinsed in PBST and 2^0 antibodies (biotinylated goat anti-rat IgG and goat anti-rabbit IgG labeled to alkaline phophatase, both at 1:200 dilutions) were applied in dilution buffer for 2 hours. Biotinylated goat anti-rat IgG was detected by the peroxidase technique (Vectastain Elite ABC kit, Vector Laboratories), and alkaline phosphatase labeled goat anti-rabbit IgG was detected as previously described(151). Sections for alkaline phosphatase staining were counter stained with eosine.

cDNA's. The Notch4/int-3 cDNA corresponds to a truncated Notch4 cDNA as described previously (62). An oligonucleotide sequence encoding the haemagglutinin (HA) epitope was appended to the 3' end of the Notch4/int-3 and Notch4 cDNA's as previously described (130). The presence of each fusion was confirmed by DNA sequencing. Similarly, a Jagged-1 cDNA was modified to encode an HA-tag at the carboxy terminus.

Cell cultures and RBE4 microvessel outgrowth assay. RBE4 cells were maintained in Alpha MEM/Ham's F10 (1:1) supplemented with 2 mM glutamine, 10% fetal calf serum and penicillin/streptomycin. For microvessel outgrowth assay, RBE4 cell lines were plated at equal cell densities (50% confluence). After 3 to 5 days, cell cultures were photographed (100 X or 40X magnification).

Cell lines. HA-tagged cDNAs were inserted into the retroviral vector pLHTCX wherein hygromycin-resistance gene is controlled by the murine leukemia virus (MLV) long terminal repeat (LTR), and cDNA transcription is controlled by an internal cytomegalovirus (CMV) promoter. Distinct populations of RBE4 cells, either expressing Notch4/int-3 or Jagged-1 cDNA, were prepared by retroviral infection as described previously (130). The resultant populations, each comprised of at least 50 clones, were used in cellular and biochemical assays described below. Notch4 expressing cell lines were established by transfecting RBE4 cells directly by calcium phosphate transfection.

Immunoblot analysis. HA epitope-tagged or non-tagged Notch4/int-3, Jagged-1 and Notch4 proteins from lysates of RBE4 cells were analyzed by immunoblotting as described previously (130). Lysates containing 20 μg protein were electrophoresed and transferred to nitrocellulose filters, and subsequently, blocked in TBST (10 mM Tris, pH 8.0, 150 mM NaCl, 0.2% Tween-20) containing 1% BSA (TBST-BSA). Blots were then incubated with 1^0 antibody diluted (1:100 for 12CA5 (Berkeley Antibody Co.); 1:2000 for anti-Notch4) in TBST-BSA for 4 hours, washed in TBST, and incubated with 2^o antibody in TBST-BSA for 1 hour. After 3 washes, the signal was visualized by chemiluminescence (Amersham, ECL).

Histochemical enzyme assay. Gamma-glutamyl transpeptidase (γGTP) activity was demonstrated histochemically in cell cultures fixed in acetone, as described previously (147): L-gamma-glutamyl-4-methoxy-2-naphthylamide was used as substrate and glycyl-glycine as acceptor. In a simultaneous azo coupling reaction with Fastblue BB, a red azo dye is produced. Alkaline phosphatase (ALP) activity was determined in cell cultures fixed in citrate-buffered acetone, using the reaction mixture Sigma kit N85, with naphtol AS-MX phosphate as substrate and fast blue RR salt as diazonium salt, as previously described (147).

Northern Blot analysis. Total RNA was isolated from RBE4 cell and Northern blot analysis was performed as described previously (62). ^{32}P-radiolabeled riboprobes were transcribed (Maxiscript, Ambion) from *Notch1*, *Notch3*, *Notch4* and *Jagged-1* cDNA's. Comparable amounts and integrity of the RNA were tested by hybridization with a b-actin probe.

FIGURE LEGENDS

Figure 1.
Immunohistochemical analysis on adult mouse kidney sections. Endothelial cells within the cortical kidney glomeruli can be detected by using either an anti-PECAM antibody (B) or an antibody generated against the carboxy terminus of Notch4 (D). No anti- PECAM antibody was used in panel A, and both panel A and B were processed for horse radish peroxidase detection which results in a brown staining. Pre-immune serum at identical dilution was used in panel C, and both panel C and D were processed for alkaline phosphatase detection which results in a blue-purple staining. Panels C and D were counterstained with eosin.

Figure 2.
Schematic representation of the Notch4, Notch4/int-3 and Jagged-1 proteins (A). Conserved domains within each proteins are indicated. Imunnoblot analysis on lysates of 293 cells transiently transfected with either epitope tagged or non-epitope tagged cDNA's of Notch4/int-3 or Notch4 (B and C) using anti-HA antibody (B) or anti-Notch4 antibody (C). Immunoblot analysis on lysates of RBE4 cells programmed to express LacZ, Notch4/int-3, Jagged-1 or Notch4 using the anti-HA antibody, demonstrates expression of each respective protein (D).

Figure 3.
RBE4 cells that are programmed to express either LacZ (A) or Notch4 (B) display a cobble stone morphology when grown on collagen coated plates. RBE4 cells programmed to express Notch4/int-3 (C and E) or Jagged-1 (D and E) display a spindle shape morphology and spontaneously form microvessel structures. Structures were more prominent in RBE-Notch4/int-3 than in RBE-Jagged-1 cell cultures (compare E to F). Photographs A to D were taken at 100X magnification whereas photographs E and F were taken at 40X magnification.

Figure 4.
Histochemical analysis of alkaline phosphatase (B) and gamma-glutamyl transpeptidase (C) activities in microvessel structures induced by RBE4 cells expressing Notch4/int-3 (B) or Jagged-1 (C). RBE4 cells surrounding the microvessel structures do not express either enzyme activity (B and C). Panel A is control.

Figure 5.
Northern blot analysis on RBE4 cells. Panel A, 40 mg total RNA from RBE4 cells was hybridized to riboprobes for either *Notch1*, *Notch3*, *Notch4* or *Jagged-1*. Panel B, 40 mg of total RNA (lane 1, 3, 5, 6) or 20 mg of total RNA (lane 2 and 4) from RBE4 cells programmed to express either LacZ, Notch4/int-3, Notch4 or Jagged-1, was hybridized to riboprobes for either *Jagged-1*, *Notch1*, *Notch4*, or *b-actin*. LTR-driven transcripts are denoted (LTR).

Chapter VII

Figure 1

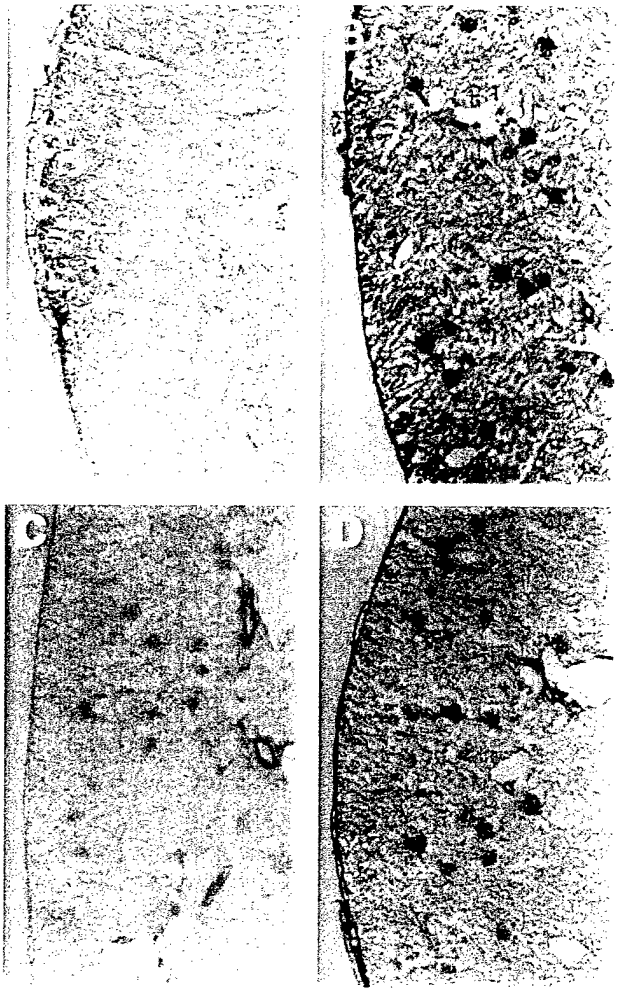

Chapter VII

Figure 2

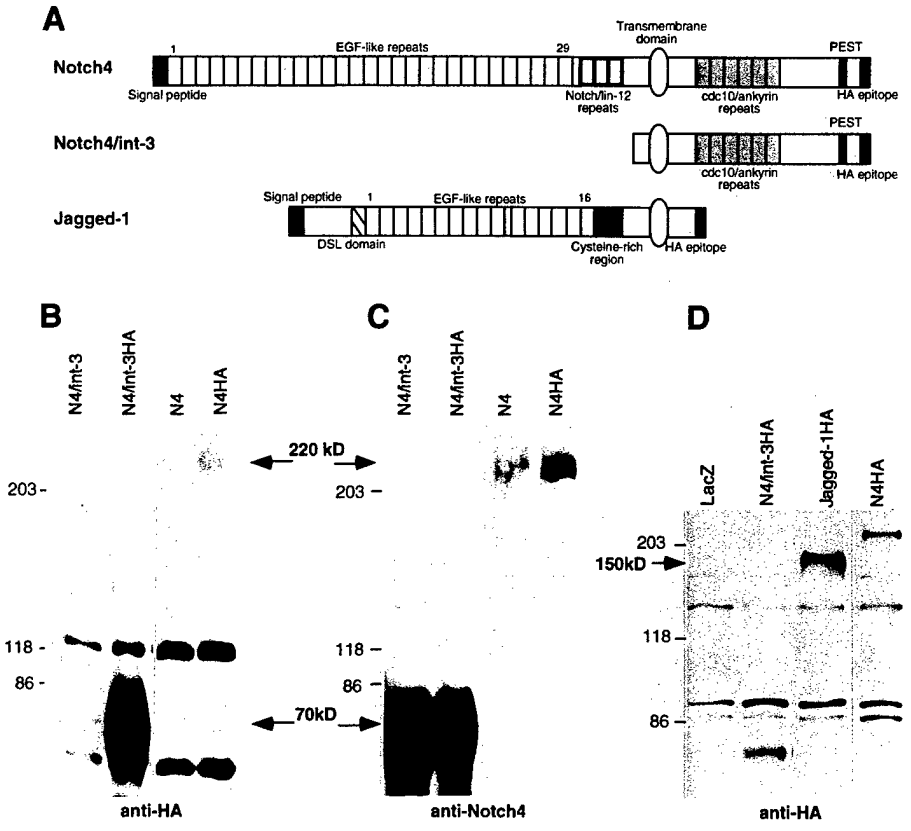

Chapter VII

Figure 3

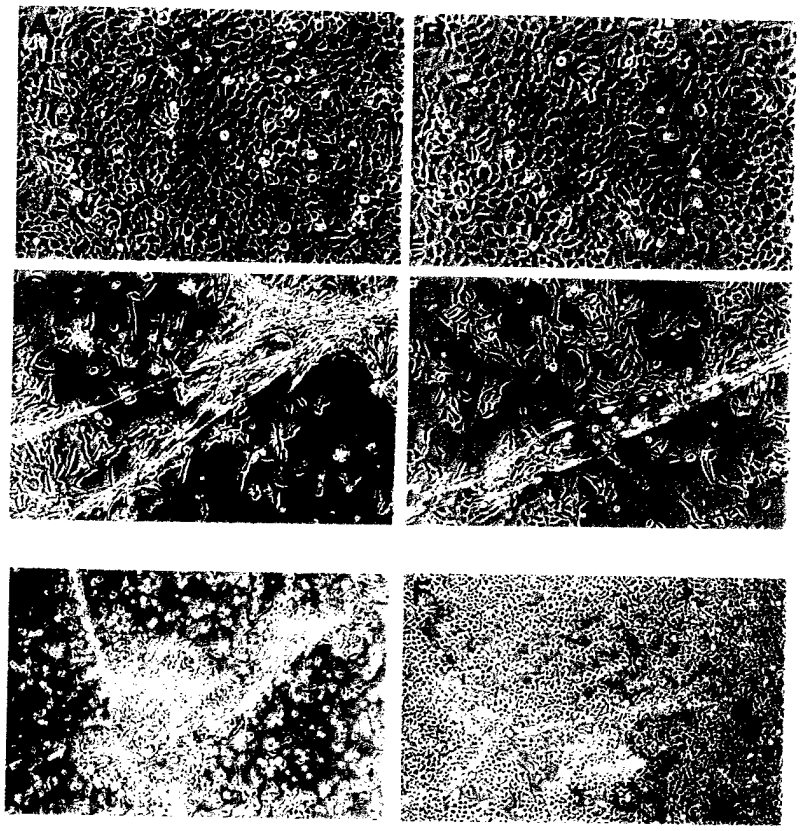

Chapter VII

Figure 4

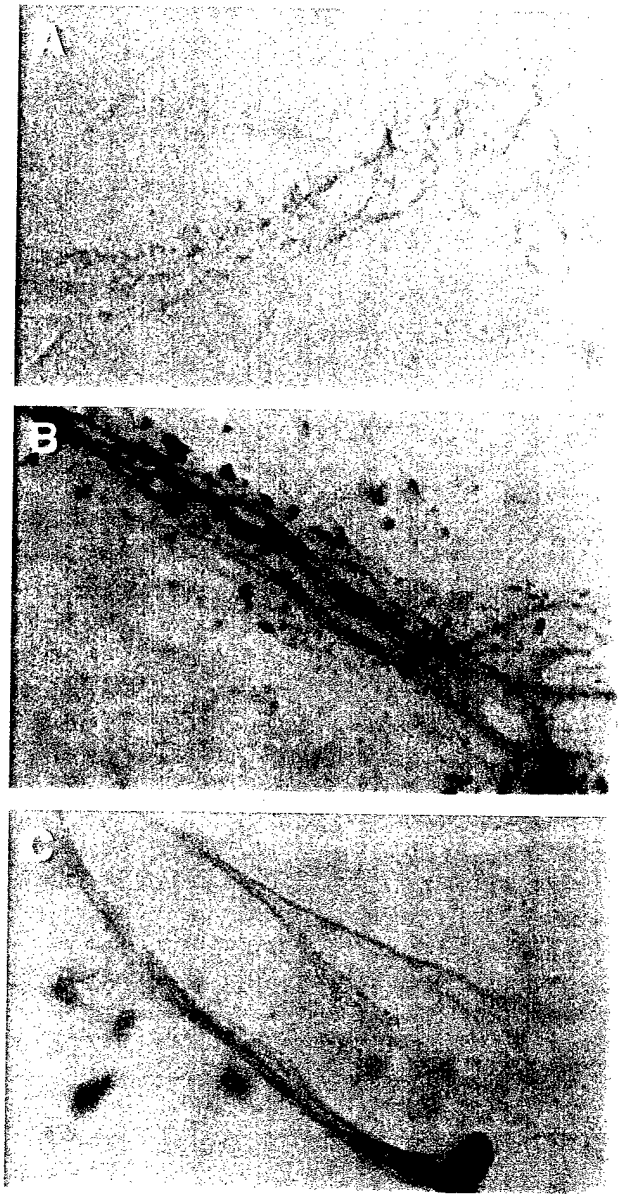

Chapter VII

Figure 5

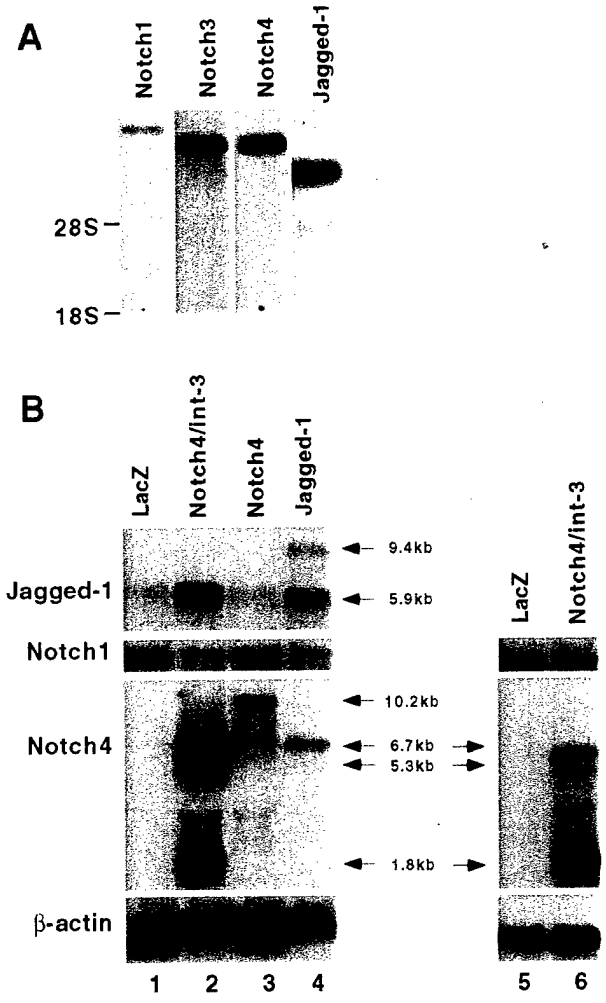

CONCLUSIONS

Data presented in this final report represent our progress in the experiments outlined in the specific aims of the research proposal. As outlined in the statement of work in the research proposal, we have largely completed the aims as scheduled for months 1-48. A new modified aim is provided, aim 3*. We have largely completed this aim.

The cloning of *int-3/Notch4* is completed. The deduced amino acid sequence of the Notch4 protein displays high homology with the *Notch/lin-12* gene family members, identifying this gene as the fourth murine *Notch* gene. We have proposed to rename this gene *Notch4*, reserving the *int-3* nomenclature for the activated and truncated form. The deduced amino acid sequence of Notch4 reveals 29 EGF-like repeats and 3 Notch/lin-12 repeats in the extracellular domain, a transmembrane domain, and an intracellular domain containing six ankyrin repeats. Comparison of the *int-3* gene to *Notch4* suggests that loss of the extracellular domain of Notch4 leads to constitutive activation of this receptor. The above data confirms the initial hypothesis that *int-3* is a bona fide member of the *Notch/lin-12* gene family.

The truncated *int-3* gene and the full length *Notch4* gene has been assembled, epitope tagged, and cloned into an eukaryotic expression vector. Cell lines have been generated that are programmed to express Notch4/int-3 proteins. Branching morphogenesis of mammary TAC-2 cells was used to examine Notch function in mammary gland development. Notch4(int-3) oncoprotein inhibited branching morphogenesis induced by HGF and TGF-β2. Co-expression of Wnt-1 and Notch4(int-3) demonstrates that Wnt-1 overrides the Notch-mediated inhibition of ductal morphogenesis. Wnt and Notch signaling may play opposite roles in mammary gland development. In this assay, the int-3 oncoprotein can prevent growth factor mediated differentiation, in an analogous matter to the *int-3* transgenic mouse phenotype.

In aim 2, we sought to identify and characterize int-3 binding proteins. SEL-10, a negative regulator of the Notch/lin-12 signaling pathway was identified in C. elegans. SEL-10 is a member of the CDC4 family of proteins that promotes ubiquitination. We confirmed that SEL-10 interacts with murine Notch4/int-3 suggesting that it may be a regulator of Notch protein turnover. We have shown SEL-10 proteins complexes with both LIN-12 and Notch4, indicating the regulatory function of *Sel-10* is conserved among different species. A human homologue of *Sel-10* has been identified.

The expression analysis of the *Notch4 mRNA* was analyzed in adult tissues as well as during mouse development. The *Notch4* transcript consists of a 6.5 kb mRNA species, that is specifically expressed in embryonic and adult endothelial cells. A rabbit polyclonal antibody was successfully raised against the intracellular domain of Notch4. This antisera was used to document an endothelial specific expression pattern for Notch4 in murine kidney. Based upon our documentation of Notch4 as a endothelially-expressed Notch gene we did not pursue expression analysis of Notch4/int-3 in mammary epithelium, as originally proposed. Activation of expression of the truncated Notch4 gene, int-3, in mammary epithelium occurs when driven by the Mouse Mammary Tumor Virus (MMTV) LTR. One can propose that an alternate Notch gene plays a role in mammary gland and Notch4 activation by MMTV disrupts this role leading to oncogenesis.

We used Rat brain microvessel endothelial cells (RBE4) as a model system to study the role of Notch4 and Jagged-1 (a Notch ligand) in endothelial cell differentiation. Both Notch4/int-3 and Jagged-1 were able to induce cellular structures with morphological and biochemical properties of endothelial microvessels. Ectopic expression of full length Notch4 did not have any discernible effect in RBE4 cells. Activation of the Notch signal transduction pathway was measured by the induction of endogenous *Notch4* and *Jagged-1* genes. The observed morphological changes to RBE4 cells correlated with endogenous *Notch4* and *Jagged-1* gene activation, demonstrating a link between Notch signaling and biological activity. Our observations demonstrate that Notch signaling can promote endothelial cell differentiation.

REFERENCES

1. Gallahan, D., Kozak, C., and Callahan, R., A new common integration region (int-3) for mouse mammary tumor virus on mouse chromosome 17, *Journal of Virology, 61*, 218-20 (1987).
2. Robbins, J., Blondel, B. J., Gallahan, D., and Callahan, R., Mouse mammary tumor gene int-3: a member of the notch gene family transforms mammary epithelial cells, *Journal of Virology, 66*, 2594-9 (1992).
3. Smith, G. H., Gallahan, D., Diella, F., Jhappan, C., Merlino, G., and Callahan, R., Constitutive expression of a truncated INT-3 gene in mouse mammary epithelium impairs differentiation and functional development., *Cell Growth & Differentiation, 6*, 563-577 (1995).
4. Jhappan, C., Gallahan, D., Stahle, C., Chu, E., Smith, G. H., Merline, G., and Callahan, R., Expression of an activated *Notch*-related *int-3* transgene interferes with cell differentiation and induces neoplastic transformation in mammary and salivary glands., *Genes & Development, 6*, 345-355 (1992).
5. Sarkar, N. H., Haga, S., Lehner, A. F., Zhao, W., Imai, S., and Moriwaki, K., Insertional mutation of int protooncogenes in the mammary tumors of a new strain of mice derived from the wild in China: normal- and tumor-tissue-specific expression of int-3 transcripts, *Virology, 203*, 52-62 (1994).
6. Wharton, K. A., Johansen, K. M., Xu, T., and Artavanis-Tsakonas, S., Nucleotide sequence from the neurogenic locus notch implies a gene product that shares homology with proteins containing EGF-like repeats., *Cell, 43*, 567-581 (1985).
7. Yochem, J., Weston, K., and Greenwald, I., The *Caenorhabditis elegans lin-12* gene encodes a transmembrane protein with overall similarity to *Drosophila Notch.*, *Nature, 335*, 547-550 (1988).
8. Greenwald, I., *lin-12*, a nematode homeotic gene, is homologues to a set of mammalian proteins that includes epidermal growth factor., *Cell, 43*, 583-590 (1985).
9. Yochem, J., and Greenwald, I., *glp-1* and *lin-12*, genes implicated in distinct cell-cell interactions in C. elegans, encode similar transmembrane proteins., *Cell, 58*, 553-563 (1989).
10. Coffman, C., Harris, W., and Kintner, C., *Xotch*, the *Xenopus* homolog of Drosophila *Notch.*, *Science, 249*, 1438-1441 (1990).
11. Lardelli, M., and Lendahl, U., *Motch A* and *Motch B*-two mouse *Notch* homologues coexpressed in a wide variety of tissues., *Exp.Cell Res., 204*, 364-372 (1993).
12. Del Amo, F. F., Smith, D. E., Swiatek, P. J., Gendron-Maguire, M., Greenspan, R. J., McMahon, A. P., and Gridley, T., Expression pattern of Motch, a mouse homolog of Drosophila Notch, suggests an important role in early postimplantation mouse development, *Development, 115*, 737-44 (1992).
13. del Amo, F. F., Gendron-Maguire, M., Swiatek, P. J., Jenkins, N. A., Copeland, N. G., and Gridley, T., Cloning, analysis, and chromosomal localization of Notch-1, a mouse homolog of Drosophila Notch, *Genomics, 15*, 259-64 (1993).
14. Reaume, A. G., Conlon, R. A., Zirngibl, R., Yamaguchi, T. P., and Rossant, J., Expression analysis of a *Notch* homologue in the mouse embryo., *J. Dev. Biol., 154*, 377-387 (1992).
15. Lardelli, M., Dahlstrand, J., and Lendahl, U., The novel Notch homologue mouse Notch3 lacks specific epidermal growth factor-repeats and is expreesed in proliferating neuroepithelium., *Mechanism of Development, 46*, 123-136 (1994).
16. Weinmaster, G., Roberts, V. J., and Lemke, G. A., A homolog of Drosophila Notch expressed during mammalian development, *Development, 113*, 199-205 (1991).
17. Weinmaster, G., Roberts, V. J., and Lemke, G., *Notch* 2: a second mammalian *Notch* gene., *Development, 116*, 931-941 (1992).
18. Ellisen, L. W., Bird, J., West, D. C., Soreng, A. L., Reynolds, T. C., Smith, S. D., and Sklar, J., TAN-1, the human homolog of the Drosophila notch gene, is broken by chromosomal translocations in T lymphoblastic neoplasms, *Cell, 66*, 649-61 (1991).
19. Zagouras, P., Stifani, S., Blaumueller, C. M., Carcangiu, M. L., and Artavanis-Tsakonas, S., Alterations in Notch signaling in neoplastic lesions of the human cervix, *Proc. Natl. Acad. Sci. USA, 92*, 6414-6418 (1995).

20. Wharton, K. A., Yedvobnick, B., Finnerty, V. G., and Artavanis-Tsakonas, S., Opa: a novel family of transcribed repeats shared by the Notch locus and other developmentally regulated loci in Drosophilla melanogaster., *Cell, 40*, 55-62 (1985).
21. Struhl, G., Fitzgerald, K., and Greenwald, I., Intrinsic activity of the Lin-12 and Notch intracellular domains in vivo, *Cell, 74*, 331-45 (1993).
22. Coffman, C. R., Skoglund, P., Harris, W. A., and Kintner, C. R., Expression of an extracellular deletion of *Xotch* diverts cell fate in Xenopus Embryos., *Cell, 73*, 659-671 (1993).
23. De Celis, J. F., Mari-Beffa, M., and Garcia-Bellido, A., Cell-autonomous role of Notch,an epidermal growth factor homologue, in sensory organ differentiation in *Drosophila.*, *Proc. Natl. Acad. Sci. USA, 88*, 632-636 (1991).
24. Lieber, T., Kidd, S., Alcomo, E., Corbin, V., and Young, M. W., Antineurogenic phenotypes induced by truncated Notch proteins indicate a role in signal transduction and may point to a novel function for Notch in nuclei., *Genes Dev., 7*, 1949-1965 (1993).
25. Swiatek, P. J., Lindsell, C. E., Franco del Amo, F., Weinmaster, G., and Gridley, T., *Notch 1* is essential for postimplantation development in mice., *Genes & Development, 8*, 707-719 (1994).
26. Kooh, P. J., Fehon, R. G., Muskavitch, M. A. T., Implications of dynamic patterns of Delta and Notch expression for cellular interactions during *Drosophila* development., *Development, 117*, 493-507 (1993).
27. Fleming, R. J., Scottgale, T. N., Diederich, R. J., and Artavanis-Tsakonas, S., The gene Serrate encodes a putative EGF-like transmembrane protein essential for proper ectodermal development in Drosophila melanogaster, *Genes & Development, 4*, 2188-201 (1990).
28. Henderson, S. T., Gao, D., Lambie, E. J., and Kimble, J., *lag-2* may encode a signaling ligand for the GLP-1 and LIN-12 receptors of *C. elegans*, *Development, 120*, 2913-2924 (1994).
29. Lindsell, C. E., Shawber, C. J., Boulter, J., and Weinmaster, G., Jagged: a mammalian ligand that activates Notch1, *Cell, 80*, 909-17 (1995).
30. Bettenhausen, B., Hrabe de Angelis, M., Simon, D., Guenet, J. L., and Gossler, A., Transient and restricted expression during mouse embryogenesis of *Dll*, a murine gene closely related to *Drosophila Delta.*, *Development, 121*, 2407-18 (1995).
31. Diederich, R. J., Matsuno, K., Hing, H., and Artavanis-Tsakonas, S., Cytosolic interaction between deltex and Notch ankyrin repeats implicates deltex in the Notch signaling pathway, *Development, 120*, 473-81 (1994).
32. Matsuno, K., Diederich, R. J., Go, M. J., Blaumeueller, C. M., and Atavanis-Tsakonas, S., Deltex acts as a positive regulator of Notch signaling through interactions with the Notch ankyrin repeats., *Development, 121*, 2633-44 (1995).
33. Fortini, M. E., Rebay, I., Caron, L. A., and Artavanis-Tsakonas, S., An activated Notch receptor blocks cell-fate commitment in the developing Drosophila eye, *Nature, 365*, 555-7 (1993).
34. Kopan, R., and Cagan, R., Notch on the cutting edge, *Trends Genet, 13*, 465-7 (1997).
35. Schroeter, E. H., Kisslinger, J. A., and Kopan, R., Notch-1 signalling requires ligand-induced proteolytic release of intracellular domain [see comments], *Nature, 393*, 382-6 (1998).
36. Struhl, G., and Adachi, A., Nuclear Access and Action of Notch In Vivo, *Cell, 93*, 1-20 (1998).
37. Ohara, O., Dorit, R. L., and Gilbert, W., One-sided polymerase chain reaction: the amplification of cDNA., *Proc.Natl.Acad.Sci.USA, 86*, 5673-5677 (1989).
38. Apte, A. N., and Siebert, P. D., Anchor-ligated cDNA libraries: a technique for generating a cDNA library for the immediate cloning of the 5' ends of mRNAs., *Bio. Techniques, 15*, 890-893 (1993).
39. Greenwald, I., and Seydoux, G., Analysis of gain-of-function mutations of the lin-12 gene of Caenorhabditis elegans, *Nature, 346*, 197-9 (1990).
40. Kolodziej, P. A., and Young, R. A., Epitope tagging and protein surveillance, *Methods Enzymol., 194*, 508-519 (1991).
41. Wilson, I. A., Niman, H. L., Houghten, R. A., Cherenson, A. R., Connolly, M. L., and Lerner, R. A., The structure of an antigenic determinant of a protein, *Cell, 37*, 767-778 (1984).
42. Miller, A. D., and Rosman, G. J., Improved retroviral vectors for gene transfer and expression., *Bio. Techniques, 7*, 980-990 (1989).
43. Soriano, J. V., Pepper, M. S., Nakamura, T., Orci, L., and Montesano, R., Hepatocyte growth factor stimulates extensive development of branching duct-like structures by cloned mammary gland epithelial cells, *Journal of Cell Science, 108*, 413-30 (1995).

44. Osborn, M., and Weber, K., Immunofluorescence and immunocytochemical procedures with affinity purified antibodies: Tubulin-containing structures., *Methods Cell Biol., 24*, 97-132 (1982).
45. Haslam, S. Z., Counterman, L. J., and Nummy, K. A., EGF receptor regulation in normal mouse mammary gland, *Journal of Cellular Physiology, 152*, 553-7 (1992).
46. Coleman-Krnacik, S., and Rosen, J. M., Differential temporal and spatial gene expression of fibroblast growth factor family members during mouse mammary gland development, *Mol. Endocrinol., 8*, 218-229 (1994).
47. Bates, P., Fisher, R., Ward, A., Richardson, L., Hill, D. J., and Graham, C. F., Mammary cancer in transgenic mice expressing insulin-like growth factor II (IGF-II)., *British Journal of Cancer, 72*, 1189-93 (1995).
48. Yang, Y., Spitzer, E., Meyer, D., Sachs, M., Niemann, C., Hartmann, G., Weidner, K. M., Birchmeier, C., and Birchmeier, W., Sequential requirement of hepatocyte growth factor and neuregulin in the morphogenesis and differentiation of the mammary gland, *Journal of Cell Biology, 131*, 215-26 (1995).
49. Daniel, C. W., Robinson, S., and Silberstein, G. B., The Role of TGF-β in Patterning and Growth of the Mammary Ductal Tree., *J. Mam. Gland Biol. Neoplasia, 1*, 331-341 (1996).
50. Pierce, D. F., Jr., Johnson, M. D., Matsui, Y., Robinson, S. D., Gold, L. I., Purchio, A. F., Daniel, C. W., Hogan, B. L., and Moses, H. L., Inhibition of mammary duct development but not alveolar outgrowth during pregnancy in transgenic mice expressing active TGF-beta 1, *Genes & Development, 7*, 2308-17 (1993).
51. Niranjan, B., Buluwela, L., Yant, J., Perusinghe, N., Atherton, A., Phippard, D., Dale, T., Gusterson, B., and Kamalati, T., HGF/SF: a potent cytokine for mammary growth, morphogenesis and development, *Development, 121*, 2897-908 (1995).
52. Pepper, M. S., Soriano, J. V., Menoud, P. A., Sappino, A. P., Orci, L., and Montesano, R., Modulation of hepatocyte growth factor and c-met in the rat mammary gland during pregnancy, lactation, and involution, *Experimental Cell Research, 219*, 204-10 (1995).
53. Smith, G. H., TGF-β and Functional Differentiation., *J. Mam. Gland Biol. Neoplasia, 1*, 343-352 (1996).
54. Kordon, E. C., McKnight, R. A., Jhappan, C., Hennighausen, L., Merlino, G., and Smith, G. H., Ectopic TGF beta 1 expression in the secretory mammary epithelium induces early senescence of the epithelial stem cell population, *Developmental Biology, 168*, 47-61 (1995).
55. Soriano, J. V., Orci, L., and Montesano, R., TGF-beta1 induces morphogenesis of branching cords by cloned mammary epithelial cells at subpicomolar concentrations, *Biochemical & Biophysical Research Communications, 220*, 879-85 (1996).
56. Nusse, R., and Varmus, H. E., *Wnt* genes, *Cell, 69*, 1073-1087 (1992).
57. Gavin, B. J., and McMahon, A. P., Differential regulation of the *Wnt*-gene family during pregnancy and lactation suggests a role in postnatal development of the mammary gland., *Mol. Cell. Biol., 12*, 2418-2423 (1992).
58. Weber-Hall, S. J., Phippard, D. J., Niemeyer, C. C., and Dale, T. C., Developmental and hormonal regulation of Wnt gene expression in the mouse mammary gland, *Differentiation, 57*, 205-14 (1994).
59. Buhler, T. A., Dale, T. C., Kieback, C., Humphreys, R. C., and Rosen, J. M., Localization and quantification of wnt-2 gene expression in mouse mammary development., *Dev. Biol., 155*, 87-96 (1993).
60. Nusse, R., van Ooyen, A., Cox, D., Fung, Y. K., and Varmus, H., Mode of proviral activation of a putative mammary oncogene (*int*-1) on mouse chromosome 15., *Nature, 307*, 131-136 (1984).
61. Tsukamoto, A. S., Grosschedl, R., Guzman, R. C., Parslow, T., and Varmus, H. E., Expression of the *int*-1 gene in transgenic mice is associated with mammary gland hyperplasia and adenocarcinomas in male and female mice., *Cell, 55*, 619-625 (1988).
62. Uyttendaele, H., Marazzi, G., Wu, G., Yan, Q., Sassoon, D., and Kitajewski, J., Notch4/int-3, a mammary proto-oncogene, is an endothelial cell-specific mammalian Notch gene, *Development, 122*, 2251-9 (1996).
63. Gallahan, D., and Callahan, R., The mouse mammary tumor associated gene INT3 is a unique member of the NOTCH gene family (NOTCH4), *Oncogene, 14*, 1883-90 (1997).

64. Daniel, C. W., and Silberstein, G. B., Postnatal Development of the Rodent Mammary Gland, in *The Mammary Gland*, Neville, M. C., and Daniel, C. W., Eds., Plenum Press, New York and London, pp. 3-31 (1987).
65. Pitelka, D. R., Hamamoto, S. T., Duafala, J. G., and Nemanic, M. K., Cell contacts in the mouse mammary gland. I. Normal gland in postnatal development and the secretory cycle, *Journal of Cell Biology, 56*, 797-818 (1973).
66. Russo, I. H., Tewari, M., and Russo, J., Morphology and Development of the Rat Mammary Gland, in *Integument and Mammary Glands*, Jones, T. C., Mohr, V., and Hunt, R. D., Eds., Springer-Verlag, Berlin, pp. 233-252 (1989).
67. Edwards, P. A. W., Hiby, S. E., Papkoff, J., and Bradbury, J. M., Hyperplasia of mouse mammary epithelium induced by expression of the Wnt-1 (int-1) oncogene in reconstituted mammary gland, *Oncogene, 7*, 2041-2051 (1992).
68. Edwards, P. A., Tissue reconstitution models of breast cancer., *Cancer Surveys, 16*, 79-96 (1993).
69. Miller, J. R., and Moon, R. T., Signal transduction through beta-catenin and specification of cell fate during embryogenesis., *Genes & Development, 10*, 2527-39 (1996).
70. Lin, K., Wang, S., Julius, M. A., Kitajewski, J., Moos, M., Jr., and Luyten, F. P., The cysteine-rich frizzled domain of Frzb-1 is required and sufficient for modulation of Wnt signaling, *Proc Natl Acad Sci U S A, 94*, 11196-200 (1997).
71. Shimizu, H., Julius, M. A., Giarre, M., Zheng, Z., Brown, A. M. C., and Kitajewski, J., Transformation by Wnt family proteins correlates with regulation of β-catenin., *Cell Growth & Differentiation, 8*, 1349-58 (1997).
72. Morin, P. J., Sparks, A. B., Korinek, V., Barker, N., Clevers, H., Vogelstein, B., and Kinzler, K. W., Activation of beta-catenin-Tcf signaling in colon cancer by mutations in beta-catenin or APC., *Science, 275*, 1787-90 (1997).
73. Molenaar, M., van de Wetering, M., Oosterwegel, M., Peterson-Maduro, J., Godsave, S., Korinek, V., Roose, J., Destree, O., and Clevers, H., XTcf-3 transcription factor mediates beta-catenin-induced axis formation in Xenopus embryos, *Cell, 86*, 391-9 (1996).
74. Yost, C., Torres, M., Miller, J. R., Huang, E., Kimelman, D., and Moon, R., The axis-inducing activity, stability, and subcellular distribution of β-catenin is regulated in *Xenopus* embryos by glycogen synthase kinase 3, *Genes & Development, 10*, 1443-1454 (1996).
75. Gumbiner, B. M., Cell Adhesion: The Molecular Basis of Tissue Architecture and Morphogenesis., *Cell, 84*, 345-357 (1996).
76. Hoschuetzky, H., Aberle, H., and Kemler, R., Beta-catenin mediates the interaction of the cadherin-catenin complex with epidermal growth factor., *J. Cell. Biol., 127*, 1375-1380 (1994).
77. Shibamoto, S., Hayakawa, M., Takeuchi, K., Hori, T., Oku, N., Miyazawa, K., Kitamura, N., Takeichi, M., and Ito, F., Tyrosine phosphorylation of beta-catenin and plakoglobin enhanced by hepatocyte growth factor and epidermal growth factor in human carcinoma cells, *Cell Adhesion & Communication, 1*, 295-305 (1994).
78. Hartmann, G., Weidner, K. M., Schwarz, H., and Birchmeier, W., The motility signal of scatter factor/hepatocyte growth factor mediated through the receptor tyrosine kinase met requires intracellular action of Ras, *Journal of Biological Chemistry, 269*, 21936-9 (1994).
79. Behrens, J., Vakaet, L., Friis, R., Winterhager, E., Van Roy, F., Mareel, M. M., and Birchmeier, W., Loss of epithelial differentiation and gain of invasiveness correlates with tyrosine phosphorylation of the E-cadherin/β-catenin complex in cells transformed with a temperature-sensitive v-Src gene, *Journal of Cell Biology, 120*, 757-766 (1993).
80. Daniel, J. M., and Reynolds, A. B., The tyrosine kinase substrate p120cas binds directly to E-cadherin but not to the adenomatous polyposis coli protein or alpha-catenin, *Molecular & Cellular Biology, 15*, 4819-24 (1995).
81. Kinch, M. S., Clark, G. J., Der, C. J., and Burridge, K., Tyrosine phosphorylation regulates the adhesions of ras-transformed breast epithelia, *Journal of Cell Biology, 130*, 461-71 (1995).
82. Campbell, G., Weaver, T., and Tomlinson, A., Axis specification in the developing Drosophila appendage: The role of wingless, decapentaplegic, and the homeobox gene aristaless., *Cell, 74*, 1113-1123 (1993).

83. Diaz-Benjumea, F. J., Cohen, B., and Cohen, S. M., Cell interaction between compartments establishes the proximal-distal axis of Drosophila legs, *Nature, 372*, 175-9 (1994).
84. Riese, J., Yu, X., Munnerlyn, A., Eresh, S., Hsu, S. C., Grosschedl, R., and Bienz, M., LEF-1, a nuclear factor coordinating signaling inputs from wingless and decapentaplegic, *Cell, 88*, 777-87 (1997).
85. Greenwald, I., and Rubin, G. M., Making a difference: the role of cell-cell interactions in establishing separate identities for equivalent cells, *Cell, 68*, 271-81 (1992).
86. Artavanis-Tsakonas, S., Matsuno, K., and Fortini, M. E., Notch signaling, *Science, 268*, 225-232 (1995).
87. Gallahan, D., Jhappan, C., Robinson, G., Hennighausen, L., Sharp, R., Kordon, E., Callahan, R., Merlino, G., and Smith, G. H., Expression of a truncated Int3 gene in developing secretory mammary epithelium retards lobular differentiation resulting in tumorigenesis, *Cancer Research, 56*, 1775-85 (1996).
88. Hubbard, E. J., Dong, Q., and Greenwald, I., Evidence for physical and functional association between EMB-5 and LIN-12 in Caenorhabditis elegans, *Science, 273*, 112-5 (1996).
89. Hsieh, J. J., Henkel, T., Salmon, P., Robey, E., Peterson, M. G., and Hayward, S. D., Truncated mammalian Notch1 activates CBF1/RBPJk-repressed genes by a mechanism resembling that of Epstein-Barr virus EBNA2, *Molecular & Cellular Biology, 16*, 952-9 (1996).
90. Greenwald, I., Structure/function studies of lin-12/Notch proteins, *Current Opinion in Genetics & Development, 4*, 556-62 (1994).
91. Axelrod, J. D., Matsuno, K., Artavanis-Tsakonas, S., and Perrimon, N., Interaction between Wingless and Notch signaling pathways mediated by dishevelled., *Science, 271*, 1826-32 (1996).
92. Pear, W. S., Nolan, G. P., Scott, M. L., and Baltimore, D., Production of high-titer helper-free retroviruses by transient transfection., *Proc. Natl. Acad. Sci. USA, 90*, 8392-8396 (1993).
93. Kimble, J., and Hirsh, D., The postembryonic cell lineages of the hermaphrodite and male gonads in Caenorhabditis elegans, *Dev Biol, 70*, 396-417 (1979).
94. Kimble, J., Alterations in cell lineage following laser ablation of cells in the somatic gonad of Caenorhabditis elegans, *Dev Biol, 87*, 286-300 (1981).
95. Seydoux, G., and Greenwald, I., Cell autonomy of lin-12 function in a cell fate decision in C. elegans, *Cell, 57*, 1237-45 (1989).
96. Greenwald, I. S., Sternberg, P. W., and Horvitz, H. R., The lin-12 locus specifies cell fates in Caenorhabditis elegans, *Cell, 34*, 435-44 (1983).
97. Wilkinson, H. A., Fitzgerald, K., and Greenwald, I., Reciprocal changes in expression of the receptor lin-12 and its ligand lag-2 prior to commitment in a C. elegans cell fate decision, *Cell, 79*, 1187-98 (1994).
98. Sundaram, M., and Greenwald, I., Suppressors of a lin-12 hypomorph define genes that interact with both lin-12 and glp-1 in Caenorhabditis elegans, *Genetics, 135*, 765-83 (1993).
99. King, R. W., Deshaies, R. J., Peters, J. M., and Kirschner, M. W., How proteolysis drives the cell cycle, *Science, 274*, 1652-9 (1996).
100. Jiang, J., and Struhl, G., Regulation of the hedgehog and wingless pathways by the F-box/WD40-repeat protein Slimb., *Nature, 391*, 493-6 (1998).
101. Altschul, S. F., Gish, W., Miller, W., Myers, E. W., and Lipman, D. J., Basic local alignment search tool, *J Mol Biol, 215*, 403-10 (1990).
102. Kumar, A., and Paietta, J. V., The sulfur controller-2 negative regulatory gene of Neurospora crassa encodes a protein with beta-transducin repeats, *Proc Natl Acad Sci U S A, 92*, 3343-7 (1995).
103. Bai, C., Sen, P., Hofmann, K., Ma, L., Goebl, M., Harper, J. W., and Elledge, S. J., SKP1 connects cell cycle regulators to the ubiquitin proteolysis machinery through a novel motif, the F-box, *Cell, 86*, 263-74 (1996).
104. Neer, E. J., Schmidt, C. J., Nambudripad, R., and Smith, T. F., The ancient regulatory-protein family of WD-repeat proteins [published erratum appears in Nature 1994 Oct 27;371(6500):812], *Nature, 371*, 297-300 (1994).
105. Fields, S., and Song, O. K., A novel genetic system to detect protein-protein interactions., *Nature, 340*, 245-246 (1989).
106. Ciechanover, A., The ubiquitin-mediated proteolytic pathway: mechanisms of action and cellular physiology, *Biol Chem Hoppe Seyler, 375*, 565-81 (1994).

107. Goebl, M. G., Yochem, J., Jentsch, S., McGrath, J. P., Varshavsky, A., and Byers, B., The yeast cell cycle gene CDC34 encodes a ubiquitin-conjugating enzyme, *Science, 241*, 1331-5 (1988).
108. Mathias, N., Johnson, S. L., Winey, M., Adams, A. E., Goetsch, L., Pringle, J. R., Byers, B., and Goebl, M. G., Cdc53p acts in concert with Cdc4p and Cdc34p to control the G1-to-S- phase transition and identifies a conserved family of proteins, *Mol Cell Biol, 16*, 6634-43 (1996).
109. Rogers, S., Wells, R., and Rechsteiner, M., Amino acid sequences common to rapidly degrade proteins: The PEST hypothesis, *Science, 234*, 364-368 (1986).
110. Mango, S. E., Maine, E. M., and Kimble, J., Carboxy-terminal truncation activates glp-1 protein to specify vulval fates in Caenorhabditis elegans, *Nature, 352*, 811-5 (1991).
111. Drexler, H. G., MacLeod, R. A., Borkhardt, A., and Janssen, J. W., Recurrent chromosomal translocations and fusion genes in leukemia-lymphoma cell lines. [Review] [247 refs], *Leukemia, 9*, 480-500 (1995).
112. Roth, M. B., Zahler, A. M., and Stolk, J. A., A conserved family of nuclear phosphoproteins localized to sites of polymerase II transcription, *J Cell Biol, 115*, 587-96 (1991).
113. Durfee, T., Becherer, K., Chen, P. L., Yeh, S. H., Yang, Y., Kilburn, A. E., Lee, W. H., and Elledge, S. J., The retinoblastoma protein associates with the protein phosphatase type 1 catalytic subunit, *Genes Dev, 7*, 555-69 (1993).
114. Evan, G. I., Lewis, G. K., Ramsay, G., and Bishop, J. M., Isolation of monoclonal antibodies specific for human c-myc proto-oncogene product, *Molecular & Cellular Biology, 5*, 3610-6 (1985).
115. Hardy, J., Amyloid, the presenilins and Alzheimer's disease, *Trends Neurosci, 20*, 154-9 (1997).
116. Neve, R. L., and Robakis, N. K., Alzheimer's disease: a re-examination of the amyloid hypothesis [In Process Citation], *Trends Neurosci, 21*, 15-9 (1998).
117. Kovacs, D. M., Fausett, H. J., Page, K. J., Kim, T. W., Moir, R. D., Merriam, D. E., Hollister, R. D., Hallmark, O. G., Mancini, R., Felsenstein, K. M., Hyman, B. T., Tanzi, R. E., and Wasco, W., Alzheimer-associated presenilins 1 and 2: neuronal expression in brain and localization to intracellular membranes in mammalian cells, *Nat Med, 2*, 224-9 (1996).
118. Duff, K., Eckman, C., Zehr, C., Yu, X., Prada, C. M., Perez-tur, J., Hutton, M., Buee, L., Harigaya, Y., Yager, D., Morgan, D., Gordon, M. N., Holcomb, L., Refolo, L., Zenk, B., Hardy, J., and Younkin, S., Increased amyloid-beta42(43) in brains of mice expressing mutant presenilin 1, *Nature, 383*, 710-3 (1996).
119. Levitan, D., and Greenwald, I., Facilitation of lin-12-mediated signalling by sel-12, a Caenorhabditis elegans S182 Alzheimer's disease gene, *Nature, 377*, 351-4 (1995).
120. Levitan, D., Doyle, T. G., Brousseau, D., Lee, M. K., Thinakaran, G., Slunt, H. H., Sisodia, S. S., and Greenwald, I., Assessment of normal and mutant human presenilin function in Caenorhabditis elegans, *Proc Natl Acad Sci U S A, 93*, 14940-4 (1996).
121. Li, X., and Greenwald, I., HOP-1, a Caenorhabditis elegans presenilin, appears to be functionally redundant with SEL-12 presenilin and to facilitate LIN-12 and GLP-1 signaling, *Proc Natl Acad Sci U S A, 94*, 12204-9 (1997).
122. Hubbard, E. J. A., Wu, G., Kitajewski, J., and Greenwald, I., sel-10, a negative regulator of lin-12 activity in C. elegans, encodes a member of the CDC4 family of proteins., *Genes Dev., 11*, 3182-93 (1997).
123. Kim, T. W., Pettingell, W. H., Hallmark, O. G., Moir, R. D., Wasco, W., and Tanzi, R. E., Endoproteolytic cleavage and proteasomal degradation of presenilin 2 in transfected cells, *J Biol Chem, 272*, 11006-10 (1997).
124. Fraser, P. E., Levesque, G., Yu, G., Mills, L. R., Thirlwell, J., Frantseva, M., Gandy, S. E., Seeger, M., Carlen, P. L., and St George-Hyslop, P., Presenilin 1 is actively degraded by the 26S proteasome, *Neurobiol Aging, 19*, S19-21 (1998).
125. Marambaud, P., Ancolio, K., Lopez-Perez, E., and Checler, F., Proteasome inhibitors prevent the degradation of familial Alzheimer's disease-linked presenilin 1 and potentiate A beta 42 recovery from human cells, *Mol Med, 4*, 147-57 (1998).
126. Patton, E. E., Willems, A. R., and Tyers, M., Combinatorial control in ubiquitin-dependent proteolysis: don't Skp the F-box hypothesis, *Trends Genet, 14*, 236-43 (1998).
127. Zhou, J., Liyanage, U., Medina, M., Ho, C., Simmons, A. D., Lovett, M., and Kosik, K. S., Presenilin 1 interaction in the brain with a novel member of the Armadillo family, *Neuroreport, 8*, 2085-90 (1997).

128. Yu, G., Chen, F., Levesque, G., Nishimura, M., Zhang, D. M., Levesque, L., Rogaeva, E., Xu, D., Liang, Y., Duthie, M., St George-Hyslop, P. H., and Fraser, P. E., The presenilin 1 protein is a component of a high molecular weight intracellular complex that contains beta-catenin, *J Biol Chem, 273*, 16470-5 (1998).
129. Takashima, A., Murayama, M., Murayama, O., Kohno, T., Honda, T., Yasutake, K., Nihonmatsu, N., Mercken, M., Yamaguchi, H., Sugihara, S., and Wolozin, B., Presenilin 1 associates with glycogen synthase kinase-3beta and its substrate tau, *Proc Natl Acad Sci U S A, 95*, 9637-41 (1998).
130. Uyttendaele, H., Soriano, J. V., Montesano, R., and Kitajewski, J., Notch4 and Wnt-1 proteins function to regulate branching morphogenesis of mammary epithelial cells in an opposing fashion., *Dev. Biol., 196*, 204-217 (1998).
131. Capobianco, A. J., Zagouras, P., Blaumueller, C. M., Artavanis-Tsakonas, S., and Bishop, J. M., Neoplastic transformation by truncated alleles of human NOTCH1/TAN1 and NOTCH2, *Mol Cell Biol, 17*, 6265-73 (1997).
132. Vassin, H., Bremer, K. A., Knust, E., and Campos-Ortega, J. A., The neurogenic gene Delta of Drosophila melanogaster is expressed in neurogenic territories and encodes for a putative transmembrane protein with EGF-like repeats, *EMBO J., 6*, 3431-3440 (1987).
133. Tax, F. E., Yeargers, J. J., and Thomas, J. H., Sequence of C. elegans lag-2 reveals a cell-signalling domain shared with Delta and Serrate of Drosophila, *Nature, 368*, 150-4 (1994).
134. Mello, C. C., Draper, B. W., and Priess, J. R., The maternal genes apx-1 and glp-1 and establishment of dorsal-ventral polarity in the early C. elegans embryo, *Cell, 77*, 95-106 (1994).
135. Dunwoodie, S. L., Henrique, D., Harrison, S. M., and Beddington, R. S., Mouse Dll3: a novel divergent Delta gene which may complement the function of other Delta homologues during early pattern formation in the mouse embryo, *Development, 124*, 3065-76 (1997).
136. Luo, B., Aster, J. C., Hasserjian, R. P., Kuo, F., and Sklar, J., Isolation and functional analysis of a cDNA for human Jagged2, a gene encoding a ligand for the Notch1 receptor, *Mol Cell Biol, 17*, 6057-67 (1997).
137. Shirayoshi, Y., Yuasa, Y., Suzuki, T., Sugaya, K., Kawase, E., Ikemura, T., and Nakatsuji, N., Proto-oncogene of int-3, a mouse Notch homologue, is expressed in endothelial cells during early embryogenesis, *Genes Cells, 2*, 213-24 (1997).
138. Lindsell, C. E., Boulter, J., diSibio, G., Gossler, A., and Weinmaster, G., Expression patterns of Jagged, Delta1, Notch1, Notch2, and Notch3 genes identify ligand-receptor pairs that may function in neural development, *Molecular & Cellular Neuroscience, 8*, 14-27 (1996).
139. Franco Del Amo, F., Smith, D. E., Swiatek, P. J., Gendron-Maguire, M., Greenspan, R. J., McMahon, A. P., and Gridley, T., Expression pattern of *Motch*, a mouse homolog of *Drosophila Notch*, suggests an important role in early postimplantation mouse development., *Development, 115*, 737-744 (1992).
140. Myat, A., Henrique, D., Ish-Horowicz, D., and Lewis, J., A chick homologue of Serrate and its relationship with Notch and Delta homologues during central neurogenesis, *Developmental Biology, 174*, 233-47 (1996).
141. Zimrin, A. B., Pepper, M. S., McMahon, G. A., Nguyen, F., Montesano, R., and Maciag, T., An antisense oligonucleotide to the notch ligand jagged enhances fibroblast growth factor-induced angiogenesis in vitro, *Journal of Biological Chemistry, 271*, 32499-502 (1996).
142. Hrabe de Angelis, M., McIntyre II, J., and A., G., Maintenance of simite borders in mice requires the *Delta* homologue *Dll1.*, *Nature, 386*, 717-721. (1997).
143. Wong, P. C., Zheng, H., Chen, H., Becher, M. W., Sirinathsinghji, D. J. S., Trumbauer, M. E., H.Y., C., Price, D. L., Van der Ploeg, L. H. T., and Sisodia, S. S., Presenilin 1 is required for *Notch1* and *Dll1* expression in the paraxial mesoderm., *Nature, 387*, 288-292 (1997).
144. Shen, J., Bronson, R. T., Chen, D. F., Xia, W., Selkoe, D. J., and Tonegawa, S., Skeletal and CNS defects in Presenilin-1-deficient mice, *Cell, 89*, 629-39 (1997).
145. Baudrimont, M., Dubas, F., Joutel, A., Tournier-Lasserve, E., and Bousser, M. G., Autosomal dominant leukoencephalopathy and subcortical ischemic stroke. A clinicopathological study, *Stroke, 24*, 122-5 (1993).
146. Joutel, A., Corpechot, C., Ducros, A., Vahedi, K., Chabriat, H., Mouton, P., Alamowitch, S., Domenga, V., Cecillion, M., Marechal, E., Maciazek, J., Vayssiere, C., Cruaud, C., Cabanis, E. A., Ruchoux, M. M., Weissenbach, J., Bach, J. F., Bousser, M. G., and Tournier-Lasserve, E.,

Notch3 mutations in CADASIL, a hereditary adult-onset condition causing stroke and dementia, *Nature, 383*, 707-10 (1996).
147. Roux, F., Durieu-Trautmann, O., Chaverot, N., Claire, M., Mailly, P., Bourre, J. M., Strosberg, A. D., and Couraud, P. O., Regulation of gamma-glutamyl transpeptidase and alkaline phosphatase activities in immortalized rat brain microvessel endothelial cells, *Journal of Cellular Physiology, 159*, 101-13 (1994).
148. Hsieh, J. J., Nofziger, D. E., Weinmaster, G., and Hayward, S. D., Epstein-Barr virus immortalization: Notch2 interacts with CBF1 and blocks differentiation, *J Virol, 71*, 1938-45 (1997).
149. Bigas, A., Martin, D., and Milner, L., Notch1 and Notch2 inhibit myeloid differentiation in response to different cytokines., *Molecular and Cellular Biology, 18*, 2324-2333 (1998).
150. Hanahan, D., Signaling vascular morphogenesis and maintenance, *Science, 277*, 48-50 (1997).
151. Zhang, Q., Ahuja, H. S., Zakeri, Z. F., and Wolgemuth, D. J., Cyclin-dependent kinase 5 is associated with apoptotic cell death during development and tissue remodeling, *Dev Biol, 183*, 222-33 (1997).

BIBLIOGRAPHY

1. Uyttendaele, H., G. Marazzi, G. Wu, Q. Yan, D. Sassoon, and **J. Kitajewski.** (1996) *Notch4/int-3*, a mammary proto-oncogene, is an endothelial cell-specific *Notch* gene. *Development*, **122**: 2251-59.

2. Uyttendaele, H., J. Soriano, R. Montesano, and **J. Kitajewski**. (1998) Notch and Wnt proteins function to regulate branching morphogenesis of mammary epithelial cells in opposing fashion. *Dev. Biol.*, **196**: 204-217.

3. Hubbard, E.J.A., G. Wu, **J. Kitajewski**, and I. Greenwald. (1997) *sel-10*, a negative regulator of *lin-12* activity in *C. elegans*, encodes a member of the CDC4 family of proteins. *Genes Dev.*, **11**: 3182-93.

4. Wu, G., E.J.A. Hubbard, **J. Kitajewski**, and I. Greenwald. (1998) Evidence for functional and physical association between *Caenorhabditis elegans* SEL-10, a Cdc4p-related protein, and SEL-12 presenilin. *Proc. Natl. Acad. Sci. USA*, **in press.**

5. Uyttendaele, H., G. Wu, F. Roux, G. Weinmaster, and **J. Kitajewski.** (1998) Notch4 and Jagged-1 induce microvessel differentiation of rat brain endothelial cells. Submitted.

MEETING ABSTRACTS

1. Uyttendaele, H. and **J. Kitajewski.** 1994. Expression of epitope tagged *int*-3 in mouse mammary epithelial cells. Meeting on Oncogenes, Frederick, Maryland.

2. **Kitajewski, J.** and H. Uyttendaele. 1995. Expression of epitope tagged int-3 in mouse mammary epithelial cells. Keystone Symposia on Molecular and Cellular Biology. Oncogenes: 20 Years Later. Keystone, Colorado.

3. Uyttendaele, H., G. Wu, and **J. Kitajewski.** 1996. Cloning and analysis of the int-3 mammary oncogene. Keystone Symposia on Molecular & Cellular Biology. Breast and Prostrate Cancer: Basic Mechanisms. Taos, New Mexico.

4. Wu, G., Uyttendaele, H., Marazzi, G., Yan, Q., Sassoon, D. and **J. Kitajewski**. 1996. *Notch4/int-3*, a mammary proto-oncogene, is an endothelial cell specific mammalian Notch gene. Meeting on Oncogenes, Frederick, Maryland.

5. Wu, G., J. Hubbard, H. Uyttendaele, I. Greenwald and **J. Kitajewski.** 1997. The int-3 mammary oncoprotein interacts with sel-10, a *C. Elegans* member of the CDC4 family of proteins. Breast Development, Physiology, and Cancer. NIH conferenece, Bethesda, Maryland

6. Uyttendaele, H., J. V. Soriano, R. Montesano and **J. Kitajewski.** 1997. The Notch4/int-3 and Wnt-1 mammary oncoproteins display opposite effects on branching morphogenesis of mammary epithelial cells. Breast Development, Physiology, and Cancer. NIH conferenece, Bethesda, Maryland

7. Uyttendaele, H. and **J. Kitajewski**. 1997. Notch Signaling in mammary gland development and tumorigenesis. Department of Defense Breast Cancer Research Program "Era of Hope". Washingtion, DC.

8. **Kitajewski, J.**, M. Julius, G. Wu, C. Young, Z. Zheng, Q. Yan, and H. Uyttendaele. 1997. Wnt and Notch signaling in mammary gland development and tumorigenesis. Department of Defense Breast Cancer Research Program "Era of Hope". Washingtion, DC.

9. **J. Kitajewski**. 1997. Wnt and Notch signaling in angiogenesis and epithelial morphogenesis. Thirteenth International Syposium on Cellular Endocrinology, Lake Placid, New York.

10. Uyttendaele, H., M. Julius, Q. Yan, and **J. Kitajewski**. 1998. The Wnt-1 and Notch4/int-3 mammary oncoproteins display opposite effects on branching morphogenesis of mammary epithelial cells. Wnt Meeting, Harvard University, Cambridge MA.

PERSONNEL FOR THIS EFFORT

Guangyu Wu

Hendrik Uyttendaele

Jan Kitajewski

Zhili Zheng

Qingyou Yan